



universität
wien

DIPLOMARBEIT

Titel der Diplomarbeit

„Temporal trends of ion concentration and deposition in
high alpine snow packs from 1983-2011
(Hohe Tauern, Austria)“

Verfasserin

Marion Rothmüller

angestrebter akademischer Grad

Magistra der Naturwissenschaften (Mag. rer. nat.)

Wien, 2012

Studienkennzahl lt. Studienblatt:

A 415

Studienrichtung lt. Studienblatt:

Meteorologie

Betreuer:

O. Univ.-Prof. Dr. Reinhold Steinacker

“There is a sufficiency in the world for man’s need
but not for man’s greed.”

Mohandas K. Gandhi

“Our environmental problems originate in the hubris of imagining
ourselves as the central nervous system or the brain of nature. We’re
not the brain, we are a cancer on nature.”

Dave Foreman

Contents

Abstract	1
Zusammenfassung	3
Acknowledgments	5
1. Introduction	7
1.1. Ionic compounds in snow	8
1.2. Aerosols	10
1.2.1. Sources	10
1.2.2. Sinks	11
1.3. Study Area	13
2. Methods	17
2.1. Snow Sampling	17
2.2. Chemical Analysis	18
2.3. Measure Units and Statistical Analysis	20
2.4. Analytical Quality Control	20
2.4.1. Ion Balance	20
2.4.2. Measured vs. Calculated Conductivity	22
2.5. Spatial Variability and Representativeness	24
2.5.1. Analytic representativeness	24
2.5.2. Microscale variability (10cm to 1m)	26
2.5.3. Mesoscale variability (10m to 1km)	26
2.5.4. Macroscale variability (>10km)	27
2.5.5. Conclusion on the spatial variability of the ion concentration in the snow	27
3. Source Analysis	29
3.1. Chemical Composition of the snow based on ion concentrations . . .	29
3.2. Principal Component Analysis	30
3.3. Non sea salt proportion	33
4. Analysis of temporal trends in ion concentration and deposition	37
4.1. Trends in acidity	38
4.2. Trends in acid compounds	39

4.3. Trends in neutralizing compounds	42
4.3.1. NH ₃ emissions and N-Fertilization	43
4.3.2. Sahara dust events	45
4.4. Trends from other Ions	47
4.4.1. Potash	47
4.4.2. Magnesium as part of sea salt and dust events	49
5. Comparison WUK and GOK	51
5.1. Comparison of ion concentration and deposition	52
5.2. Discussion of the differences of WUK and GOK	53
5.3. Outlier discussion - 1997	61
6. Main Findings and Conclusion	65
6.1. Main findings	65
6.2. Conclusion and outlook	66
A. Mean, Median and Deposition	81
B. Source Analysis	85
B.1. PCA WUK	86
B.2. PCA GOK	87
C. Boxplots	91
C.1. 3*Interquantil range (WUK)	92
C.2. 3*Interquantil range (GOK)	93
C.3. 1,5*Interquantil range (WUK)	94
C.4. 1,5*Interquantil range (GOK)	95
D. Depth profiles for all years	97
D.1. WUK	98
D.2. GOK	101

Abstract

The input of atmospheric trace elements to high alpine snow covers could cause an acidification of high alpine glaciers and of outflowing meltwater which could in turn lead to an “acid shock” of affected ecosystems like rivers, lakes or soil.

This work tries to identify the sources and long term trends of acidity of two high alpine glaciers (Goldbergkees and Wurtenkees) in the Nationalpark Hohe Tauern in Austria from 1983 to 2011.

The chemical composition of the snow packs is verified and shows that the primary ions of high alpine snow packs are Nitrate (NO_3^-), Sulfate (SO_4^{2-}), Hydron (H^+), Ammonium (NH_4^+) and Calcium (Ca^{2+}). It is shown, that the anions are, together with H^+ , responsible for the acidification of the glaciers and are neutralized by the cations NH_4^+ and Ca^{2+} .

The source regions of the ions are identified through a Principal Component Analysis and the calculation of “non sea salt concentrations” of all ions based on the sea water ratios. It is proven that the sources for the primary ions are mainly anthropogenic and only naturally for Ca^{2+} , which originates from dust events. The secondary ions, such as Chloride (Cl^-), Sodium (Na^+) and Potassium (K^+) are found not to originate from maritime aerosols, as assumed so far, but from anthropogenic activities as well, probably from wooden biomass combustion and fertilization with potash.

The long time trend analysis shows a significant decrease for SO_4^{2-} and H^+ concentrations and depositions on both glaciers. On Wurtenkees also for NO_3^- a significant reduction in concentration and deposition is observed.

This allows the conclusion that the acidification of glaciers and hence, the acidification of outflowing meltwater is regressive. The drop of the pH in high alpine snow packs is achieved through emission reductions of Sulfur dioxide (SO_2) and Nitrogen oxides (NO_x).

Zusammenfassung

Der Eintrag atmosphärischer Spurenstoffe in eine hochalpine Schneedecke kann eine Versauerung des Gletscher und des Schmelzwassers zur Folge haben. Das abfließende Schmelzwasser kann somit einen “Säureschock” in den angrenzenden Ökosystemen wie Flüssen, Seen oder Böden hervorrufen.

Die vorliegende Arbeit untersucht die Ursache der Versauerung und deren langzeitlichen Trend anhand zweier Gletscher (Goldbergkees und Wurtenkees) im Nationalpark Hohe Tauern in Österreich für den Zeitraum von 1983 bis 2011.

Nitrat (NO_3^-), Sulfat (SO_4^{2-}), Hydron (H^+), Ammonium (NH_4^+) und Calcium (Ca^{2+}) wurden als die wichtigsten Ionen in der hochalpinen Schneedecke identifiziert. Es konnte gezeigt werden, dass die Anionen zusammen mit H^+ verantwortlich für die Versauerung sind und durch NH_4^+ und Ca^{2+} neutralisiert werden.

Die Quellen für die Ionen auf den untersuchten Gletschern wurden mittels Hauptkomponentenanalyse (PCA) und der Berechnung sogenannter “non Sea Salt” Konzentrationen ermittelt. Die Berechnung ergab, dass die genannten Ionen hauptsächlich aus anthropogenen Quellen stammen. Nur Ca^{2+} konnte einer natürlichen Ursache, nämlich Saharastaubereignissen, zugeordnet werden. Weiters konnte gezeigt werden, dass Chlorid (Cl^-), Natrium (Na^+) und Kalium (K^+) nicht, wie bisher angenommen ihren Ursprung in Meersalzaerosolen haben, sondern ebenfalls anthropogen, durch die Verbrennung von Biomasse und daraus entstehenden Holzrauch sowie durch die Düngung mit Potasche, verursacht werden.

Die Langzeittrends zeigen eine signifikante Abnahme der SO_4^{2-} und H^+ Konzentrationen und Depositionen auf beiden Gletschern. Am Wurtenkees wurde außerdem auch ein signifikanter negativer Trend für NO_3^- gefunden.

Daraus lässt sich schließen, dass die Versauerung der untersuchten Gletscher und daher auch die Versauerung des Schmelzwassers rückläufig ist. Dieser Rückgang ist mit der Reduktion der Emissionen von Schwefeldioxid (SO_2) und Stickoxiden (NO_x) erklärbar.

Acknowledgments

I would like to thank Prof. Dr. Reinhold Steinacker for accepting this kind of diploma thesis, as well as Dr. Wolfgang Schöner from the ZAMG (Zentralanstalt für Meteorologie und Geodynamik) for his supervision.

Furthermore I would like to thank Dr. Anne Kasper-Giebl and Elisabeth Schreiner of the Vienna Institute of Technology for their support with the chemical analysis and the data interpretation.

Thanks to my fellow students for helping me with all the mathematical and theoretical exercises. Without them I would not have passed all these exams.

Furthermore many thanks to Prof. Dr. Diethard Mattanovich of the University of Agriculture for his constant support in providing me with the freedom required to pursue my studies alongside my work tasks.

Last, but not least I would like to thank my parents and my family for their mental support, my friends for avocation during the writing and my boyfriend Michi for proofreading and just being.

1. Introduction

The concentration of trace elements and pollutants in the atmosphere and in precipitation is highly relevant for environmental processes, such as nutrient supply to terrestrial and aquatic ecosystems [JONES ET AL., 2001]. Analysis of the chemical composition of air and precipitation allow conclusions on the contamination of atmosphere, water and soil and the influence on vegetation, animals and human beings. A look on the global hydrological cycle (Figure 1.1) reveals the interactions between the different ecosystems and reservoirs of water. The storage of water in form of ice and snow is, after the ground-water reservoir and the storage in oceans, the largest reservoir of water [WALLACE AND HOBBS, 2006]. Thus, studies of the concentrations of different ions of ice and snow are of importance for terrestrial and stream flow ecosystems, because rivers or lakes could suffer from “acid shock” through the low pH of melt water since solutes and particulates stored over the winter period are released in a relatively short time period [FILIPPA ET AL., 2010].

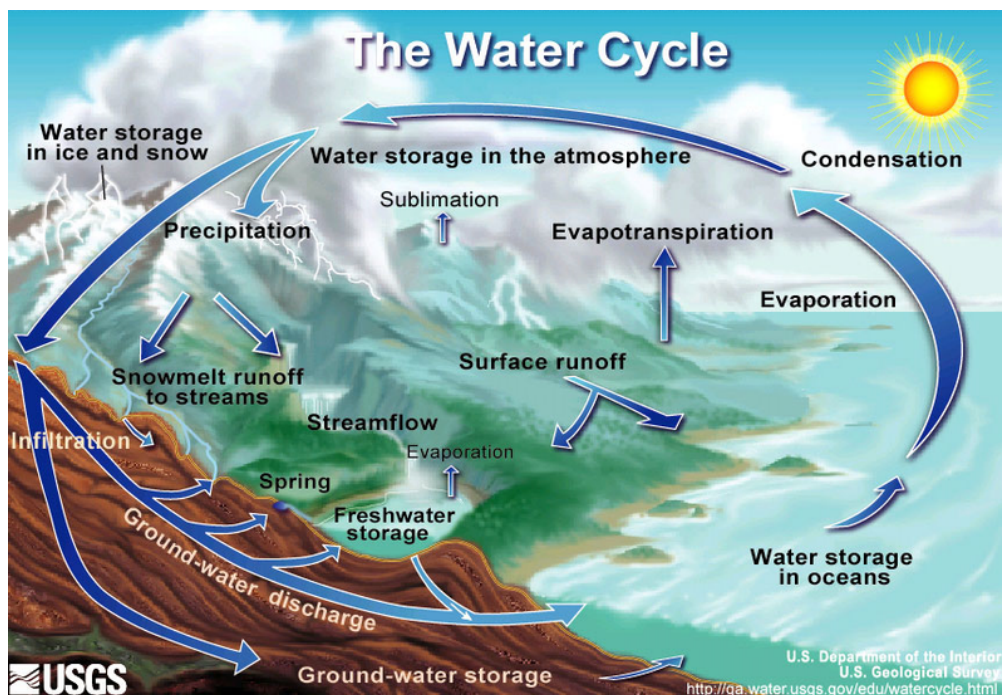


Figure 1.1.: The hydrological cycle; reveals interactions between different ecosystems and water reservoirs (Figure from the U.S. Geological Survey Homepage)

This study focuses on the snow chemistry of alpine glacier sites in the Sonnblick region (Nationalpark Hohe Tauern, Austria) with peaks higher than 3000m a.s.l. and could be described as „background monitoring stations“ in accordance with the definition of the European Environment Agency of „monitoring stations of air polluting substances, that are significant for a given region or for the globe as a whole“. For elevations higher than 3000m a.s.l. precipitation is for more than 80% solid and snow melting occurs only between May and October. Furthermore the ion concentration in the snow cover is considered to be preserved, as long as there is no melting. Thus, it is possible to determine the ionic loads which represents the total deposition for the ions during the winter accumulation period (from October to April) [AUER ET AL., 1995; SCHÖNER, 1995]. During this period, deep convection is barely present and the atmosphere is usually stably stratified. It is assumed that the top of the mixing layer lies below 3000m a.s.l. so that the air masses at higher elevations originate from remote transport as opposed to local. The snow samples therefore may be regarded as representative for the free troposphere where most of the phenomena associated with weather occur [KUHN ET AL., 1998].

Under undisturbed conditions, snow is deposited in layers which would allow a dating of the precipitation events (“snow calender”) based on the stratigraphy of the profile. This method was developed from SCHÖNER (1995) during his dissertation. Based on the information of the snow calender the origin of the “polluted” air mass can be determined. The origin could be *either continental* and thus affected mainly by anthropogenic activities (industry, agriculture, traffic) or natural sources (deserts, volcanoes) *or maritime*. The sedimentation of the pollutants is disturbed through accumulation and erosion processes due to wind with high velocities in such elevated areas. The described disturbance is a major disadvantage for the dating of the precipitation events and so also for the determination of the origin of the air mass. In contrast the already mentioned factors, such as no melting and exclusively solid precipitation during the winter accumulation period, are crucial advantages of such exposed sampling sites. SCHÖNER (1995) discussed the alteration of the ion concentration through erosion and accumulation processes and concluded that these processes play a minor role at the sampling sites analyzed in the thesis at hand, since the sites are not exposed to strong wind influence.

This work focuses on the ions in the alpine snow and aims to identify long term trends in concentrations and deposition of high alpine snow packs. Furthermore emission sources of atmospheric trace elements, their chemical composition and influence on acidity may be identified.

1.1. Ionic compounds in snow

The major ions in high alpine snow packs are known to be Chloride (Cl^-), Nitrate (NO_3^-), Sulfate (SO_4^{2-}), Ammonium (NH_4^+), Sodium (Na^+), Potassium (K^+), Calcium (Ca^{2+}), Magnesium (Mg^{2+}) and the Hydron or Proton (H^+) [JONES ET AL.,

2001]. They are incorporated to the snow cover by different mechanisms of wet, dry and occult deposition. To understand the incorporation of the ions into the snow cover, it is necessary to take a look at the physical and chemical characteristics of aerosols as well as their deposition processes (to be shown in the following chapters). LEGRAND (1987) investigated the soluble part of impurities preserved in snow and ice samples from East and West Antarctica over time periods of up to 30.000 years. He showed a very close balance between anions and cations, what suggests that nearly all ions present in Antarctic precipitation have been analyzed. This knowledge of the main constituents was adopted for glaciers, snow and ice worldwide.

Extensive studies have already been published, analyzing the chemical composition of high elevation precipitation for different regions and time periods. MAUPETIT ET AL. (1994 AND 1995) collected samples from snow cores of 4 high altitude glaciers of the French Alps from 1989 to 1991 as well as a 13m firn core below the Mont Blanc, summit drilled in 1991. Both sampling sites showed that high alpine snow is slightly acidic in absence of alkaline dust. Also KUMAI (1985) found that the acidity of snow was reduced by alkaline aerosols, fly ash and soil minerals. NICKUS ET AL. (1997) summarized the results of SNOSP, a snow sampling program in the Alps from 1991 to 1993, where a transect of up to 17 sites from the southwest French Alps to the eastern part of the Austrian Alps were analyzed. All sites showed an acidic snow cover and a neutralization through dust events. Thus, it can be concluded that high alpine snow is slightly acidic and furthermore, that the acidity is neutralized mainly by dust events and alkaline aerosols.

The temporal trends of ions in precipitation, snow and ice are of interest because conclusions on emission sources of atmospheric pollutants can be drawn from this data. RUOHO-AIROLA ET AL. (1998) reported a decrease of nearly all compounds in precipitation measured at four Finnish background stations from 1988 to 1995. SEILKOP and FINKELSTEIN (1987) published, that there is evidence of a decline in the total deposition and concentration of SO_4^{2-} , NO_3^- and H^+ in eastern North America's precipitation from 1980 to 1984. PUXBAUM ET AL. (1998) found a significant decrease of SO_4^{2-} and H^+ concentrations and depositions over a period of 10 years (1984-1993) for central Austria. AVILA (1996) found a significant decrease in SO_4^{2-} -concentration and deposition as well as an increase in the pH at a mountain site in northeastern Spain between 1983 and 1994. FISCHER and WAGENBACH (1998) analyzed ice cores from the Greenland ice sheet and documented a significant decline in SO_4^{2-} -concentration and a slight reduction of NO_3^- since the 1990s.

While the listed studies only analyzed time periods of 10 years at the most, the unique advantage of snow sampling from the Sonnblick region lies in the potential for the analysis of a long-term time period of nearly 30 years.

1.2. Aerosols

Aerosols are generally defined as the suspension of solid or liquid particles in the air. The size distribution of aerosols can be divided into three log-normal distributed modes (see Figure 1.2):

- Nucleii mode: $< 0,1\mu\text{m}$ diameter (Aitken nuclei)
- Accumulation mode: $0,1\text{--}1\mu\text{m}$ diameter (Large particles)
- Coarse particle mode: $>1\mu\text{m}$ diameter (Giant particles)

1.2.1. Sources

Mainly there are two types of aerosols in the atmosphere. Primary particles which are emitted directly, and secondary particles, which are built through chemical reactions.

Primary aerosols

Sea salt aerosols and mineral dust are the main contributors for primary aerosols. Their natural sources are the formation of sea salt aerosols generated by the bursting of bubbles on the sea surface, volcanic emissions of solid particles, mineral dust from weathering and erosion of rocks, forest fires and „living particles“ such as bacteria, spores or pollen.

Anthropogenic sources are solid particle emissions from the burning processes of oil, coal or biomass as well as traffic. On a global scale, the anthropogenic primary aerosol emissions are very low.

Primary aerosols belong to the Coarse particle mode and are exclusively giant particles.

Secondary aerosols

The main sources are anthropogenic emission gases produced in traffic, industry or agriculture such as Sulfur dioxide (SO_2), Nitrogen oxides (NO_x) or Ammonia (NH_3).

These gases act as precursors and are oxidized in the atmosphere. The most important example is the oxidation from Sulfur dioxide (SO_2) to Sulfuric acid ($\text{H}_2\text{SO}_{4(\text{gas})}$). The oxidized gases can then be deposited in the form of particles [SPIRIDINOV AND CURIC, 2005].

In situ condensation, defined as gas-to-particle-conversion, is the main process of particle formation. Gaseous molecules form particles of the dimension of Aitken nuclei through nucleation. This could happen by either homogenous nucleation, where

both molecules are in the same state of aggregation (e.g. $\text{H}_2\text{SO}_4_{(\text{gas})} + \text{H}_2\text{SO}_4_{(\text{gas})}$), or heterogeneous nucleation (e.g. $\text{H}_2\text{SO}_4_{(\text{gas})} + \text{H}_2\text{O}_{(\text{liquid})}$) where the molecules are in different phases. The Aitken nuclei coagulate among themselves, or further gases condense onto the existing molecule clusters until they reach the accumulation mode.

Estimates of the annual source strength of direct emissions and of secondary aerosol sources are summarized in Table 1.1.

Primary particle emissions		
	N-Hemisphere	Global
Sea salt [Tg/a]	1 440	3 340
Mineral dust [Tg/a]	1 800	2 150
Direct emissions of aerosol precursors		
NO_x [Tg N/a]	32	41
anthropogenic	27 (86%)	30 (75%)
natural	5 (14%)	11 (25%)
NH_3 [Tg N/a]	41	54
anthropogenic	34 (82%)	40 (75%)
natural	7 (18%)	14 (25%)
SO_2 [Tg S/a]	76	88
anthropogenic	69 (92%)	78 (89%)
natural	7 (8%)	10 (11%)
Secondary aerosol sources		
Sulfate [Tg NH_4HSO_4 /a]	145	200
natural	39	78 (39%)
anthropogenic	106	122 (61%)
Nitrate [Tg/a]	14,6	18,1
natural	2,2	3,9 (22%)
anthropogenic	12,4	14,2 (78%)

Table 1.1.: Primary particle emissions for the year 2000, source strength for emissions in the particular reference year of secondary aerosol precursors and estimates for secondary aerosol sources for the year 2000. Edited table, based on results from the Intergovernmental Panel on Climate Change (2001).

1.2.2. Sinks

The main sinks for atmospheric compounds are wet, dry and occult deposition. The effectiveness of the removal processes depend on the size distribution of atmospheric aerosols mentioned above (see Figure 1.2).

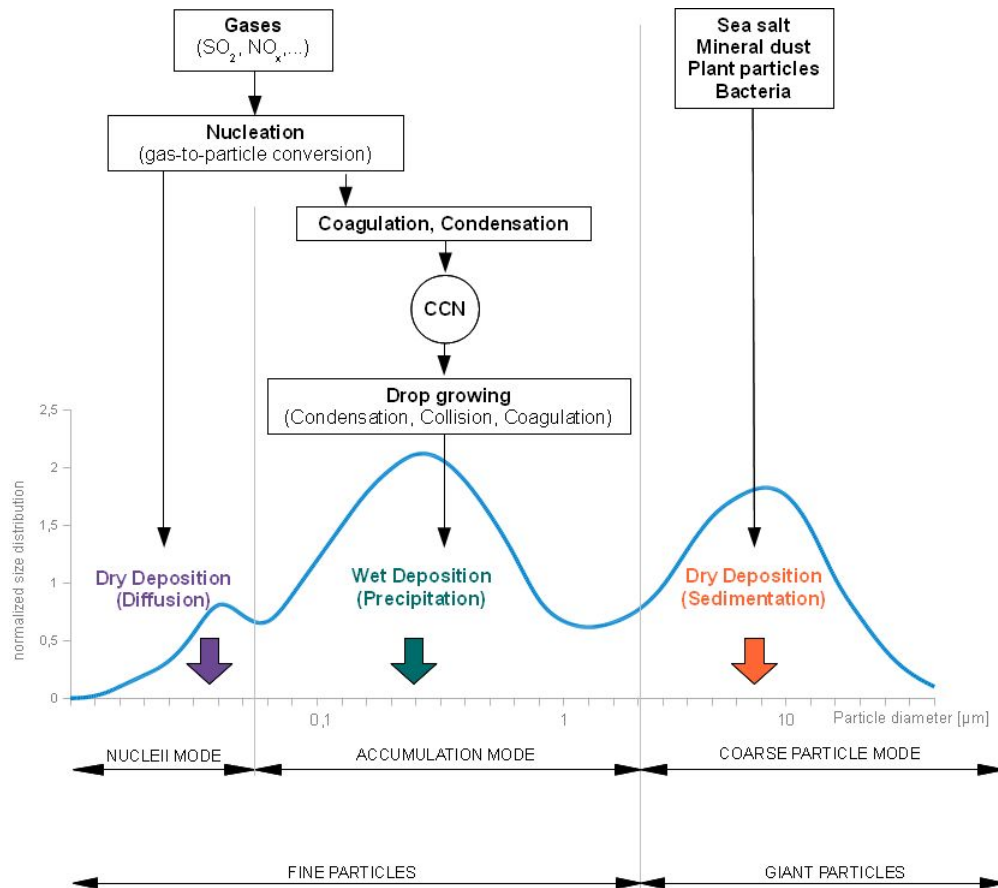


Figure 1.2.: Aerosol formation and deposition processes based on PALECZEK (1993). Small ($<0,1\mu\text{m}$) and big ($>1\mu\text{m}$) particles are deposited mainly through dry deposition processes such as diffusion and sedimentation, whereas particles between $0,1\text{--}1\mu\text{m}$ (mostly secondary aerosols) are deposited mainly through the mechanism of wet deposition.

Wet deposition

Aerosol particles of the accumulation mode act as cloud condensation nuclei (CCN) to form hydrometeors such as clouds, fog or precipitation. This happens through two different condensation effects, *either* through hygroscopic aerosols which adsorb water vapor and surround themselves with a thin water film to form a drop on which further condensation occurs *or* through soluble aerosols which reduce the saturation water pressure and advance the further condensation. These cloud droplets can be classified in “warm” and “cold” clouds, having different precipitation formation mechanisms.

In *warm clouds*, the temperature throughout the droplet is above 0°C . The drop is growing through condensation, collision and coagulation until it is big enough to precipitate. This mechanism belongs mainly to the tropical convection.

In *cold clouds*, the temperature is lower than 0°C so that a mix of ice particles

and “super-cooled” water droplets is present. Due to the saturation water pressure, which is lower over ice than over water, the air is close to saturation concerning liquid water, but is super-saturated concerning ice. This results in rapid evaporation of the “super-cooled” water droplets and rapid ice crystal growth through vapor deposition. This is known as the Bergeron-Findeisen process. The crystals can grow through ice multiplication (by bumping into each other), aggregation (at temperatures above -5°C ice crystals stick together) or accretion (ice crystals collides with “super-cooled” droplets). The ice crystals will grow large enough to precipitate. If the temperature during the way down rises above 0°C the crystals will melt and reach the ground as rain. If the melting during the fall down ceases, the crystals reach the ground as snow. The precipitation formation from “cold” clouds is most common in middle latitudes.

The wet deposition removal process is of episodic character.

Occult deposition

This includes deposition through dew, rime or hoar frost. Depending on the literature consulted occult deposition is often included in the definition of wet deposition, but for smaller droplets. Hence ion concentration is often higher and deposition is slower.

Dry deposition

This designates the deposition of aerosols and gases through sedimentation and diffusion towards the earth surface. Dry deposition is a slower process than wet deposition, but is of continuous character.

Sedimentation is most important for natural primary aerosols of the coarse particle mode. Diffusion dominates the deposition of particles of the nuclei mode.

1.3. Study Area

Snow pack samples were taken on two different sampling sites, Goldbergkees (GOK) and Wurtenkees (WUK) which are part of the Goldberggruppe in the Nationalpark Hohe Tauern (Eastern Alps, Austria, see Figure 1.3). The sampling sites are nearby the summit Hoher Sonnblick (3106m ASL), where a meteorological observatory is located. This measuring point is, since 1993, part of the "Global Atmosphere Watch" program (GAW) of the World Meteorological Organization (WMO), which is a program for the observation of the chemical composition of the atmosphere.



Figure 1.3.: Goldberggruppe, part of the Nationalpark Hohe Tauern, Eastern Alps in Austria;
Source: AMAP Austria - Bundesamt für Eich- und Vermessungswesen (BEV)

The topography of the two glaciers is shown in Figure 1.4. The orientation of the GOK sampling site is southeastward and lies on the northern side of the main ridge of the Alps. In contrast to this the WUK sampling site is orientated towards west and is located south of the main ridge of the Alps.

The different orientation and position of the sampling sites, in particular with respect to their position to the Alpine main divide, could cause differences in deposition rates and ion concentrations. Additionally a skiing region set up in 1985 on the WUK may also influence the ion deposition, due to the production of artificial snow.

The samples are taken every spring (between the end of April and the beginning of May), when the winter accumulation period is approximately maximized. At the WUK snow pack analysis are being performed since 1983, at the GOK since 1987.¹

¹year dates correspond to the year where the samples were taken

1.3 Study Area

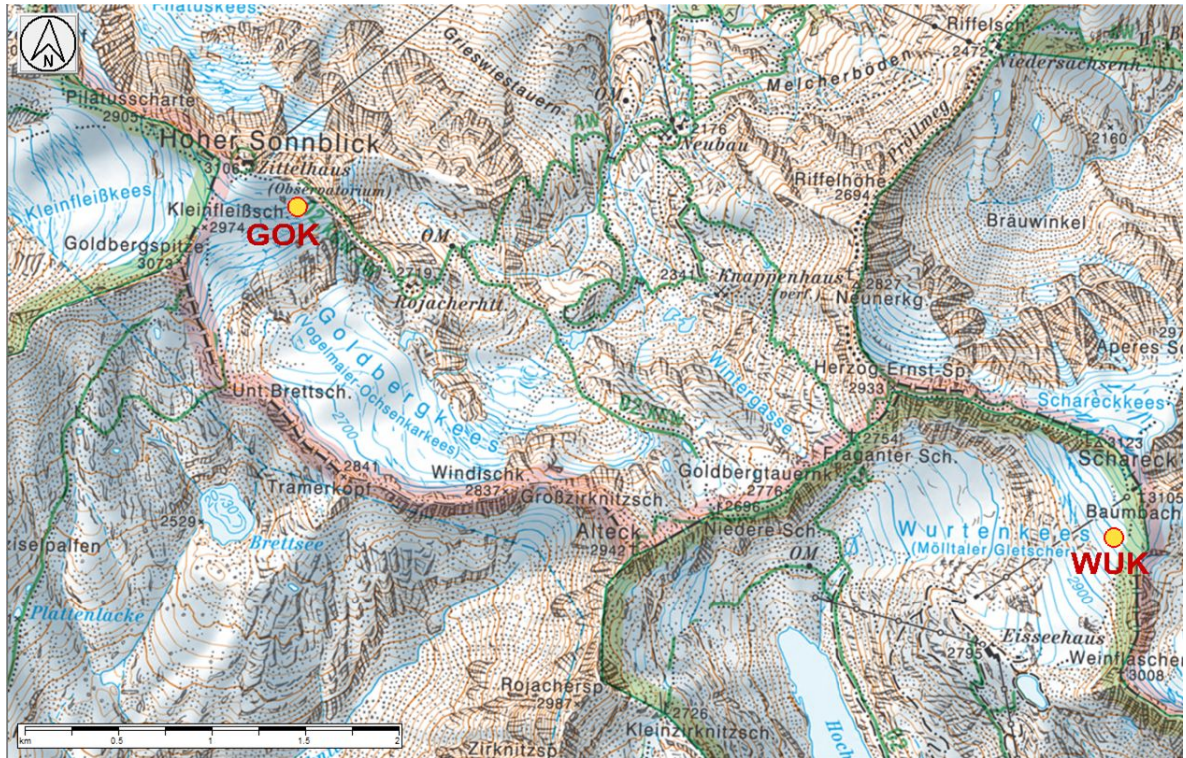


Figure 1.4.: Yellow dots represent the sampling sites on Goldbergkees (GOK) and Wurtenkees (WUK) in the Eastern Alps, Austria; Source: AMAP Austria - Bundesamt für Eich- und Vermessungswesen (BEV)

2. Methods

2.1. Snow Sampling

Snow pits down to last year's horizon have been excavated. Then samples were taken with a 10x5cm stainless steel cylinder to get values of 10cm increments over the whole profile. To avoid contamination of the samples gloves and a mask have been worn throughout the sampling. The samples were stored in small polyethylene plastic bags and were kept frozen throughout transport to the Institute of Analytic Chemistry at the Technical University in Vienna (TU). From 1983 until 1986 samples from more than one pit were collected [VITOVEC, 1988]. The different sampling techniques are listed in Table 2.1, whereas Table 2.2 summarizes the profile depth, water equivalent values and the number of samples for every year.

Besides the sampling, the snow profile was stratigraphically described using the „International Classification for Seasonal Snow on the Ground“ [COLBECK, 1985] and the temperature was measured every 10cm.

This kind of sampling was tested and established during SNOSP, a sub project of ALPTRAC [SCHWIKOWSKI ET AL., 1997], and has already been thoroughly described in the appropriate literature (e.g. see literature mentioned above).

Year	
1983-1986	<ul style="list-style-type: none">• sampling directly in plastic bottles without steel cylinder [VITOVEC, 1988]• samples from more than one pit, but from the same depth, were averaged to get a notional profile for every year
1987-1996 and 1998-2011	sampling as described in the text above
1997	different sample volume (GOK 40cm and WUK 50cm), samples stored in plastic bottles
1989 and 1990	density profile normalized with WUK profile because no data available for GOK
2005	abort of sampling on GOK at 380cm due to bad weather condition
2008	abort of sampling on GOK at 360cm due to bad weather condition

Table 2.1.: Sampling methods used in the particular years

	Goldbergkees			Wurtenkees		
	depth [cm]	water eq. [mm]	# samples	depth [cm]	water eq. [mm]	# samples
1983	-	-	-	360	1360	73
1984	-	-	-	320	910	99
1985	-	-	-	300	1120	120
1986	-	-	-	280	1170	97
1987	436	1684	44 ^{a)}	320	1089	33
1988	286	1084	27	310	1292	30
1989	410	1569	42	410	1569	41
1990	380	1564	38	225	918	23
1991	282	1039	29	320	1037	32
1992	312	1144	31	382	1548	38
1993	360	1300	36	343	1261	34
1994	340	1296	35	300	1172	30
1995	560	2115	56	445	1720	45
1996	240	900	23	253	1016	25
1997	720	2703	18 ^{c)}	532	2021	11 ^{c)}
1998	320	1244	32	386	1550	38
1999	493	2084	49	389	1477	39
2000	443	1902	44	500	2205	50
2001	410	1439	40 ^{b)}	343	1230	34
2002	473	1954	47	420	1599	42
2003	420	1681	42	375	1373	37
2004	365	1573	36	338	1331	33
2005	460	1872	38 ^{c)}	398	1620	39
2006	358	1416	36	300	1355	30
2007	218	1027	21	199	938	20
2008	500	1957	36 ^{c)}	490	1958	49
2009	589	2306	58	450	1731	44
2010	390	1707	39	229	845	22
2011	302	1343	30	280	1221	27

Table 2.2.: Snow pit depth, water equivalent and number of samples for both sampling sides and all years from 1983-2011

a) first sample from 5-15cm

b) sample for 120cm missing but two samples for 80cm

c) see Table 2.1 for sampling methods in the particular years

2.2. Chemical Analysis

The samples were melted at room temperature and than aliquoted for different measurements (pH, conductivity and ion concentrations). H^+ concentrations were

calculated from the definition of the pH value:

$$pH = -\log(c_{(H^+)})$$

The pH and the conductivity were measured using the following instruments (see Table 2.3):

Instrument	METTLER Toledo MPC 227
pH-electrode	METTLER Toledo Pure Pro pH 1...11/0-80°C
Conductivity-electrode	METTLER Toledo 720 Conductivity NTC, 0-500µS, 0-100°C

Table 2.3.: pH and conductivity instruments

The ion concentrations were measured using Ion chromatography (IC). The following instruments and adjustments were used (see Table 2.4):

Instrument	DIONEX ICS-3000
Autosampler	KNAUER Smartline 3800
Suppressor	DIONEX CSRS 4mm
Column	CS 12A
Detector	Conductivity detector
Eluent	MSA 12mM
Flow	1 ml/min
Software	Chromeleon Version 6,80 SP4 Build 2361

Table 2.4.: Instruments and adjustments of Ion chromatography

The detection limits of the different ions are listed in Table 2.5, compared with the limits reported by VITOVEC (1988). The technical advance is obvious and the detection limits are 5-10 times smaller than decades ago.

Anions	[ppm]	Cations	[ppm]	Anions	[ppm]	Cations	[ppm]
Cl ⁻	0,005	Na ⁺	0,010	Cl ⁻	0,02	Na ⁺	0,05
NO ₃ ⁻	0,004	NH ₄ ⁺	0,004	NO ₃ ⁻	0,1	NH ₄ ⁺	0,05
SO ₄ ²⁻	0,008	Ca ²⁺	0,004	SO ₄ ²⁻	0,1	Ca ²⁺	-
		Mg ²⁺	0,003			Mg ²⁺	-
		K ⁺	0,023			K ⁺	0,1

Table 2.5.: Comparison of limits of detection for the particular ions reported by SCHREINER (2011) (left) and VITOVEC (1988) (right)

The described settings are valid for the years 2010 and 2011 at the least [SCHREINER, 2011].

2.3. Measure Units and Statistical Analysis

Ion concentrations are stated in volume weighted $\mu\text{eq/l}$. The following formulas have been used for calculation:

$$c [\mu\text{eq/l}] = \frac{c [\text{mg/l}] * z * 1000}{M} \qquad c_w [\mu\text{eq/l}] = \frac{c [\mu\text{eq/l}] * WE}{\text{Mean} [WE]_{\text{Profile}}}$$

Deposition is described in meq/m^2 :

$$\text{dep} = \text{Mean} [c_w]_{\text{Profile}} * \text{Mean} [WE]_{\text{Profile}}$$

c.....concentration c_wweighted concentration z.....valence
M.....molar mass WE...water equivalent

Statistical analysis has been performed using R-scripts (*The R Project for Statistical Computing*). The long time trends were calculated with the Mann-Kendall-Test, which is based on ranks within the time series to identify and quantify significant monotonic trends. Therefore the R package *Kendall* and the function *Seasonal-MannKendall* was used. Correlations are expressed by the Spearman rank correlation coefficient included in the R package *stats*, avoiding overemphasizing of extreme values. These statistical parameters are widely used in environmental studies because they are nonparametric, which means they can be used without an assumption of the probability distribution of the data. Most of the other statistical parameters, such as the Pearson correlation coefficient, postulate a normal distribution of the data.

2.4. Analytical Quality Control

Ion balance and the comparison of measured with calculated electric conductivity were used to check the analytical quality of the data. This kind of quality control is described in detail in the appropriate literature [AUER ET AL., 1995; AVILA, 1996; MAUPETIT AND DELMAS, 1994; NOVO AND ROSSI, 1998; PUXBAUM ET AL., 1998; WINIWARTER ET AL., 1998].

2.4.1. Ion Balance

The ion balance was calculated using the following formula:

$$\sum \text{Anions} - \sum \text{Cations} = \Delta \text{Ions}$$

Under the assumption of electro neutrality, $\Delta Ions$ must be zero and the sums must equal.

Samples from both glaciers, for which concentrations of all ions are available, showed an excess of cations ($\Delta Ions$ negative) for 90% of the samples (see Figure 2.1). This can be explained by the not measured carboxylic acids and organic anions (e.g. $HCOO^-$, HCO_3^- , CH_3COO^-) [MAUPETIT AND DELMAS, 1994; MAUPETIT ET AL., 1995, PUXBAUM ET AL., 1998]. The same result is achieved if both glaciers are evaluated separately.

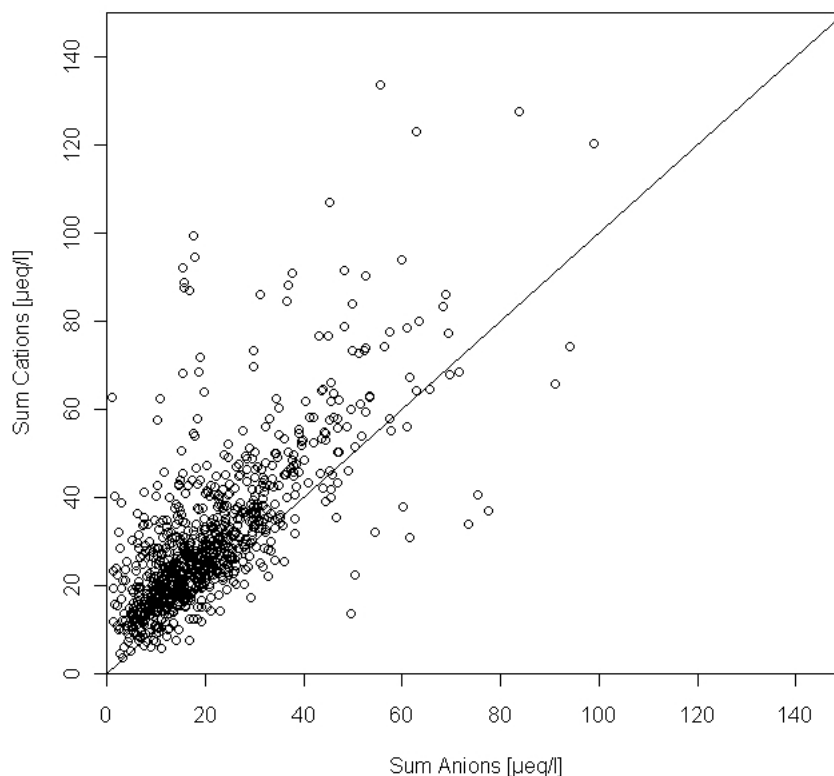


Figure 2.1.: Ion balance of samples from WUK and GOK for the period of 1983-2011 were concentrations of all ions are available. A cation excess is observed due to not measured carboxylic acids and organic anions.

The correlation of the sum of anions and sum of cations is determined, using the Spearman correlation coefficient. Results considering both glaciers together, as well as for the single sampling sites are given in Table 2.6. The observed correlation is approximately 0,7.

If a Mann-Kendall-test is performed to analyze the temporal trend, a significant decrease for anions can be found in all three data sets from 1983-2011. Correspond-

ingly also the $\Delta Ions$ shows a significant decrease in all data sets from 1983-2011. The trend of the cations is not as significant as the trend of the anions or even does not show any significance at all.

		Spearman	τ
WUK&GOK	$\Delta Ions$	0,730	-0,161 ^{c)}
	$\sum An$	-	-0,135 ^{c)}
	$\sum Cat$	-	0,058 ^{a)}
WUK	$\Delta Ions$	0,768	-0,156 ^{c)}
	$\sum An$	-	-0,262 ^{c)}
	$\sum Cat$	-	-0,092 ^{b)}
GOK	$\Delta Ions$	0,708	-0,228 ^{c)}
	$\sum An$	-	-0,118 ^{c)}
	$\sum Cat$	-	n.s.

Table 2.6.: Spearman Correlation coefficient and Kendall Trend Analysis of the Ion balance for the sites analyzed from 1983-2011; Significance levels: ^{a)} $p < 0,05$; ^{b)} $p < 0,01$; ^{c)} $p < 0,001$; n.s. = not significant

2.4.2. Measured vs. Calculated Conductivity

In aqueous solutions the conductivity is composed of the contribution of the single ions, which can be calculated with the equivalent conductivity Λ_0 , a material constant. For every single ion the conductivity is calculated using the following formula and summarized afterwards.

$$\Lambda_{calculated} = \frac{c[mg/l]}{M[g/mol]} * \Lambda_0[Scm^2/mol]$$

Ion	Na ⁺	K ⁺	Cl ⁻	$\frac{1}{2}$ SO ₄ ²⁻	NO ₃ ⁻	NH ₄ ⁺	$\frac{1}{2}$ Ca ²⁺	$\frac{1}{2}$ Mg ²⁺	H ⁺
$\Lambda_0[Scm^2/mol]$	50,1	73,5	76,8	80,0	71,5	73,6	59,5	53,1	349,5

Table 2.7.: Equivalent Conductivity Λ_0 used for the calculation of the conductivity

Analogous to the ion balance, the conductivity balance can be calculated with the subsequent formula:

$$\Lambda_{measured} - \Lambda_{calculated} = \Delta Conductivity$$

The measured conductivity values are higher than the calculated values for 80% of the samples, displayed in Figure 2.2. Here, the difference perhaps be explained with carboxylic acids and organic compounds gathered in the conductivity measurement, but not included in the calculation of the conductivity.

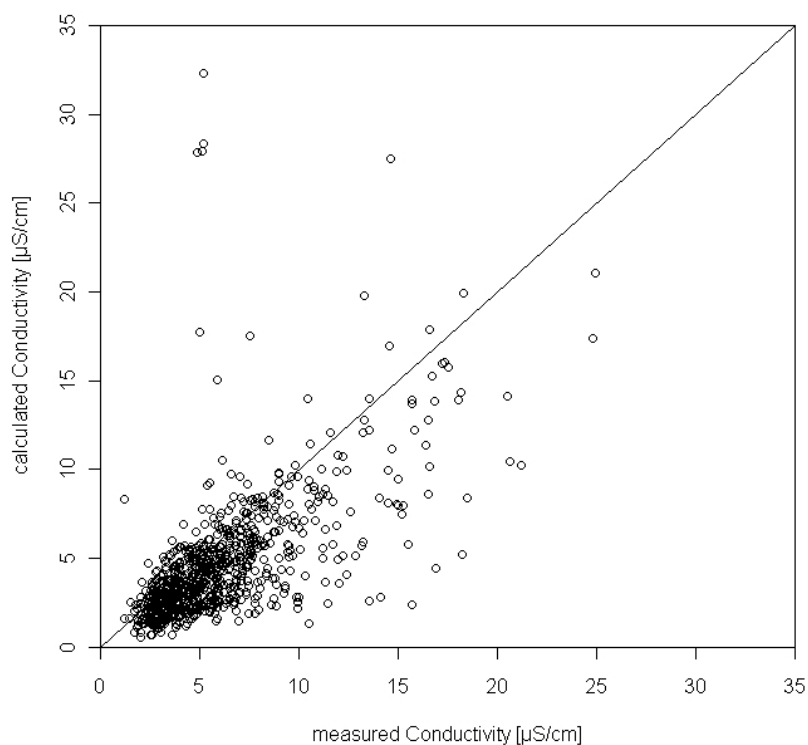


Figure 2.2.: Measured vs. calculated Conductivity of samples from WUK and GOK for the period of 1983-2011 where concentrations of all ions are available. Measured conductivity showed higher values than the calculated one, perhaps due to carboxylic acids and organic anions not included in the calculation.

The data sets used for the ion balance were also used for the calculation of correlation coefficients and trends of the conductivity balance. No significant trends are observed and the correlation of approximately 0,7 is comparable to the ion balance (also approximately 0,7).

WUK & GOK	WUK	GOK
0,698	0,718	0,677

Table 2.8.: Spearman correlation coefficients of measured and calculated Conductivity for both sampling sites from 1983-2012

The main source of errors or a further explanation of differences in the ion and conductivity balance is associated with H^+ . This concentration is calculated from the pH measurements and has a major influence on the sum of the cations. Furthermore H^+ has a very high equivalent conductivity, meaning it provides a high contribution to total conductivity (see Table 2.7). Thus the pH measurement has an important influence on ion and conductivity balance but has a high uncertainty of 0,1-0,2 pH units [AUER ET AL., 1995].

2.5. Spatial Variability and Representativeness

To see if the values for the ion concentrations are representative for a specific region, here the Sonnblick region including both sampling sites WUK and GOK, the spatial variability and the representativeness of the measurements were determined from the results of previous studies summarized in Table 2.9. Parts of this summary have already been published from STAUDINGER ET AL. (1997).

The notation of the scales used in this chapter is different from the common meteorological definition. Here Microscale denotes horizontal distances from 10cm to 1m, Mesoscale horizontal distances from 10m to 1km and Macroscale horizontal distances of more than 10km. The meteorological classification denotes horizontal distances of less than 2km as Microscale, horizontal distances between 2km to 2000km as Mesoscale and horizontal distances between 2000km to 10 000km as Macroscale.

2.5.1. Analytic representativeness

SCHWIKOWSKI ET AL. (1997) summarized two laboratory and two field intercomparison programs in order to investigate the seasonal and geographical distribution of ion concentrations in the Alps.

The laboratory intercomparison programs were performed in the winter of 1991 and in the spring of 1992, with eight and nine participating laboratories respectively. For the first program two standards (HCl and a mixture of NaCl, $NaNO_3$ and Na_2SO_4) had to be analyzed, whereas in the second one a homogenous surface sample collected at Untersberg (Salzburg, Austria) was distributed among the different groups. The laboratory intercomparison showed high agreement between the different groups revealing standard deviations of 3-13% for the anions and higher variations (11-40%) for the cations. The generally larger relative standard deviations for cations was explained with less experience in methods of cation analysis of some laboratories. Additionally the accuracy of the pH measurement has to be concerned, especially regarding H^+ .

The field intercomparison studies, each with six participating groups, were performed at Daunferner in 1989, where samples were collected from pits dug separately

Type	Na ⁺	K ⁺	Cl ⁻	SO ₄ ²⁻	NO ₃ ⁻	NH ₄ ⁺	Ca ²⁺	Mg ²⁺	H ⁺	Year/Site	Reference
Analytic	-	-	3	-	-	-	-	-	-	1991/Standard	SCHWIKOWSKI ET AL. (1997)
	-	-	13	7	13	-	-	-	-	1991/Standard	SCHWIKOWSKI ET AL. (1997)
	23	33	12	10	5	11	-	-	40	1992/Untersberg (A)	SCHWIKOWSKI ET AL. (1997)
	-	-	69	17	22	16	-	-	-	1989/Daumferner (A)	SCHWIKOWSKI ET AL. (1997)
	40	67	15	8	9	11	38	45	47	1993/Weissfluhjoch (CH)	SCHWIKOWSKI ET AL. (1997)
	12	50	10	14	10	9	13	63	70	1993/Weissfluhjoch (CH)	SCHWIKOWSKI ET AL. (1997)
	17	67	8	8	3	7	11	24	58	1993/Weissfluhjoch (CH)	SCHWIKOWSKI ET AL. (1997)
Microscale			38	28	24				26	1983-85/Wurtenkees (A)	WINIWARTER ET AL. (1998)
	29		25	9	14	27			15	1988/Wurtenkees (A)	WINIWARTER ET AL. (1998)
	-	-	79	6	15	-	-	-	-	1992/Daumferner (A) ^{a)}	NICKUS AND KUHN (1993)
	-	-	60	11	21	-	-	-	-	1992/Daumferner (A) ^{b)}	NICKUS AND KUHN (1993)
	-	-	39	21	13	-	-	-	-	1992/Daumferner (A) ^{c)}	NICKUS AND KUHN (1993)
	57	-	7	3	1	2	-	27	-	1991/Goldbergkees (A)	SCHÖNER 1995
Mesoscale	50	-	41	12	15	21	56	17	-	1992/Goldbergkees (A)	SCHÖNER 1995
	12	-	27	17	17	4	12	10	-	1991/La Grave (F)	SCHÖNER 1995
Macroscale	110	66	53	31	40	34	51	70	56	1991/Alps	NICKUS ET AL. (1997)
	86	46	77	28	42	29	120	70	79	1992/Alps	NICKUS ET AL. (1997)
	39	55	22	43	40	45	79	144	39	1993/Alps	NICKUS ET AL. (1997)

Table 2.9.: Summary of the analytical and spatial coefficients of variation; bold values are used to calculate the total variability with the Gaussian error propagation (see Chapter 2.5.5); ^{a)} samples taken at grid distances of 10cm in a rectangle of 60x50cm; ^{b)} 20 samples in a vertical line at distances of 1m; ^{c)} 24 samples in a vertical line at distances of 10m

one beside the other *and*, at Weissfluhjoch in 1993 where samples were collected by each group individually within a joint snow pit in a distance of 1m between the sampling positions. The variation for NO_3^- , SO_4^{2-} and NH_4^+ were reasonable, whereas the one for Cl^- showed very high discrepancy. This was interpreted with either contamination during sampling with sweat or analytical problems.

Furthermore two snow samples from the profile at Weissfluhjoch (surface and 1m depth) were distributed between the participating groups and analyzed individually. The agreement was good for the anions as well as for NH_4^+ but less satisfying for the other cations. The results of these sampling are in general agreement with the laboratory intercomparison and represent the analytical capabilities of the laboratories.

2.5.2. Microscale variability (10cm to 1m)

WINIWARTER ET AL. (1998) describes the investigation on the reliability and therefore analyzed multiple samples in one pit on WUK. From 1983 to 1988 3-5 samples have been taken from certain depth whereas in 1988 replicate samples over the whole profile have been taken. The results indicated that the variation within a glacier is larger than the sampling induced uncertainty. WINIWARTER ET AL. (1998) referred that this may indicate variations by “natural differences” such as snow erosion and accumulation processes. Snow from one event (possibly with higher concentrations) may be accumulated stronger at one site of the glacier than another.

NICKUS AND KUHN (1993) took surface snow samples from the uppermost 30cm at Daunferner in 1992. 42 of these samples were taken at grid distances of 10cm in a rectangle of 60x50cm^{a)}, 20 samples in a vertical line at distances of 1m^{b)} and 24 samples in a vertical line at distances of 10m^{c)}. For SO_4^{2-} and NO_3^- the local variability was small, but very high for Cl^- which is explained by values close to the detection limit.

SCHÖNER (1995) compared 3 parallel samples of 10cm increments over the whole depth from one pit at Goldbergkees in 1991. He found, that the variability in the single layers is very high because it is difficult to always sample the exact same layer. In contrast, the variations of the mean weighted concentrations over the whole profile are very low.

2.5.3. Mesoscale variability (10m to 1km)

SCHÖNER (1995) summarized the analysis of 4 snow pits on the Goldbergkees in 1992 and 3 profiles at La Grave (France) in order to investigate the regional representativeness. The snow pits in the particular region were situated approximately 500m apart. High variabilities were achieved for Cl^- , Na^+ and Ca^{2+} . The latter one can be interpreted with the high local variability of dry deposition of Saharan dust,

the main source for Ca^{2+} in the Alps [DE ANGELIS AND GAUDICHET, 1991]. The relative standard deviations for SO_4^{2-} , NO_3^- and NH_4^+ are reasonable. Furthermore the anion composition showed good accordance within the respective regions.

2.5.4. Macroscale variability (>10km)

NICKUS ET AL. (1997) compared the results of up to 17 sampling sites at different glaciers in the Alps and found that ion concentrations show a West to East increase in weighted mean concentrations. Only Calcium showed an reversed distribution with higher concentrations in the west. For most of the ions high variabilities were observed with high annual variations. Only for SO_4^{2-} , NO_3^- , NH_4^+ and Mg^{2+} the annual variation is comparatively small.

2.5.5. Conclusion on the spatial variability of the ion concentration in the snow

Based on the results of the analytic and mesoscale variability (variabilities used are bold in Table 2.9) a total variability for the ion concentrations can be calculated with the Gaussian Error Propagation [SCHÖNER, 1995]. This kind of error calculation is necessary because the error of the analytic measurements and the spatial variability summarize. The results for the individual ions are given in Table 2.10.

Na^+	K^+	Cl^-	SO_4^{2-}	NO_3^-	NH_4^+	Ca^{2+}	Mg^{2+}	H^+
51	61	41	12	15	22	56	17	58

Table 2.10.: Total variability [%] calculated with the Gaussian error propagation from the analytic and mesoscale variability marked bold in Table 2.9

The total variability of SO_4^{2-} , NO_3^- , NH_4^+ and Mg^{2+} is relatively low with values between 12% and 22%. For the other ions the total variability is higher than 40%. For Cl^- and Na^+ the possible contamination with sweat has to be regarded which could falsify the results of the concentrations. The high variability of Ca^{2+} could be explained with the local different dry deposition, which is the main deposition mechanism. For K^+ and H^+ no mesoscale variability is available. Thus, the value in Table 2.9 for these ions accounts only for the analytical variability, which is already very high since the pH measurement has a high measurement error with 0,1-0,2 pH units and the concentration of K^+ is near the limit of detection.

The variability, especially for SO_4^{2-} , NO_3^- and NH_4^+ , is with variabilities between 12-22% acceptable compared to the cost, time and material investments. The listed ions are known to be the main ions influencing the acidification and neutralization of high alpine snow packs.

The result of the analysis of the uncertainty is, that the ion concentrations measured on the sampling sites WUK and GOK can be regarded representative for the Sonnblick region. Furthermore, information on the signal-to-noise ratio was obtained, giving the information if trends in the time series are significant or not. This result is very important for the time trend analysis of acidity and the comparison between the two glaciers [SCHÖNER, 1995].

3. Source Analysis

3.1. Chemical Composition of the snow based on ion concentrations

The general composition of high alpine snow was described in the introduction. Figure 3.1 shows the mean ion composition of the two glaciers analyzed in this thesis. The values are based on the weighted mean concentrations of all snow layers from 1983 to 2011 when all ions have been measured. Primary ions, contributing the main part of the ion composition, are SO_4^{2-} , NO_3^- , H^+ , NH_4^+ and Ca^{2+} , whereas secondary ions are Cl^- , Na^+ , Mg^{2+} and K^+ .

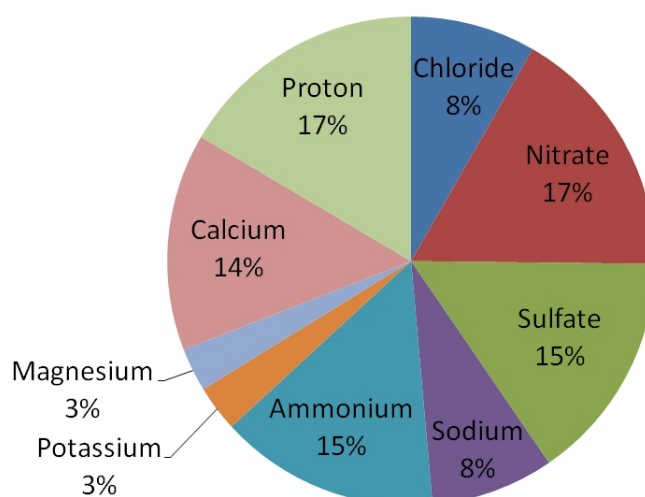


Figure 3.1.: Mean ion composition of the snow cover of the analyzed sites based on the ion concentrations

The correlation matrix with the Spearman correlation coefficient is given in Table 3.1 and shows if two ions are linked or not. The correlation coefficient is used as advanced information regarding the origin of the single ions and is a widely used method [AUER ET AL., 1995; FILIPPA ET AL., 2010; MAUPETIT AND DELMAS, 1994; WILLEY AND KIEFER, 1990; WINIWARTER ET AL., 1998].

	K ⁺	Na ⁺	Cl ⁻	SO ₄ ²⁻	NO ₃ ⁻	NH ₄ ⁺	Ca ²⁺	Mg ²⁺	H ⁺
K ⁺	1	0,763	0,631	0,130	0,043	-0,024	0,270	0,365	0,022
Na ⁺		1	0,796	0,115	0,101	0,102	0,323	0,352	-0,075
Cl ⁻			1	0,339	0,261	0,154	0,340	0,349	0,080
SO ₄ ²⁻				1	0,626	0,541	0,219	0,382	0,428
NO ₃ ⁻					1	0,544	0,204	0,226	0,374
NH ₄ ⁺						1	0,155	0,165	0,085
Ca ²⁺							1	0,477	-0,203
Mg ²⁺								1	0,008
H ⁺									1

Table 3.1.: Spearman correlation matrix including ion concentrations of both sampling sites from 1983-2012

A high correlation between Na⁺ and Cl⁻ occurs, and is assumed to have maritime origin. K⁺ is supposed to have a high correlation with Na⁺ and Cl⁻ because of similar chemical reactivity to Na⁺ in the atmosphere but is generally assigned to dust events. NO₃⁻ and SO₄²⁻ are correlated with H⁺ because these ions are presumed to be responsible for the acidity by forming either Nitric (HNO₃) or Sulfuric acid (H₂SO₄) [MAUPETIT AND DELMAS, 1994]. NH₄⁺ is related with SO₄²⁻ and NO₃⁻ because for all three an anthropogenic source is assumed. Mg²⁺ is linked with Ca²⁺, which are supposed to share a common origin from dust events. Ca²⁺ is negatively correlated with H⁺, which is obvious because it is supposed to be a neutralizing compound. Thus, from the correlation matrix the assumption for the following different sources is comprehensible:

1. sea salt origin for Cl⁻, Na⁺
2. anthropogenic origin for NO₃⁻, SO₄²⁻ and NH₄⁺
3. origin from dust events for Ca²⁺, Mg²⁺ and K⁺

These or similar clusters have already been published in e.g. SCHÖNER (1995).

3.2. Principal Component Analysis

To validate the assumptions made above, a Principal Component Analysis (PCA) with varimax rotation was performed using the R package *psych* and the function *principal()*. This method is often used for the evaluation of sources of the ion content in the snow cover and precipitation in general [FILIPPA ET AL., 2010; MAUPETIT AND DELMAS, 1994; SCHÖNER, 1995; WILLEY AND KIEFER, 1990]. The PCA uses an orthogonal transformation to transform a set of observations of possibly correlated variables into a set of linearly uncorrelated variables called principal components or factors. So, the possibly correlated ion concentrations are

grouped in uncorrelated principal components, where each component accounts for a different source region.

The two examined sampling sites are either considered jointly or separately in the PCA and the calculation was performed using either 3 or 4 factors *and* including or excluding the H^+ concentrations. The data set consists of weighted concentrations of the ions in all layers measured in the period from 1983 to 2011.

Excluding H^+ , the same results were obtained if both sampling sites were taken into account (see Table 3.2) or when both sites were considered separately. Factor 1 is loaded with the Cl^- , Na^+ (corresponding to the maritime cluster) and K^+ , factor 2 with NO_3^- , SO_4^{2-} and NH_4^+ (anthropogenic ions) and factor 3 with Ca^{2+} and Mg^{2+} (dust events but without K^+). 77% of the total variance can be explained with three factors excluding H^+ .

	F1	F2	F3	Commonality ^{a)}
Cl^-	0,95	0,10	0,12	0,92
NO_3^-	0,00	0,82	0,02	0,67
SO_4^{2-}	0,11	0,79	0,16	0,66
Na^+	0,94	0,01	0,12	0,90
NH_4^+	0,00	0,84	0,00	0,71
K^+	0,91	0,01	0,09	0,84
Mg^{2+}	0,15	0,07	0,84	0,74
Ca^{2+}	0,08	0,06	0,86	0,75

	F1	F2	F3
SS loadings ^{b)}	2,65	2,03	1,51
Proportion Var. ^{c)}	0,33	0,25	0,19
Cumulative Var. ^{d)}	0,33	0,58	0,77

Table 3.2.: PCA WUK and GOK excl. H^+ and 3 factors

a) Sum of the squared factor loads in one row

b) Sum of the squares of the factor loads in one column.

c) SS loadings divided through the number of variables which is the variance explained through this factor.

d) Cumulative part of the explained variances

For 4 factors excluding H^+ different results were obtained whether looking at both sites jointly or separately. In Table 3.3 the result for the data set including both sampling sides can be seen. F1, F2 and F3 are loaded with the same ions as before. Considering both sites Factor 4 is loaded with SO_4^{2-} and Mg^{2+} . 84% of the total variance can be explained with four factors excluding the H^+ . Considering only GOK F4 is loaded with Ca^{2+} , whereas for WUK F4 is loaded with NH_4^+ and NO_3^- (Tables see Appendix B.1 and B.2).

	F1	F2	F3	F4	Commonality
Cl ⁻	0,95	0,09	0,07	0,08	0,92
NO ₃ ⁻	0,02	0,85	0,18	-0,21	0,81
SO ₄ ²⁻	0,10	0,73	-0,08	0,51	0,82
Na ⁺	0,94	0,01	0,10	0,03	0,90
NH ₄ ⁺	0,00	0,84	-0,02	0,09	0,71
K ⁺	0,91	0,00	0,04	0,07	0,84
Mg ²⁺	0,15	0,00	0,56	0,71	0,84
Ca ²⁺	0,10	0,07	0,93	0,12	0,89

	F1	F2	F3	F4
SS loadings	2,67	1,98	1,23	0,85
Proportion Var.	0,33	0,25	0,15	0,11
Cumulative Var.	0,33	0,58	0,73	0,84

Table 3.3.: PCA WUK and GOK excl. H⁺ and 4 factors

If **H⁺ is included** in the PCA F1, F2 and F3 are again loaded with the same ions as before and H⁺ is accredited to the anthropogenic factor (see Table 3.4). 71% of the total variance can thus be explained. These factor loads are also achieved if the glaciers are considered separately.

	F1	F2	F3	Commonality
Cl ⁻	0,95	0,11	0,11	0,92
NO ₃ ⁻	0,00	0,79	0,07	0,64
SO ₄ ²⁻	0,12	0,81	0,15	0,70
Na ⁺	0,94	0,00	0,12	0,90
NH ₄ ⁺	-0,02	0,76	0,11	0,59
K ⁺	0,91	0,00	0,09	0,84
Mg ²⁺	0,16	0,08	0,81	0,68
Ca ²⁺	0,09	0,04	0,86	0,74
H ⁺	0,03	0,54	-0,31	0,39

	F1	F2	F3
SS loadings	2,66	2,18	1,55
Proportion Var.	0,30	0,24	0,17
Cumulative Var.	0,30	0,54	0,71

Table 3.4.: PCA WUK and GOK incl. H⁺ and 3 factors

With 4 factors, H⁺ is attributed with SO₄²⁻ in a separate factor (see Table 3.5) whereas the other factor loads are the same as before. 81% of the total variance can thus be explained.

One exception is given for GOK including H^+ and 4 factors. Here F4 is loaded with H^+ , SO_4^{2-} and NO_3^- , but the loads of the last two ions are very low (Table see Appendix B.2).

	F1	F2	F3	F4	Commonality
Cl^-	0,95	0,08	0,12	0,07	0,92
NO_3^-	0,01	0,81	0,03	0,15	0,67
SO_4^{2-}	0,11	0,70	0,19	0,40	0,71
Na^+	0,94	0,02	0,11	-0,04	0,90
NH_4^+	0,01	0,89	0,00	-0,11	0,81
K^+	0,91	0,01	0,08	-0,01	0,84
Mg^{2+}	0,15	0,04	0,85	0,06	0,75
Ca^{2+}	0,08	0,08	0,85	-0,11	0,75
H^+	-0,01	0,15	-0,08	0,95	0,94

	F1	F2	F3	F4
SS loadings	2,66	1,98	1,52	1,13
Proportion Var.	0,30	0,22	0,17	0,13
Cumulative Var.	0,30	0,52	0,68	0,81

Table 3.5.: PCA WUK and GOK incl. H^+ and 4 factors

Hence, the above clustering could be verified with the PCA, with one exception. K^+ is not associated to dust events, but to the maritime factor, together with Cl^- and Na^+ . The factor with the highest explained variance for the ions at the analyzed sampling sites is the maritime factor, followed by the anthropogenic (NO_3^- , SO_4^{2-} , NH_4^+) and dust event cluster (Ca^{2+} , Mg^{2+}).

3.3. Non sea salt proportion

The result, that the maritime factor dominates in the region examined, is surprising. As Austria is in Central Europe, it could be expected that the anthropogenic induced ions dominate. For example even for snow packs in the Aosta Valley in the Italian Alps, where the influence of the Atlantic should be greater than in Austria, the maritime factor is nondominant [FILIPPA ET AL., 2010]. Also for the French Alps, the maritime factor does not dominate over the anthropogenic one [MAUPETIT AND DELMAS, 1994].

Assuming that all the Cl^- or Na^+ in the snow samples originate from sea salt the non sea salt (nSS) proportion of the single ions can be calculated based on the chemical composition of seawater (see Figure 3.2). The ratio between the concentration of the specific ion and the concentration of either Cl^- or Na^+ in sea water is used. This method was often described [FISCHER AND WAGENBACH, 1998; MAUPETIT AND DELMAS, 1994; WILLEY AND KIEFER, 1990].

$$nSS\ Ion_{(Cl^-)} = c_{Ion}[\mu\text{eq/l}] - Ratio(\frac{Ion}{Cl^-}) * c_{Cl^-}[\mu\text{eq/l}]$$

$$nSS\ Ion_{(Na^+)} = c_{Ion}[\mu\text{eq/l}] - Ratio(\frac{Ion}{Na^+}) * c_{Na^+}[\mu\text{eq/l}]$$

Results given in Table 3.6 are based on the calculation of all layers from both sampling sites and subsequent averaging.

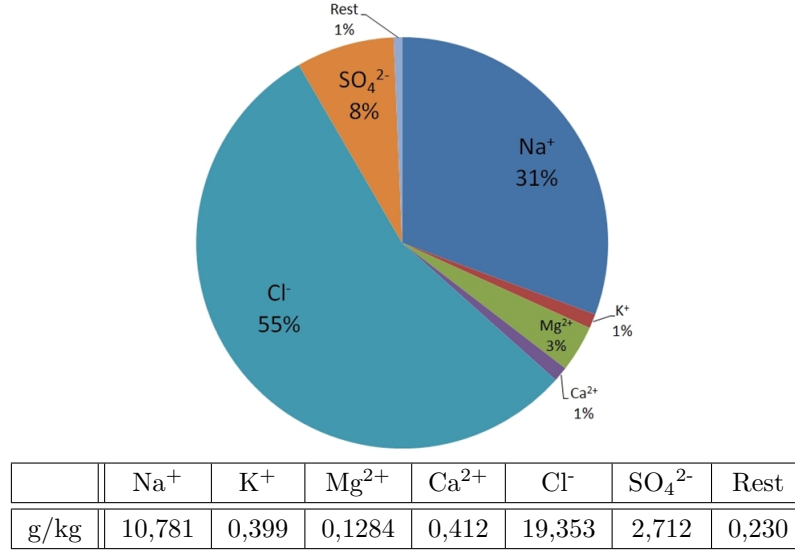


Figure 3.2.: Surface Seawater Composition [PILSON, 1998]

		nSS Na ⁺	%	nSS SO ₄ ²⁻	%	nSS K ⁺	%	nSS Mg ²⁺	%	nSS Ca ²⁺	%
based on ratio $\frac{Ion}{Cl^-}$	Mean	1,77	43	6,42	89	1,40	92	1,11	77	6,95	98
	Median	0,70	43	4,38	93	0,75	94	0,74	83	4,43	99
		nSS Cl ⁻	%	nSS SO ₄ ²⁻	%	nSS K ⁺	%	nSS Mg ²⁺	%	nSS Ca ²⁺	%
based on ratio $\frac{Ion}{Na^+}$	Mean	3,25	82	6,09	84	1,32	88	0,84	70	6,91	97
	Median	1,84	84	4,00	91	0,71	90	0,58	78	4,38	98

Table 3.6.: Non sea salt proportions given in [$\mu\text{eq/l}$] or [%] of the specific ion, based on the sea water ratio with Cl⁻ (Top) or Na⁺ (Bottom) and either the mean or median of the time series

It can be shown from the calculation of nSS proportions, that Na⁺ originates with 60% and Cl⁻ with only 20% from sea salt. K⁺ is attributed in the PCA to the same factor as Cl⁻ and Na⁺ but has a nSS amount of 90% and higher.

The nSS proportion of Na⁺, Cl⁻, K⁺ can possibly be associated with aerosols produced during biomass combustion (especially wood charcoal) and fertilization with potash in agriculture. Potash, which is an umbrella term for various salts that contain K⁺ in water-soluble form, is the main Potassium containing fertilizer

[CHESWORTH, 2008]. The major constituents from potash are Halit (NaCl) and Sylvin (KCl). This result disproves the assumption of many similar studies mentioned above, that these ions originate from natural sources like sea salt.

The nSS proportion of Ca^{2+} is more than 90% which coincides with the result of the PCA, that Ca^{2+} originates from dust events. The calculation shows, that 30% of Mg^{2+} originate from sea salt, the other 70% are assumed to originate from dust events as well, according to the PCA.

The results of the PCA and the nSS proportions allow the conclusion that the source classification mentioned previously has to be modified as to:

1. *potash* and only a small proportion from sea salt (Cl^- , Na^+ , K^+)
2. anthropogenic activities (NO_3^- , SO_4^{2-} , NH_4^+)
3. dust events (Ca^{2+} , Mg^{2+})

Now clusters 1 *and* 2 are of anthropogenic origin. Thus the majority of the ions in the high alpine sampling sites analyzed in the thesis at hand are anthropogenically induced and not naturally, as assumed so far. Furthermore the PCA confirms that the acidity in the snow originates from SO_4^{2-} and partly from NO_3^- together with H^+ .

4. Analysis of temporal trends in ion concentration and deposition

The annual volume weighted mean concentrations of all measured compounds were calculated, as well as the median and the deposition, in order to investigate temporal trends. To identify these trends in the data set, the already before used Mann-Kendall test was performed. The results are shown in Table 4.1, where the numbers account for Kendall's tau.

	GOK			WUK		
	Mean	Median	Deposition	Mean	Median	Deposition
K ⁺	n.s.	n.s.	n.s.	n.s.	n.s.	n.s.
Na ⁺	n.s.	0,244	n.s.	n.s.	n.s.	n.s.
Cl ⁻	n.s.	n.s.	n.s.	-0,274	-0,348	n.s.
SO ₄ ²⁻	-0,680	-0,620	-0,640	-0,655	-0,690	-0,560
NO ₃ ⁻	-0,250	-0,257	n.s.	-0,298	-0,374	-0,287
NH ₄ ⁺	n.s.	n.s.	n.s.	n.s.	n.s.	n.s.
Ca ²⁺	n.s.	n.s.	n.s.	n.s.	0,278	n.s.
Mg ²⁺	-0,361	-0,260	-0,281	n.s.	n.s.	n.s.
H ⁺	-0,373	-0,344	-0,353	-0,483	-0,576	-0,374
pH	0,323	0,313	-	0,432	0,528	-
Conductivity	-0,268	n.s.	-	-0,530	-0,509	-

Table 4.1.: Kendall test for temporal trends of the annual volume weighted mean concentrations, the median or the deposition; colors account for different significance levels: n.s. = not significant; red: $p < 0,1$; orange: $p < 0,05$; yellow: $p < 0,01$; green: $p < 0,001$

To visualize the trends in the data set and to get information on the inter-annual variation a Box-Whisker-Plot for every single ion is presented. The box includes the lower quartile, the median and the upper quartile. The whiskers show the lowest and highest value within $1.5 \cdot \text{IQR}$ (Interquartile range). Values outside of this range are counted as outliers. Usually values between $1.5 \cdot \text{IQR}$ and $3 \cdot \text{IQR}$ are considered as „smooth“ outliers and values larger than $3 \cdot \text{IQR}$ as “extreme“ outliers. The outliers were not drawn in the following diagrams but are given in the Appendix.

The outliers identified in the Box-Whisker-Plots were not excluded in previous calculation, because it is not clear if they arise through contamination, errors in the

measurement or if there really was a high concentration. Further investigation in this direction is required. If the outliers were excluded in the PCA and the calculation of the nSS proportions, no differences in interpretation arose.

Results are compared with the publication of WINIWARTER ET AL. (1998) which analyzed trends from 1983 to 1993 on WUK.

4.1. Trends in acidity

For the pH value, a significantly increasing trend can be seen in Table 4.1 and Figure 4.2. Due to the definition of the pH-value, the trend of H^+ has to be inverse, obviously indicated by its decreasing trend.

WINIWARTER ET AL. (1998) found no trend in pH in the time period from 1983 to 1993 at WUK. Now, after the analysis of a time span of nearly 30 years, an increase is present at the same sampling site.

The decline in acidity allows the conclusion of a decreasing trend of the acidifying ions or an increase of the neutralizing ions. Thus, the conductivity must also show a trend. As displayed in Table 4.1 and Figure 4.1 a decrease in conductivity is significant, which means that the decline in acidity is determined by a decrease in acid compounds. Otherwise, if the reduction of acidity would be induced through an increase in neutralizing compounds, the conductivity would have to show an increasing trend too.

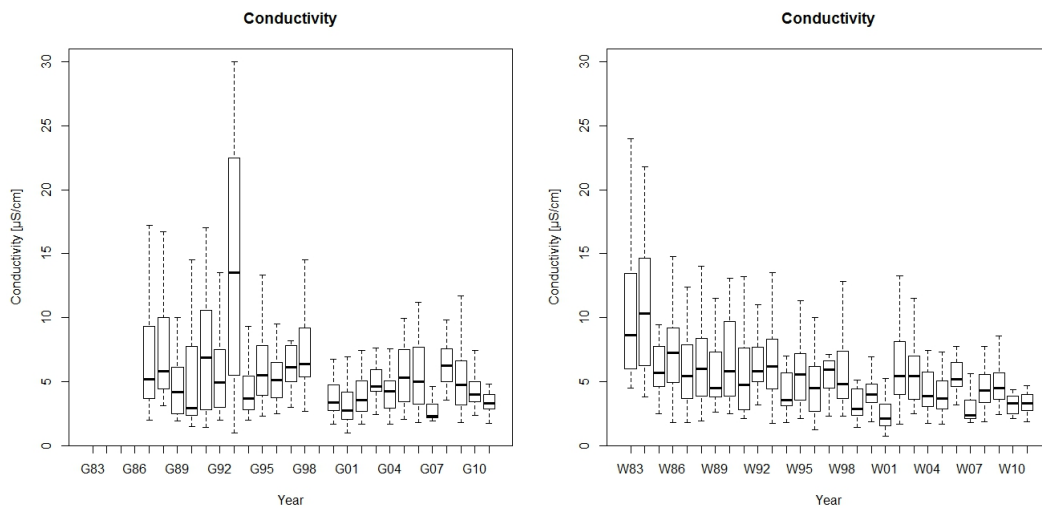


Figure 4.1.: Box-Whisker-Plot of measured conductivity including all layers where values are available from 1983-2011; left GOK, right WUK; A decreasing trend is present, due to the decrease of acidifying anions.

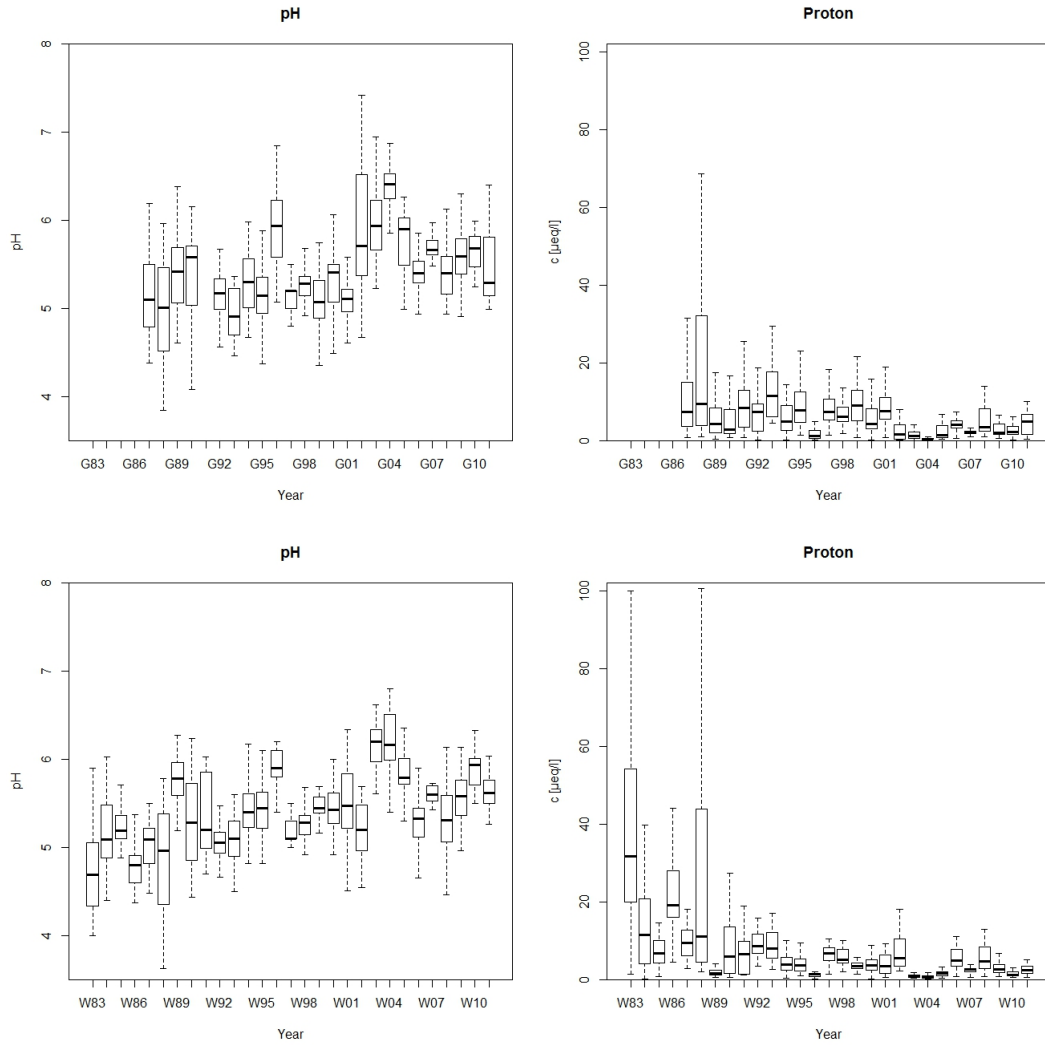


Figure 4.2.: Box-Whisker-Plot of acidity expressed in terms of the pH-value and the resulting proton concentration including all snow layers where values are available from 1983-2011; Top: GOK, Bottom: WUK; A decline in H^+ concentration and, according to this, an increase in pH is observed.

4.2. Trends in acid compounds

As already proven through the PCA, SO_4^{2-} and NO_3^- are known to be the main source of acidity in high alpine snow packs [MAUPETIT AND DELMAS, 1994].

For both ions a significant decreasing trend is present in the snow pack of both sampling sites (see Table 4.1 and Figure 4.3) which coincides with the result of the pH and conductivity measurements. These results are achieved through controlled reduction of emission gases such as SO_2 and NO_x which act as precursors for the

mentioned ions. The anions are generated by the oxidation of SO_2 and NO_x and, after the gas-to-particle conversion, deposited as SO_4^{2-} and NO_3^- (see Chapter 1.1). The main sources of these ions are known to be anthropogenic induced such as fossil fuel combustion and bio mass burning [WALLACE AND HOBBS, 2006]. Since the industrial revolution a significant increase in SO_2 emissions occurred but since the Eighties of the 20th century industry and energy suppliers were forced to reduce emission (see Figure 4.4 and 4.5).

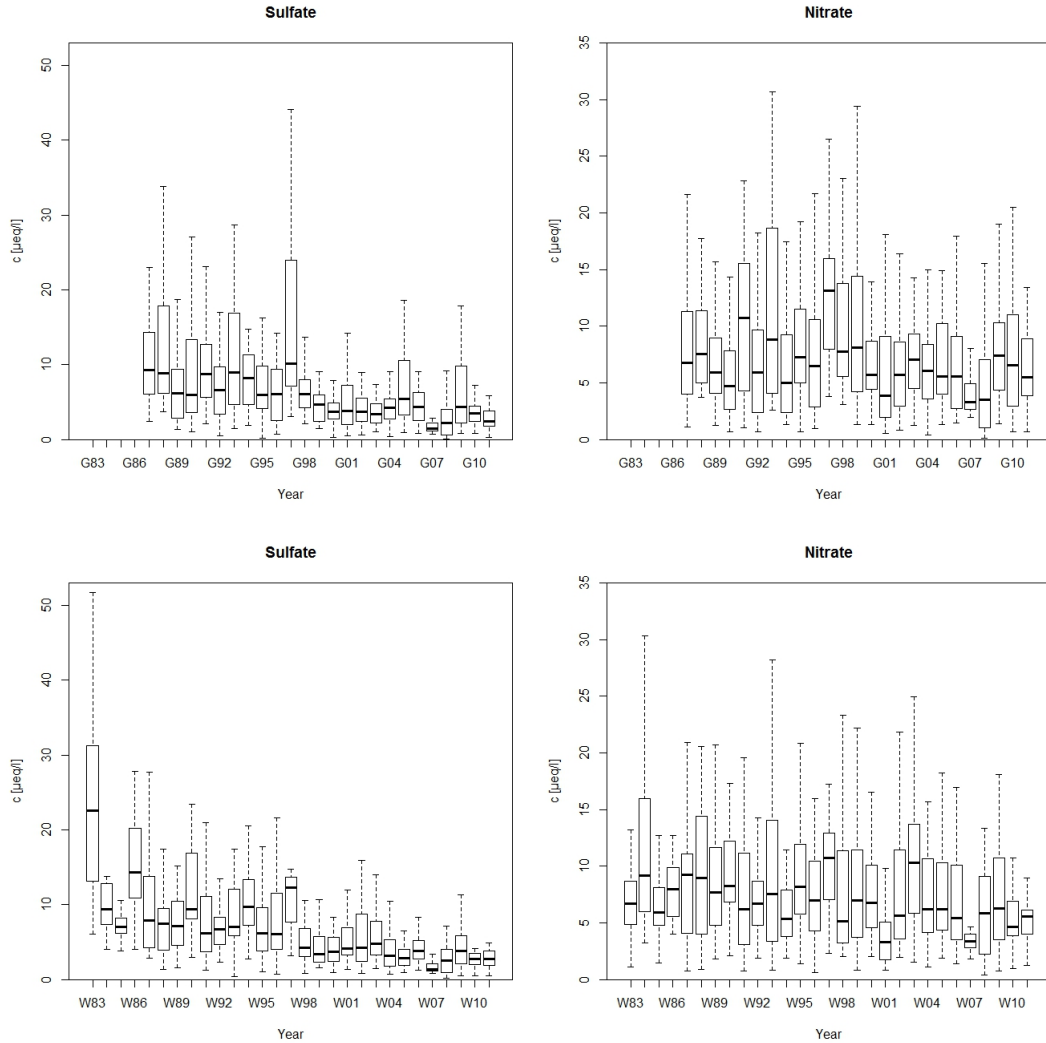


Figure 4.3.: Box-Whisker-Plot of Sulfate and Nitrate of all layers where concentrations are available from 1983-2011; Top: GOK, bottom: WUK; A decrease in the concentration of both anions can be seen due to the emission reduction of their precursor gases.

To prove the emission reduction true, a Kendall test for the European Union emission data is computed. The decreasing trend is significant with $p < 0,001$ and values of -1 for SO_2 (1990-2008) and -0,775 for NO_x (1987-2008).

4.2 Trends in acid compounds

A different result was published from WINIWARTER ET AL. (1998), where neither NO_3^- nor NO_x indicated a trend at WUK. Also a trend in SO_4^{2-} concentration and deposition was not observed. Therefore the decrease in acidifying ions did not become significant within a 10 year time period but did indeed become significant within a nearly 30 year long time period.

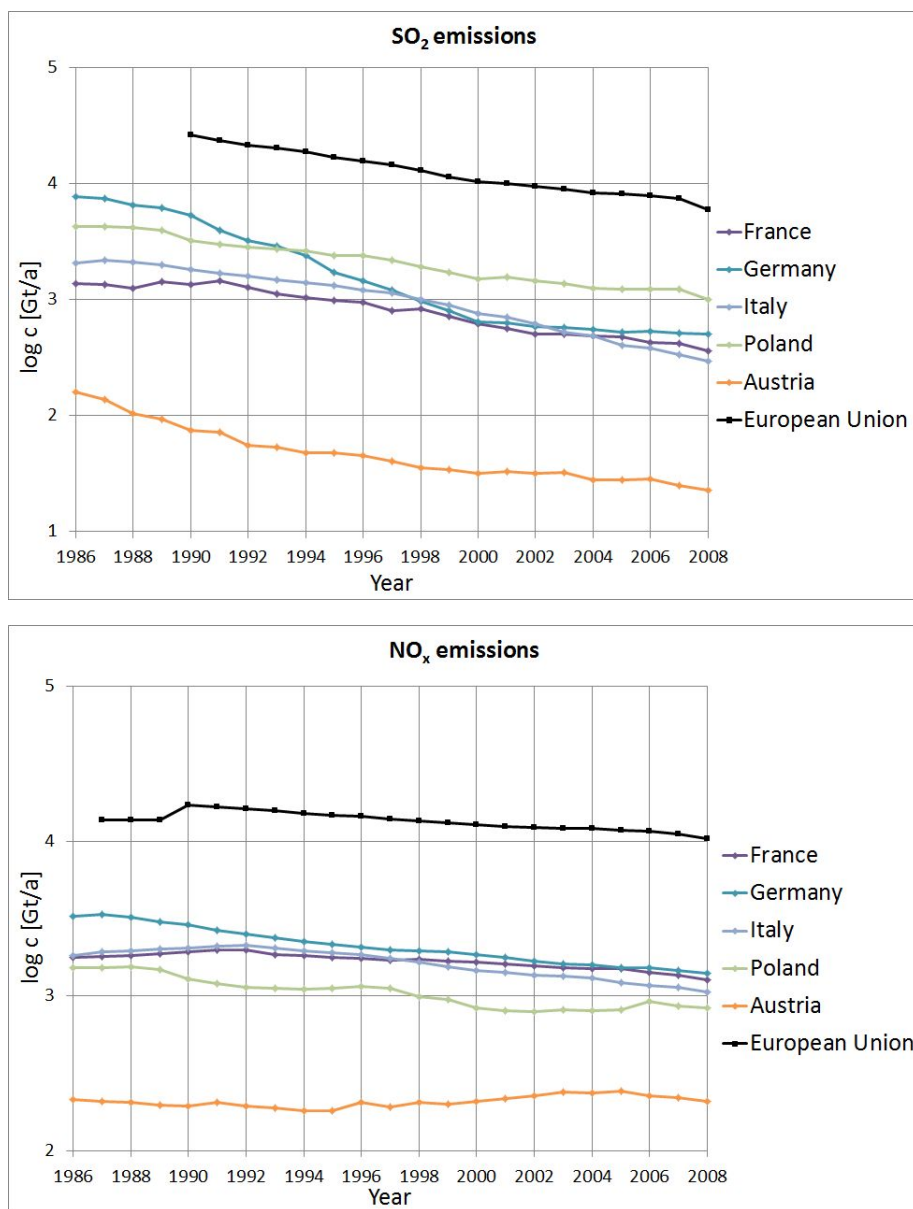


Figure 4.4.: SO_2 emissions (top) and NO_x emissions (bottom) of Europe, the European states with the highest emissions and Austria from 1986 - 2008; Data source: The EMEP Centre on Emission Inventories and Projections (CEIP); The reduction in emission is obvious.

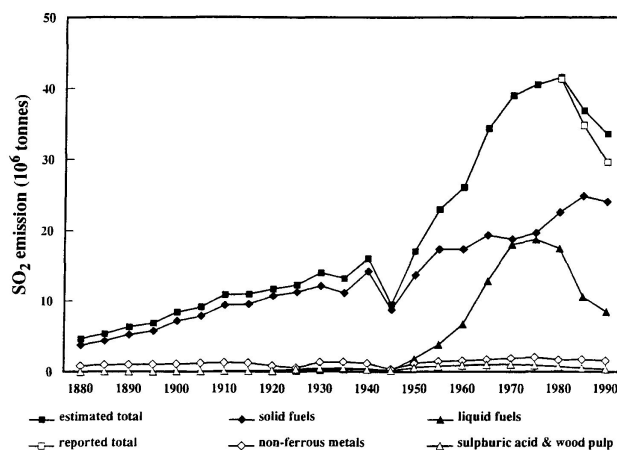


Figure 4.5.: Estimated historical anthropogenic emissions of SO_2 in Europe from 1880-1990. Reported total refers to emissions submitted by European countries to UN-ECE/EMEP [?]; Since the industrial revolution (1750-1850) the industrial SO_2 emissions increased rapidly, but since the 1980's emissions are decreasing.

4.3. Trends in neutralizing compounds

NH_4^+ and Ca^{2+} are assumed to act as neutralizers by forming secondary aerosols like Ammonium sulfate ($(\text{NH}_4)_2\text{SO}_4$), Ammonium nitrate (NH_4NO_3) or Calcium nitrate ($\text{Ca}(\text{NO}_3)_2$) instead of Sulfuric or Nitric acid [ASMAN AND SUTTON, 1998; KUMAI, 1985].

Based on the concentrations of the acid and neutralizing compounds a neutralization factor can be calculated.

$$\frac{[\text{NH}_4^+]}{[\text{SO}_4^{2-}] + [\text{NO}_3^-]} \quad \text{or} \quad \frac{[\text{NH}_4^+] + [\text{Ca}^{2+}]}{[\text{SO}_4^{2-}] + [\text{NO}_3^-]}$$

If this factor is smaller than 1, the acid is not completely neutralized. Vice versa, the acid becomes neutralized if the factor is exceeding 1. For the calculation of neutralization only with NH_4^+ as the neutralizing compound (left formula), 12% of all samples are neutralized. If Ca^{2+} is included in the calculation (right formula), the value of neutralized samples maximizes to 48%. This is also shown in Figure 4.6 where a shift of the scatter plot towards the 45° line is observed.

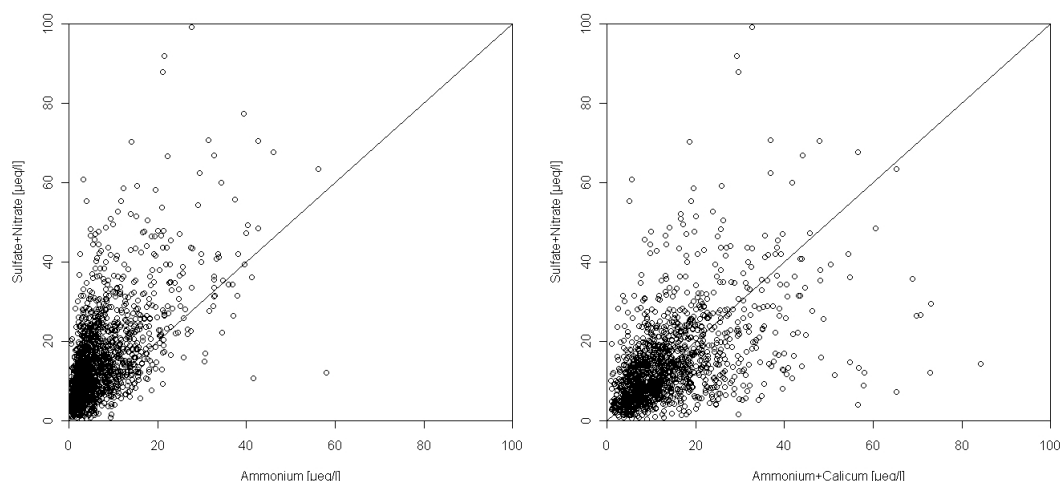


Figure 4.6.: Neutralization of acidic compounds (NO_3^- and SO_4^{2-}) with NH_4^+ (left) or NH_4^+ and Ca^{2+} (right); the 45° line represents neutralization of the samples; the shift towards neutralization is obvious when NH_4^+ and Ca^{2+} are regarded as neutralizers

4.3.1. NH_3 emissions and N-Fertilization

NH_4^+ was classified by the PCA as an ion originating from anthropogenic activities, mainly from animal husbandry and fertilization [ASMAN AND SUTTON, 1998; WAGENBACH AND MÜNICH, 1998]. Figure 4.8 displays the time series of NH_3 emissions and Nitrogen fertilizer consumption. A slight significant decreasing trend is denoted in European NH_3 emissions (Kendall's tau -1 with $p < 0,001$) but the N-fertilizer consumption shows a significant increase on nearly all continents and hence worldwide (Kendall's tau 0,7 with $p < 0,001$). The only exception is Europe, where a decreasing trend also in N-fertilizer consumption is observed (Kendall's tau -0,8 with $p < 0,001$).

Even though decreasing of trends in the sources of atmospheric NH_4^+ are present, there is no trend in the NH_4^+ concentration and deposition in high alpine snow packs observed yet (see Table 4.1 and Figure 4.7).

Again, a different result here was published from WINIWARTER ET AL. (1998), where an increasing trend in deposition was significant for WUK from 1983 to 1993 whereas emissions decreased.

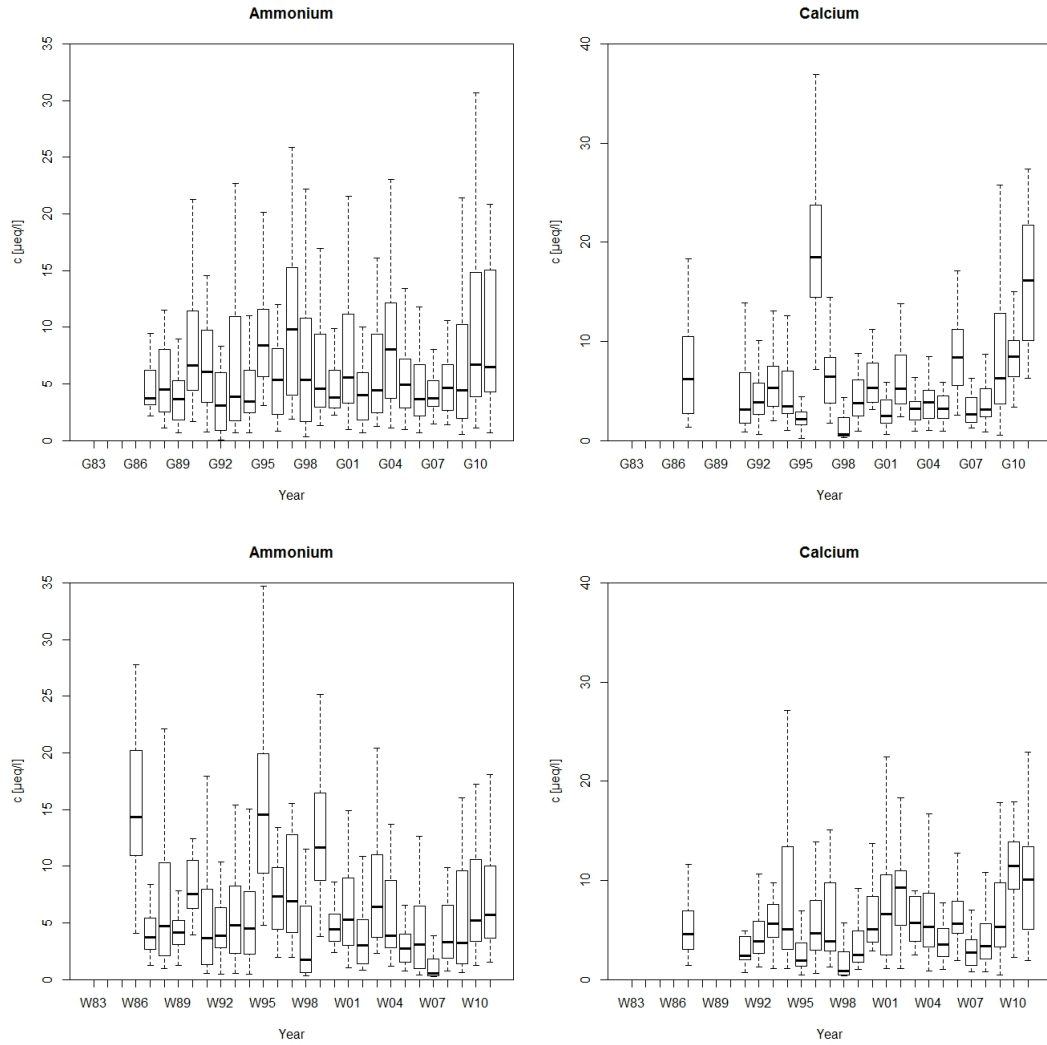


Figure 4.7.: Box-Whisker-Plot of Ammonium and Calcium of all layers where concentrations are available from 1983-2011; Top: GOK, bottom: WUK; No significant trends were observed for these ions.

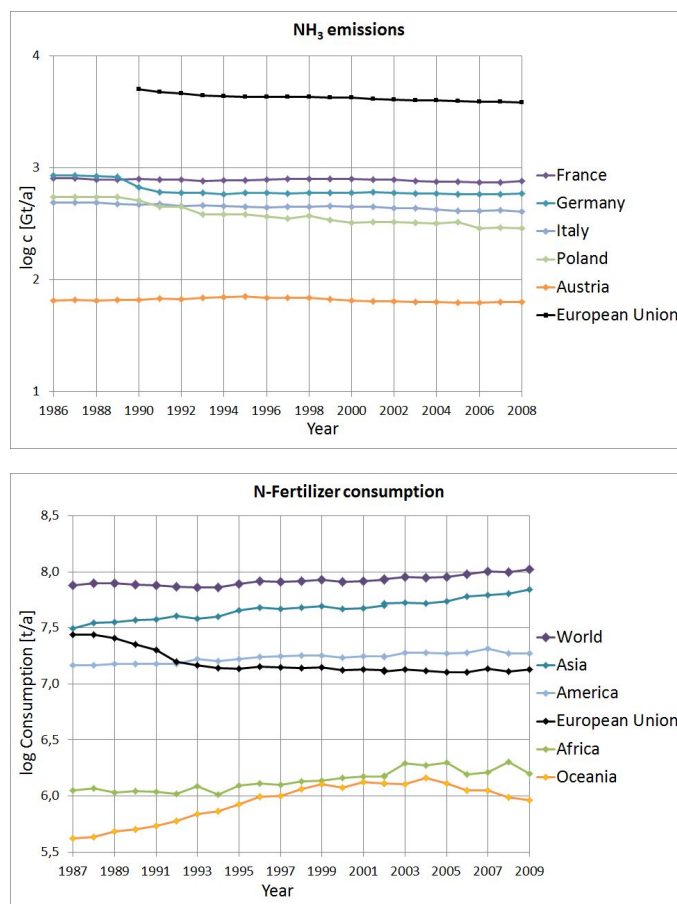


Figure 4.8.: NH₃ emissions (top) of Europe, the European states with the highest emissions and Austria from 1986 - 2008 and time trend of N-Fertilizer consumption (bottom) where values from 1987-2002 represent the consumption in tonnes whereas from 2002-2009 values represent the consumption in nutrients in tonnes of nutrients; Emission data source: The EMEP Centre on Emission Inventories and Projections (CEIP); Fertilizer data source: Food and Agriculture Organization of the United Nations (FAOSTATS)

4.3.2. Sahara dust events

Dust events are responsible for Ca²⁺ in the high alpine snow cover. For the sampling sites analyzed in the thesis at hand, the main input comes from the North-West Sahara, such as Morocco, Algeria, Tunisia and Libya [DE ANGELIS AND GAUDICHET, 1991; RODRIGUEZ ET AL., 2011].

BARKAN ET AL. (2005) found that the strength and position of two circulation patterns are the governing factors of providing suitable flows for the Saharan dust to be transported over the Mediterranean towards Italy and Central Europe. These are a trough deepening southward from an Icelandic low and the eastern cell of the subtropical high (compare Figure 4.9 and 4.10).

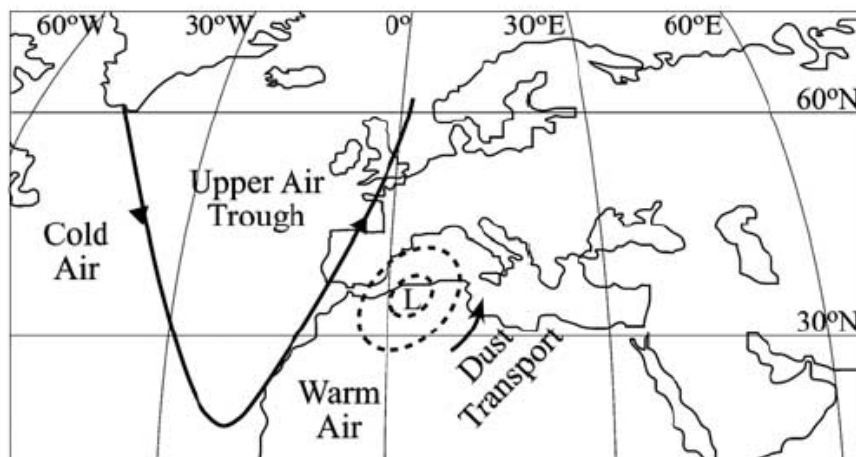


Figure 4.9.: Schematic map of the general synoptic situation in periods of dust outbreaks from the Sahara to Europe (solid line: 700 hPa; dashed line: surface pressure) [BARKAN ET AL., 2005]

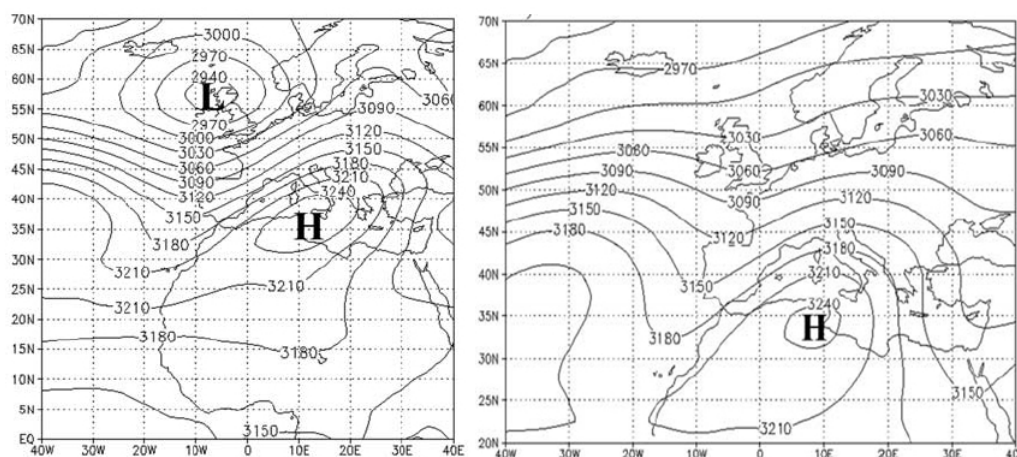


Figure 4.10.: Left: Average geopotential height of the dusty cases at 700 hPa, July 1979–1992; Right: Average geopotential height of the dusty period 5–9 July 1988 at 700 hPa [BARKAN ET AL., 2005]

For Ca^{2+} only in the median of the concentration of WUK a significant increase could be observed. A slight increase can also be seen in the Box-Whisker-Plots of both sampling sites, but not yet showing significance.

This result is a quite interesting, since for several years no dust events were optically identified in the snow through the observation of reddish color of the snow.

To interpret this data, further investigations on the identification of Saharan dust events appear necessary.

4.4. Trends from other Ions

4.4.1. Potash

As mentioned before, Na^+ , Cl^- and K^+ are assumed to be introduced to the snow cover mainly as aerosols produced during biomass (wood charcoal) combustion and agricultural fertilization with potash. All three ions show no significant trends in the time series of deposition (see Table 4.1 and Figure 4.12). WUK shows a decreasing trend in the concentration of Cl^- whereas GOK shows an increasing trend in the concentration of Na^+ . The magnitude of the sources which are responsible for the introduction of Na^+ , Cl^- and K^+ into the snow could not be estimated yet. It is not known yet to what extent the “woodsmoke” from charcoal combustion or the usage of potash as fertilizer affect the concentration and deposition of the respective ions.

Generally, for the usage of potash fertilization in Europe, a decreasing trend is existing (Kendall's tau -0,8 with $p < 0,001$) and an increasing trend in potash consumption in America and Asia (Kendall's tau 0,6 to 0,8 respectively with $p < 0,001$). On a global scale no trend can be seen (compare Figure 4.11).

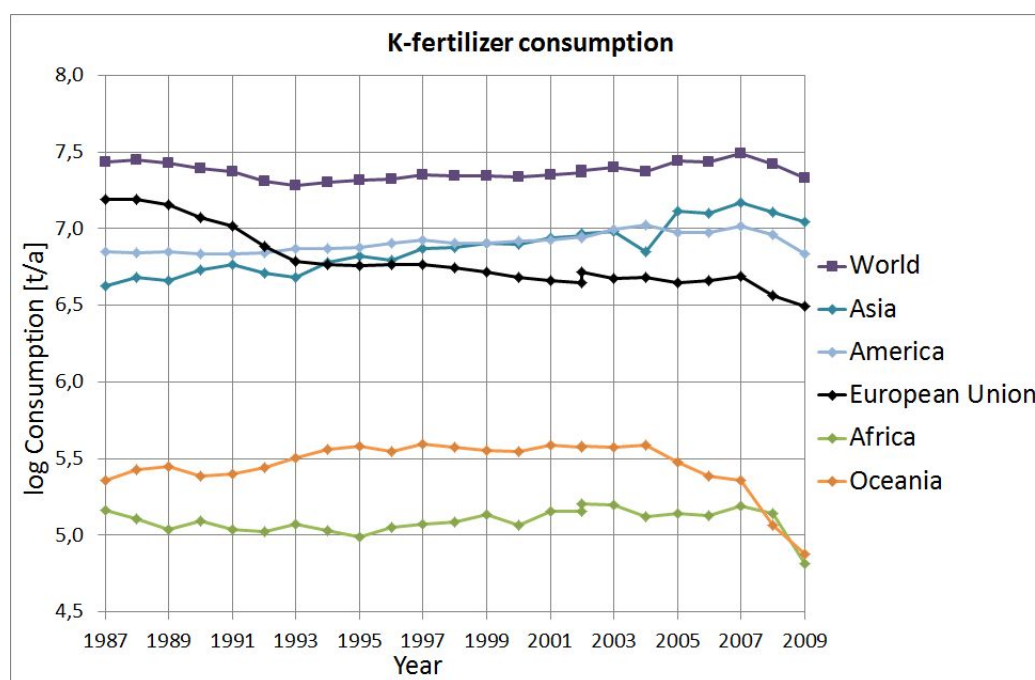


Figure 4.11.: K-fertilizer consumption where values from 1987-2002 represent the consumption in tonnes whereas from 2002-2009 values represent the consumption in nutrients in tonnes of nutrients; Data source: Food and Agriculture Organization of the United Nations (FAOSTATS)

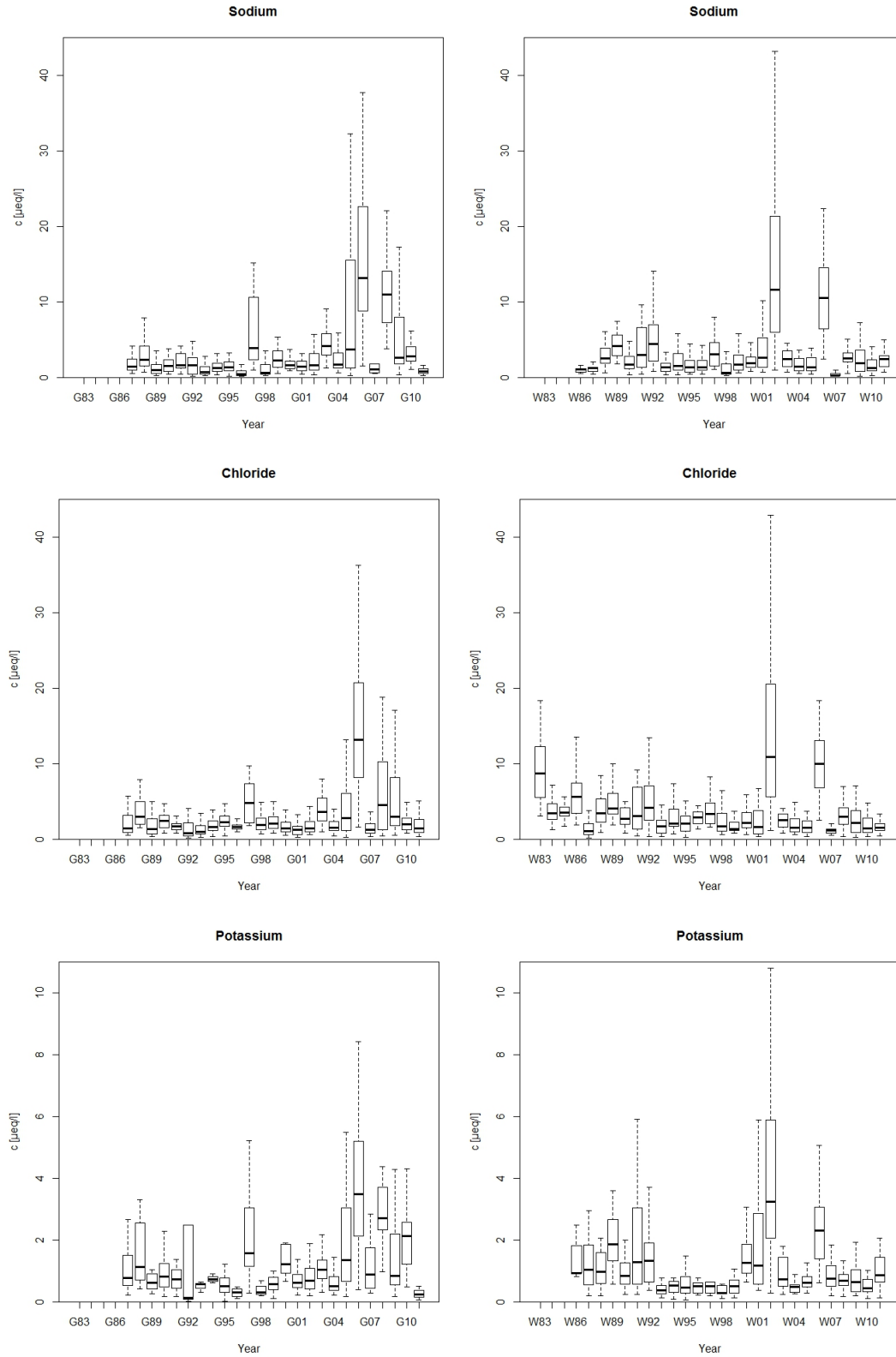


Figure 4.12.: Box-Whisker-Plot of Sodium, Chloride, Potassium of all layers where concentrations are available from 1983-2011; left: GOK, right: WUK; No significant trends were observed for the ions concerning potash.

4.4.2. Magnesium as part of sea salt and dust events

Mg^{2+} originates mainly from dust events and partly from sea salt.

It shows a significant decrease in concentration and deposition only on the GOK sampling site (see Table 4.1 and Figure 4.13). This would fit into the observation, that Saharan dust events were not optically witnessed in the snow packs over the last years.

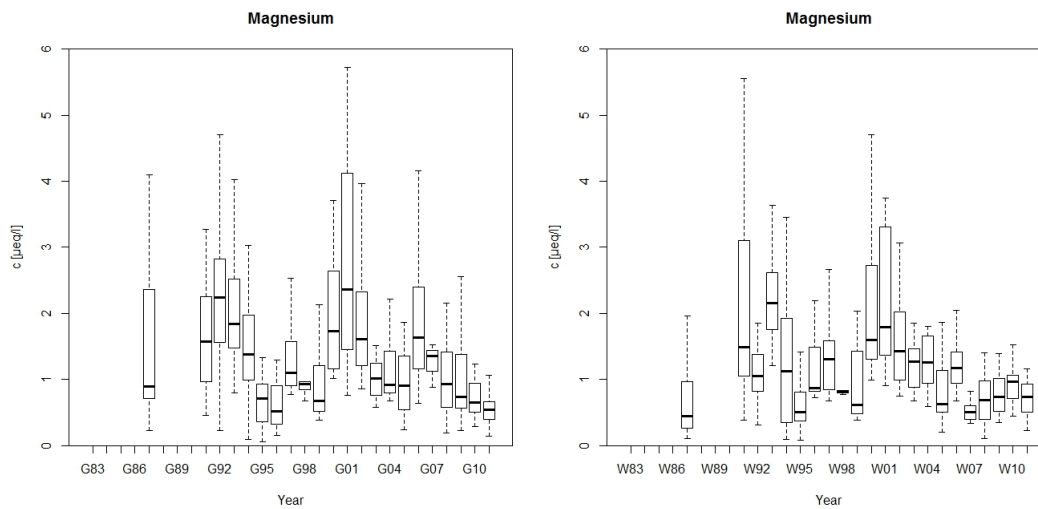


Figure 4.13.: Box-Whisker-Plot of Magnesium of all layers where concentrations are available from 1983-2011; left: GOK, right: WUK; A significant decrease was observed only for GOK.

5. Comparison WUK and GOK

The calculation of the coefficients of variation in Chapter 2.5 resulted in a total variability (sum of analytic and mesoscale variability) for each ion and the conclusion that the ion concentrations measured on WUK and GOK can be regarded representative for the Sonnblick region. But, the two sampling sites feature different orientation and position to incident atmospheric flow. This may cause relative differences in deposition and ion concentrations. The skiing resort on the WUK could be an additional source for the ion deposition due to the production of artificial snow. Thus, the time series of both sites are compared to see if differences are present. Therefore the signal-to-noise ratio, giving the information if trends in the time series are significant or not, is very important for the time trend analysis of acidity and the comparison between the two glaciers.

Na ⁺	K ⁺	Cl ⁻	SO ₄ ²⁻	NO ₃ ⁻	NH ₄ ⁺	Ca ²⁺	Mg ²⁺	H ⁺
1,14	0,09	0,92	1,07	1,65	1,18	3,15	0,71	7,97

Table 5.1.: Standard deviation in µeq/l of the specific ions, based on the calculation of the total variability (sum of analytic and mesoscale variability).

Figure 5.1 displays the profile depth and the water equivalent of both sampling sites for every year reviewed. The water equivalent (density x depth) represents the water that has accumulated on the ground. In other words, it defines the depth of water that would result from the melting of the entire snow pack¹. The profile depth and the water equivalent show a similar tendency. For the majority of the years observed, GOK had higher accumulations and, accordingly higher water equivalents. The different location of the two sites relatively to the alpine main divide could be one explanation. Since GOK is located on the northern side of the main ridge of the Alps, higher precipitation amounts are enabled, due to the Alps pondage and uplifting of incoming air masses from the Northwest, which is the dominant flow over Central Europe. On the other hand, the GOK and WUK sampling sites are both very close to the main ridge of the Alps. Thus, it can be supposed that the increased water equivalents on GOK are not only due to the relative location to the alpine main divide, but the fact that WUK is located further downstream of the incoming northwestern flow than GOK.

¹AMS Glossary of Meteorology

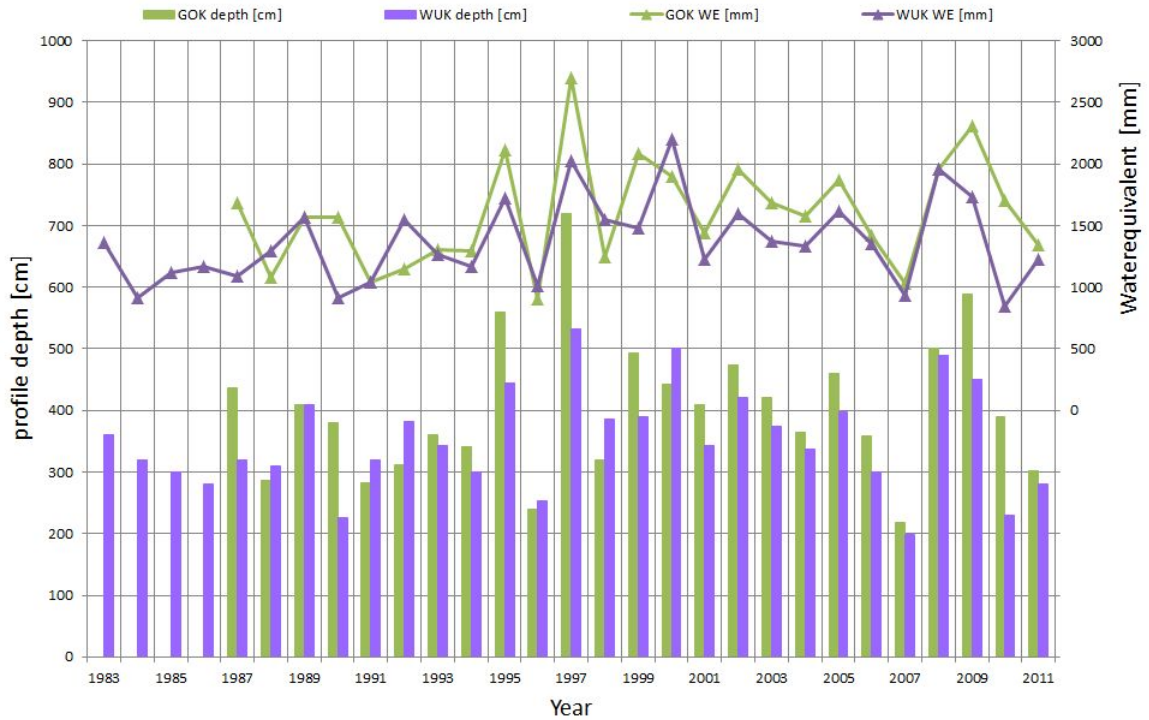


Figure 5.1.: Profile depth and Water equivalent of both sampling sites to show the similar tendency on both sampling sites. In the majority of the years the accumulation was higher on GOK due to the uplifting of incoming air masses which enables higher precipitation amounts.

5.1. Comparison of ion concentration and deposition

To see if there are differences between the two sampling sites, the annual mean concentrations and the annual depositions were compared. It has to be regarded, that, especially for K^+ and Mg^{2+} the number of samples higher as the detection limit of 0,023ppm and 0,003ppm respectively, is very low. Hence, in those cases the mean has to be computed from a very few data only (see depth profiles in Appendix D) and thus it is recommended to draw conclusions on these ions very cautious.

The tendency of the concentration of the acidifying ions, such as H^+ , SO_4^{2-} and NO_3^- as well as their deposition (see Figure 5.2) is comparable on both glaciers. For 1997, all ions showed a high value, relative to the trend, in deposition for both sites, whereas an increased concentration was only measured for SO_4^{2-} at GOK.

The tendency of the neutralizing compounds NH_4^+ and Ca^{2+} as well as Mg^{2+} applies analogously to the two glaciers. Again, the high amount in deposition of all three cations on both sites in 1997 is remarkable, while concentrations are not increased (see Figure 5.3). For NH_4^+ the concentration and deposition on WUK since 2004 was always lower compared to GOK. High Ca^{2+} concentrations ($> 10\mu eq/l$) were found

for GOK in 1996, together with a high deposition ($> 200\text{meq/m}^2$). Furthermore three years of nearly constant Ca^{2+} concentrations and depositions were observed on WUK from 2001 to 2003. Interestingly, the different construction activities, such as the renovation of the nearby Zittelhaus from 1991 to 1994 as well as the renewal of the steel constructions at the observatory from 2001 to 2004, could not be detected in concentrations and deposition of the particular years. It was expected that during construction activities cement (consists mainly of Calcium silicate) or dust from the bedrock (complex rock composition, geol. Hohe Tauern window) was dispersed and dryly deposited in the surrounding area. But higher Ca^{2+} or Mg^{2+} concentrations in relation to construction work were not explicitly found in the data.

Concerning ions originating from potash (Na^+ , Cl^- and K^+) the tendency in concentration and deposition is not as homogenous as it is for the other ions, but all three ions show a similar picture (see Figure 5.4). Increased depositions and concentrations were observed for 2002 at WUK and for 2006 at WUK and GOK. Also in 1997 and in the period from 2008 to 2010 increased concentrations and depositions were found, but only at GOK.

5.2. Discussion of the differences of WUK and GOK

When looking at the time series of ion concentration and deposition from both sites, few years could be recognized, where specific ions showed an optically distinctive aberrance from the trend. Such high values are called “peaks” in the following text. Table 5.2 summarizes the identified peaks from both sites which are discussed year by year in the following section.

	WUK		GOK	
	Deposition	Concentration	Deposition	Concentration
1996	-	-	Ca^{2+}	Ca^{2+}
1997	all ions	-	all ions	Na^+ , Cl^- , K^+ , SO_4^{2-}
2002	Na^+ , Cl^- , K^+	Na^+ , Cl^- , K^+	-	-
2006	Na^+ , Cl^- , K^+	Na^+ , Cl^- , K^+	Na^+ , Cl^- , K^+	Na^+ , Cl^- , K^+
2008-2010	-	-	Na^+ , Cl^- , K^+	Na^+ , Cl^- , K^+

Table 5.2.: Overview of the events clear peaks in the time series of WUK and GOK

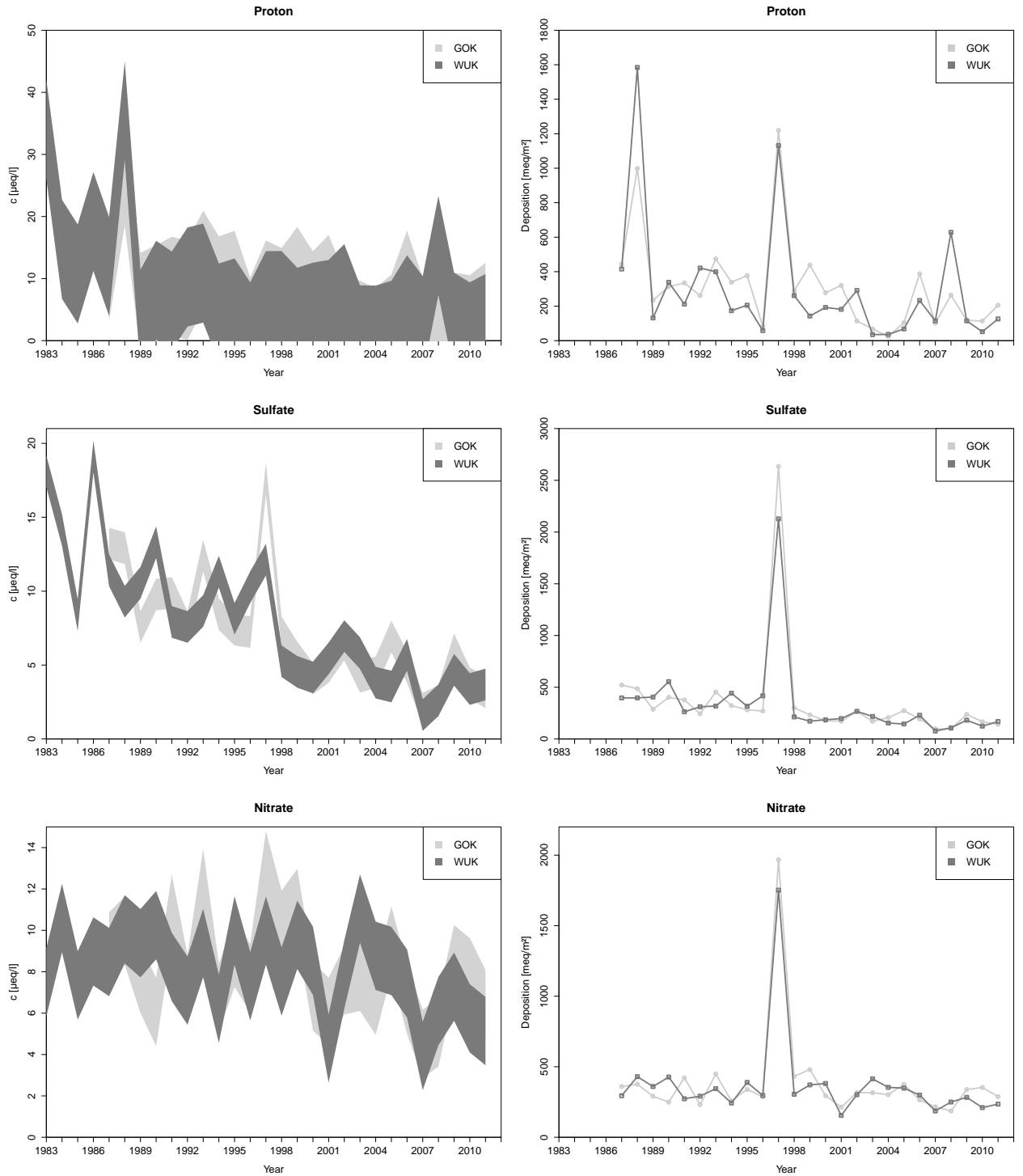


Figure 5.2.: Left: Concentration in µeq/l displayed as range from the mean \pm standard deviation; Right: Deposition in meq/m² of H⁺, SO₄²⁻ and NO₃⁻ ; In 1997 all three ions show a clear peak in deposition on both sites whereas only SO₄²⁻ shows a clear peak in the time series of concentration for 1997 especially for GOK, too. The high band in the concentration of H⁺ arises is related with the high variation of H⁺, due to the high accuracy of 0,1-0,2 pH units.

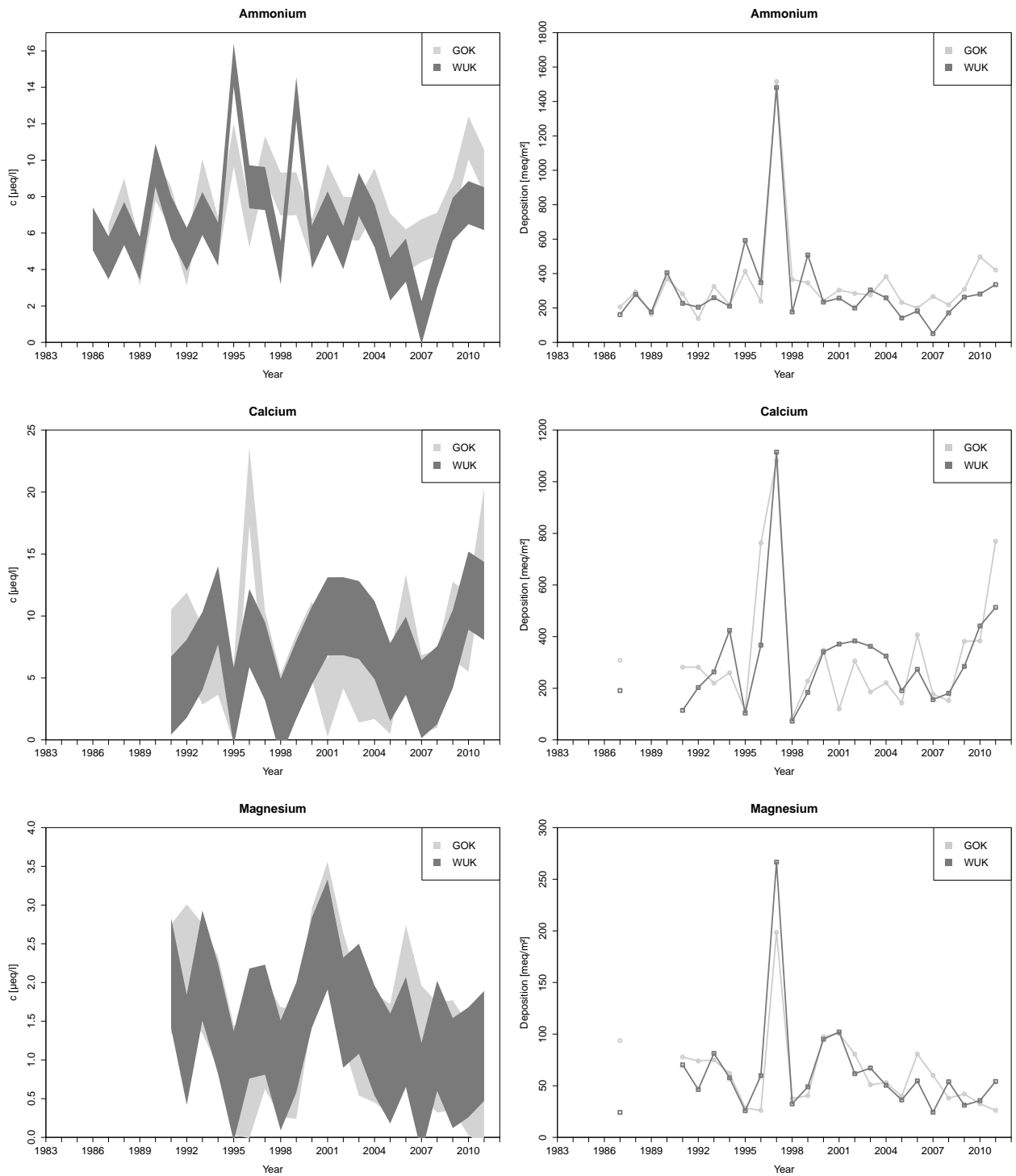


Figure 5.3.: Left: Concentration in µeq/l displayed as range from the mean \pm standard deviation; Right: Deposition in meq/m² of NH₄⁺, Ca²⁺ and Mg²⁺; In 1997 all three ions show a clear peak in deposition whereas concentrations do not. Additionally Ca²⁺ showed a peak in deposition and concentration for 1996.

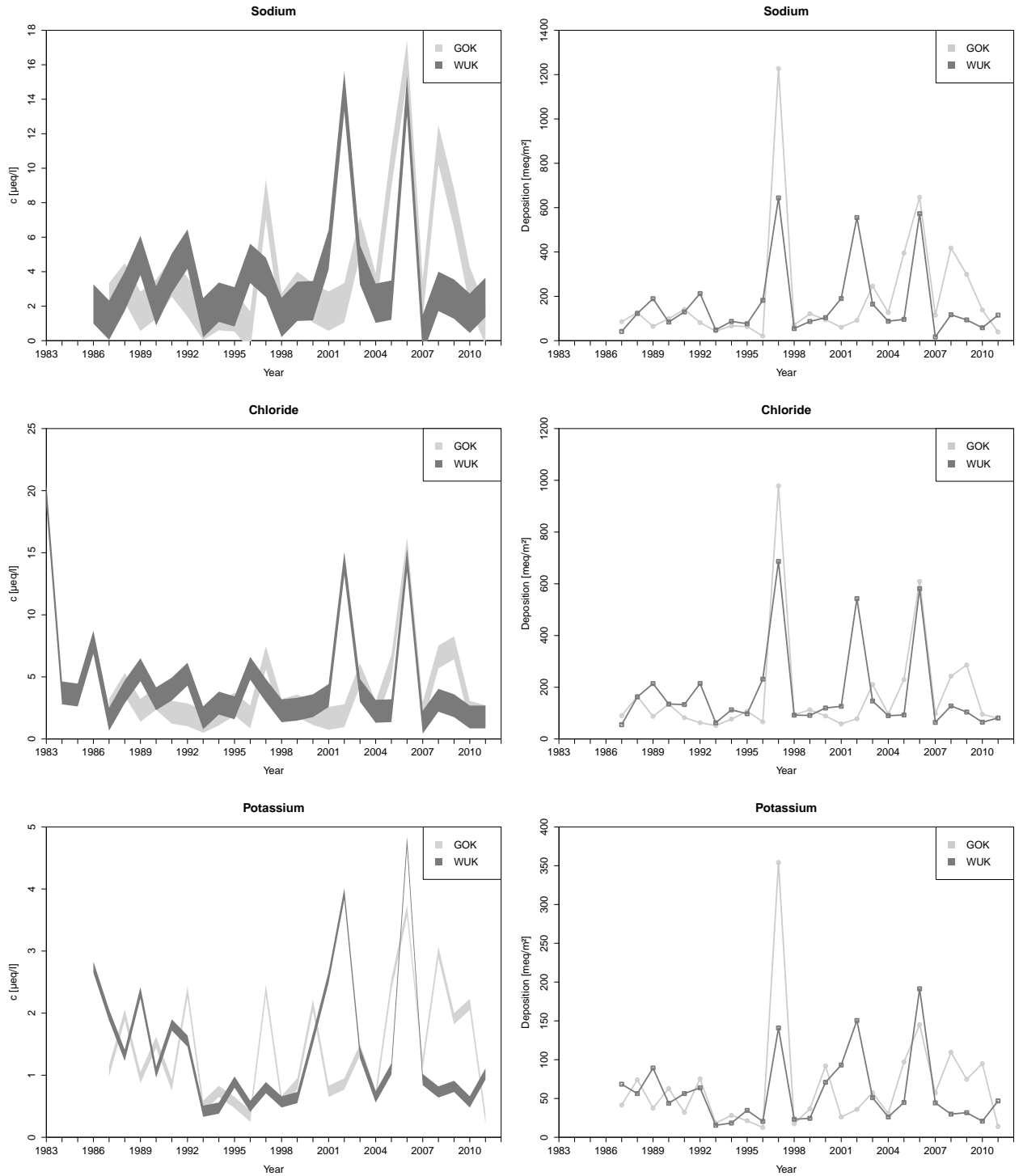


Figure 5.4.: Left: Concentration in $\mu\text{eq/l}$ displayed as range from the mean \pm standard deviation; Right: Deposition in meq/m^2 of Na^+ , Cl^- and K^+ . In 1997 all three ions show a clear peak in deposition, whereas concentration showed only a peak for the GOK sampling site. Additionally clear peaks in concentration and deposition were observed for all three ions on WUK in 2002 and 2006, and on GOK in 2006 and from 2008-2010.

All ions showed clear peaks in **1997** on both sites, whereas only for GOK high concentrations for Na^+ , Cl^- , K^+ and SO_4^{2-} were found, too. This specific year is discussed in detail in the subsequent chapter (Chapter 5.3).

In **1996** it appears like GOK had more input of Sahara dust than WUK, which can be seen in the depth profiles displayed in Figure 5.5. WUK had only one layer (100-110cm) where concentrations higher than $20\mu\text{eq/l}$ were present, whereas GOK showed concentrations higher than $20\mu\text{eq/l}$ in at least 3 layers (10-20cm, 120-130cm and 150-160cm).

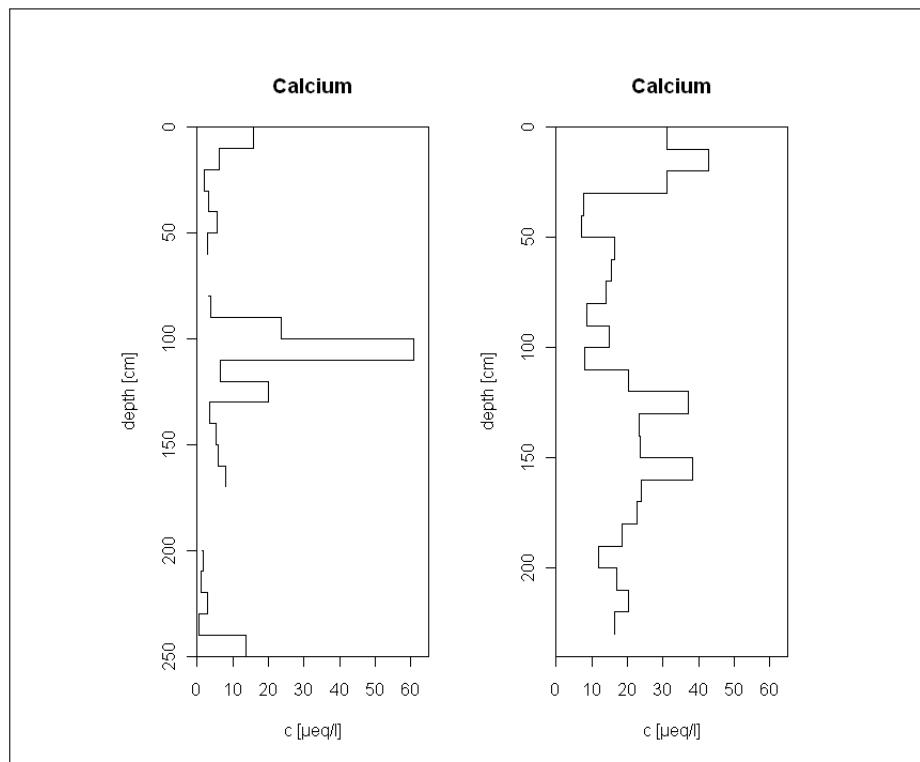


Figure 5.5.: Depth profiles for Ca^{2+} in 1996; left: WUK, right: GOK

In **2002** WUK apparently received air contaminated with ions originating from potash more often than GOK because mean concentration and deposition of Na^+ , Cl^- and K^+ were higher relative to GOK. The difference is obvious when the profiles are analyzed (see Figure 5.6). It can be seen that the concentrations of the WUK profile, especially in the lower part, are 10-30 $\mu\text{eq/l}$ higher than the once at GOK.

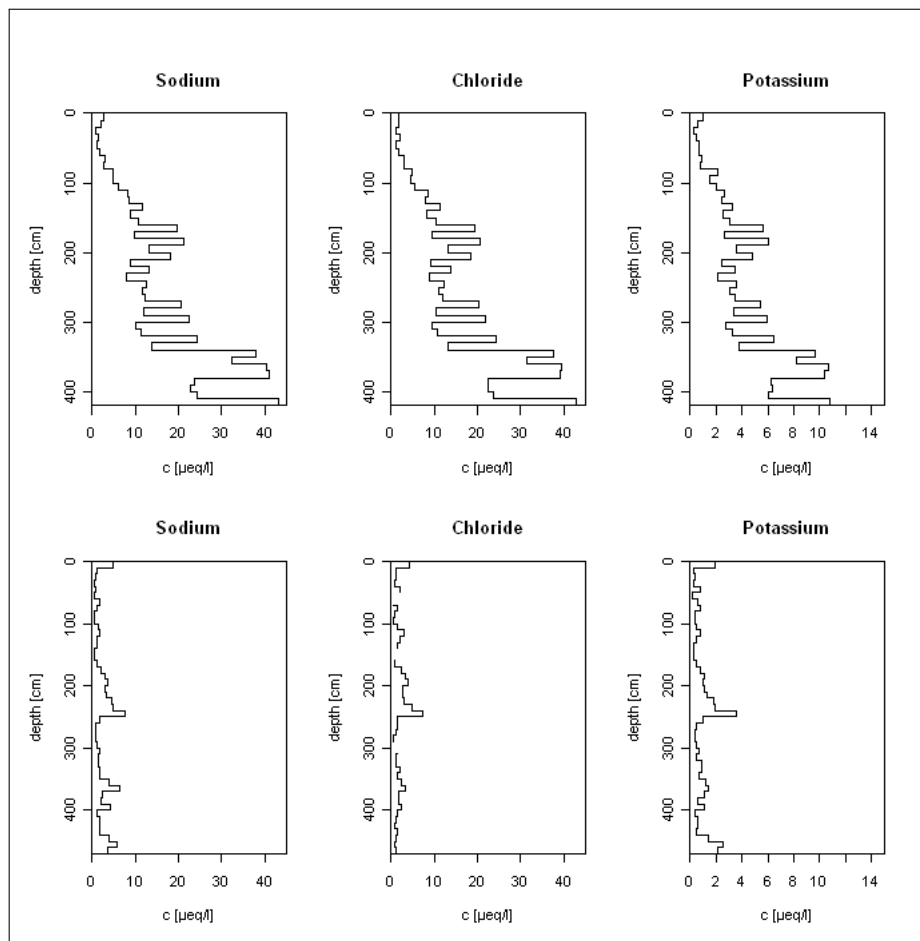


Figure 5.6.: Depth profiles for Na^+ , Cl^- and K^+ for the year 2002; top: WUK, bottom: GOK; It is shown that in this particular year it seems that WUK received more often air polluted with potash ions, originating mainly from biomass combustion (especially wood charcoal) and K-Fertilization.

For **2008-2010** it appears that it was the opposite if compared to 2002. The difference can be seen by taking a look on the depth profiles (Figure 5.7). The concentrations on WUK were between 0-10 $\mu\text{eq/l}$, whereas on GOK they reached values up to 40-50 $\mu\text{eq/l}$. Differently to the year 2002, two intercepts in the GOK profiles, from 130-230cm and 370-390cm, showed the increased ion concentrations whereas on WUK in 2002 the whole lower part of the profile ($> 200\text{cm}$) showed heightened concentration relative to the rest of the profile.

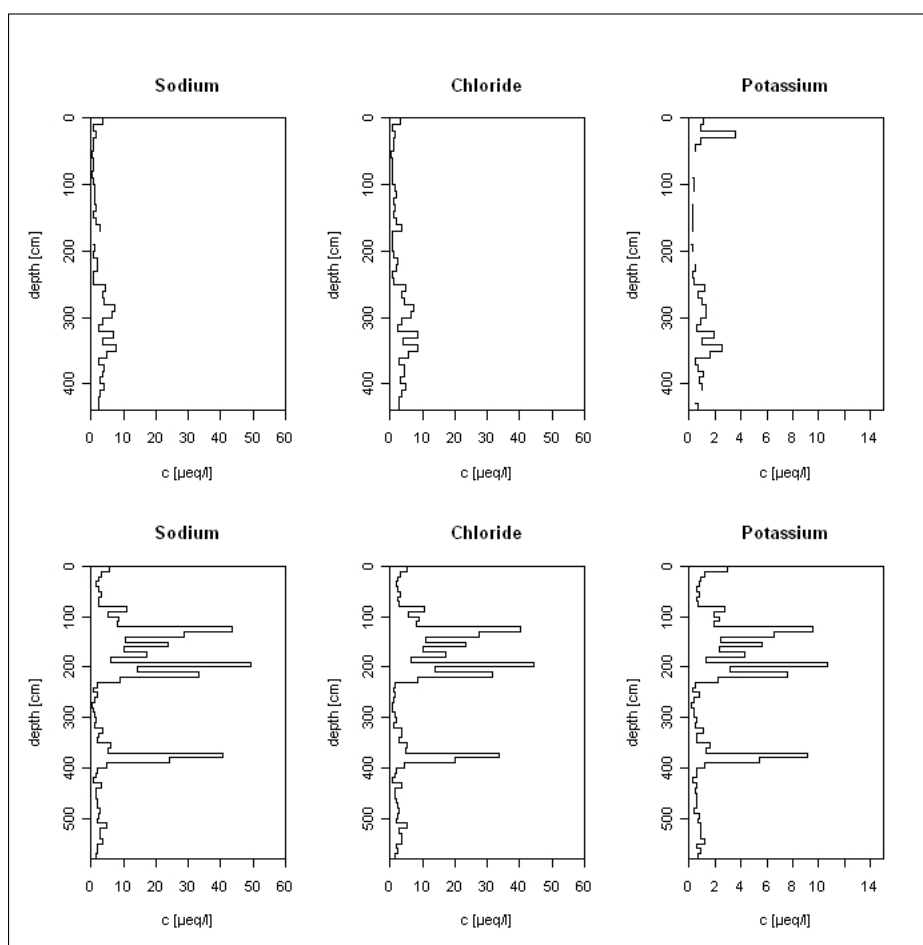


Figure 5.7.: Depth profiles for Na^+ , Cl^- and K^+ for the year 2009; top: WUK, bottom: GOK; It is shown that in this particular year it seems that GOK received more often air polluted with potash ions, originating mainly from biomass combustion (especially wood charcoal) and K-Fertilization.

In **2006**, both sites showed high concentration and deposition values of potash ions, such as Na^+ , Cl^- and K^+ . While the mean concentration and deposition for Cl^- was the same for both glaciers, WUK showed a slightly higher mean for K^+ and GOK for Na^+ (Figure 5.4). The depth profiles (Figure 5.8) display, that at WUK one layer (60-80cm) featured high concentrations ($>50\mu\text{eq/l}$) for all ions, whereas at GOK the whole profile showed increased concentrations with values between 10-40 $\mu\text{eq/l}$. For Cl^- the two different observations (one layer with heightened concentration at WUK vs. slight heightened concentration over the whole profile at GOK) do not result in a difference in the mean. Indeed, the difference in the observation is present in the mean of K^+ and Na^+ .

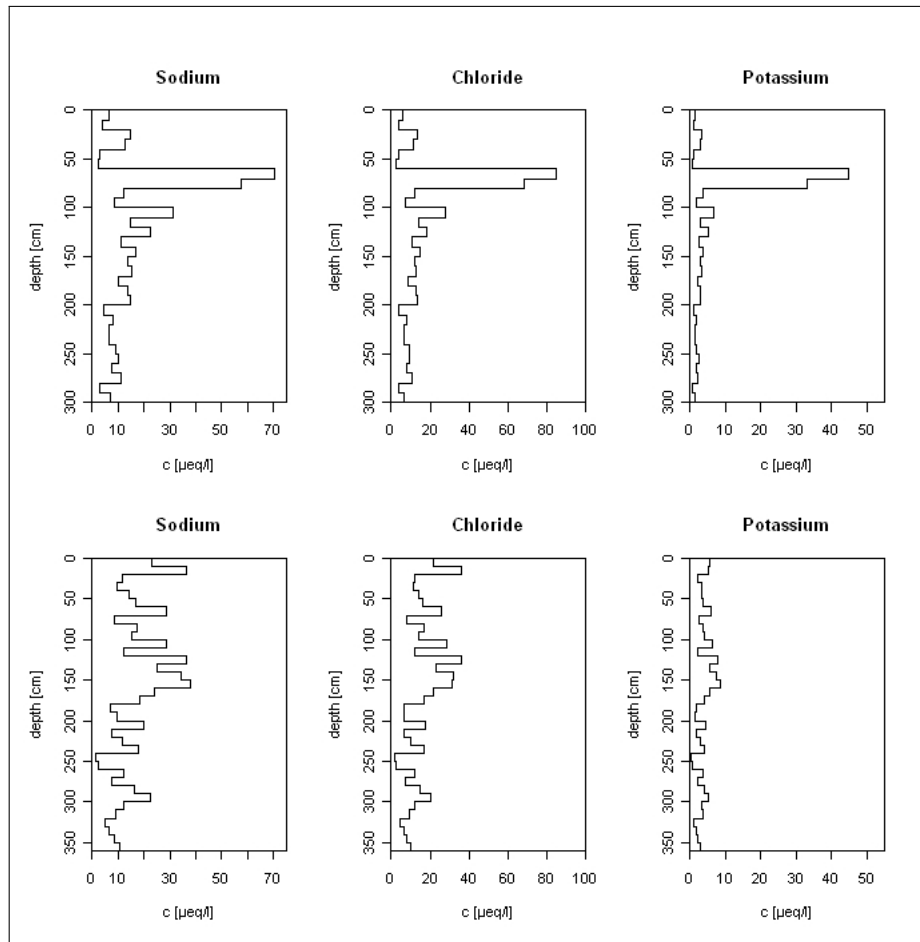


Figure 5.8.: Depth profiles for Na^+ , Cl^- and K^+ for the year 2006; top: WUK, bottom: GOK; In the WUK profile two layers (60-80cm) had increased concentrations ($> 50\mu\text{eq/l}$) of all three ions, relative to the rest of the profile. GOK showed slightly increased concentrations (10-40 $\mu\text{eq/l}$) over the whole profile.

5.3. Outlier discussion - 1997

In 1997 all ions showed an anomaly in the time series of the deposition at both sites. This might be explained with the outstanding high snow accumulation on GOK and WUK with a depth of 720cm and 532cm, respectively which caused high rates in deposition of all ions while the concentrations might not be increased. This can be highlighted through a comparison of the concentrations in 1997 on GOK with an averaged profile over the previous five years (1992-1996), both normalized to 100% depth.

The concentrations in 1997 for Ca^{2+} , NH_4^+ , Mg^{2+} , H^+ and NO_3^- were within the magnitude of the concentrations of the averaged profile. For Na^+ , Cl^- and K^+ the single year concentrations were higher than the averaged one, which indicates a high input of potash (compare Figure 5.9 and 5.10).

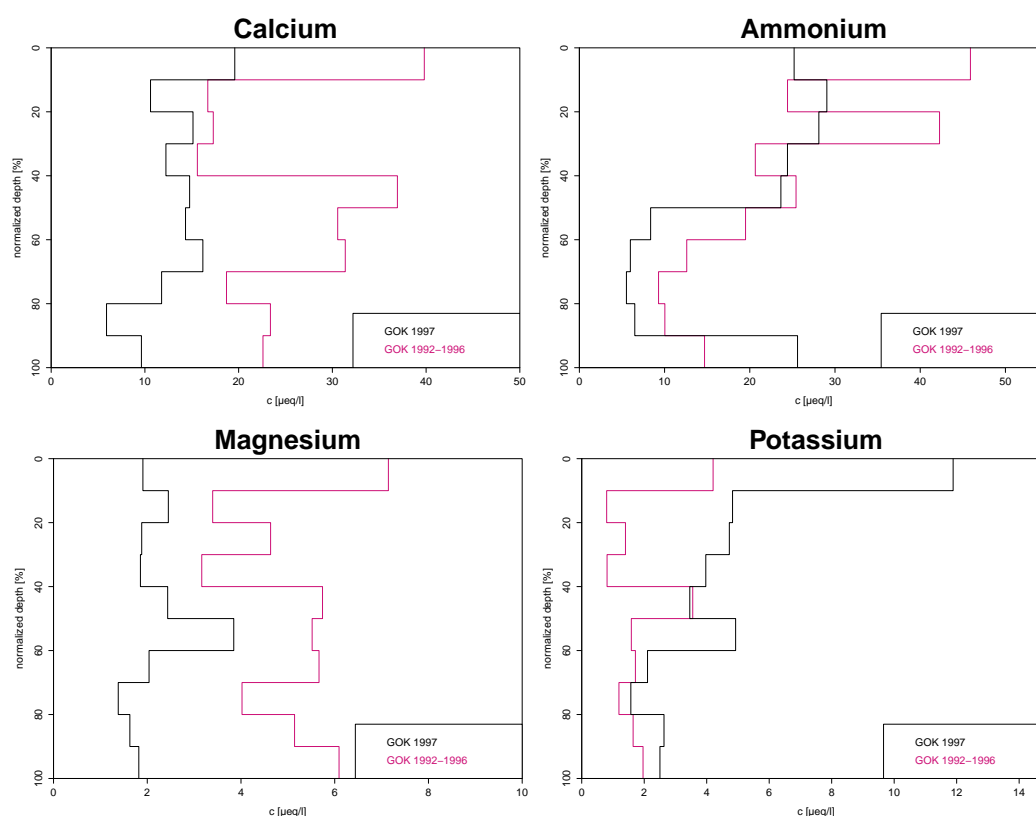


Figure 5.9.: Comparison of an average profile from 1992-1996 (pink) and the profile of 1997 (black), both normalized to 100% depth; Single year concentrations are within the magnitude of the averaged profile, except for K^+ .

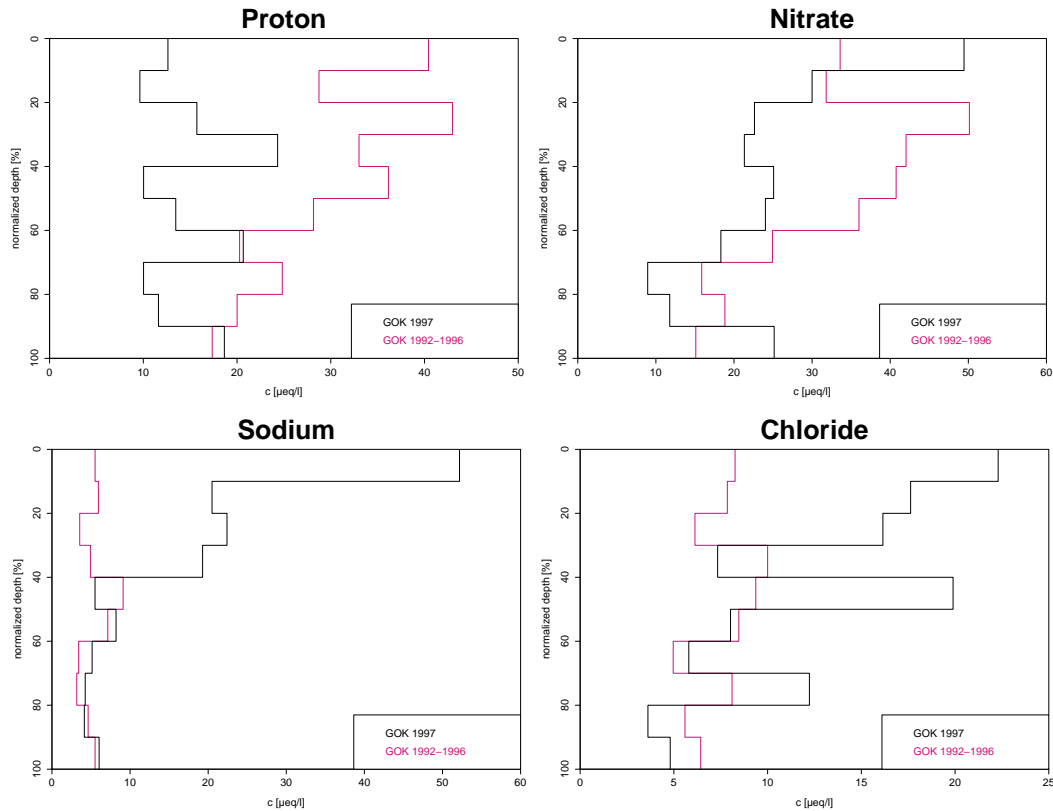


Figure 5.10.: Comparison of an average profile from 1992-1996 (pink) and the profile of 1997 (black), both normalized to 100% depth; Single year concentrations are always higher than the one from the averaged profile for Na^+ and Cl^- , but not for H^+ and NO_3^- .

The increased concentration of SO_4^{2-} (mean $> 15\mu\text{eq/l}$) relative to the trend is interesting, because the corresponding acidifying ions like H^+ and NO_3^- did not show increased concentrations. Therefore the question arises if the increased concentration of SO_4^{2-} was due to a different sampling method performed this year (see Table 2.2), the result of contamination or if it arises from remote transport of air masses.

Analyzing the time series of WADOS (usually **Wet And Dry Only**, but here *only Wet*) precipitation Sampler positioned nearby the Sonnblick observatory, no extreme value can be found for the SO_4^{2-} concentration in 1997 (see Figure 5.11). It can be assumed that the heightened SO_4^{2-} concentration arises through the proportion of dry deposition, which is mainly the deposition mechanism for local influence. Thus, it is supposed that there was no origin from remote transport for the heightened SO_4^{2-} concentration observed in the profile.

If the two profiles displayed on the left side in Figure 5.12 are compared, two layers could be identified in the profile of 1997 (black line) which showed much higher concentrations ($> 40\mu\text{eq/l}$) relative to the averaged profile of the previous five years (pink line). In contrast, the non-normalized profile from 1997, on the right side

in Figure 5.12, showed three layers with heightened concentrations of more than 30 µeq/l. These layers are not as clearly visible in the normalized picture as in the not normalized one. The difference arises from the normalization, where the concentrations of a few layers are averaged and the extreme values are thus put into perspective. According to this, the lower two layers (310-320cm and 510-520cm) seem to be outliers since the concentration of the single year is higher than the average of the previous five years.

But, in the Box-Whisker-Plots merely the layer from 510 to 520cm was identified as outlier only within the 1,5*IQR (given in Appendix C) . Therefore this layer can be regarded as “smooth” outlier and could be removed from the time series according to statistic rules. The other two layers can not be removed, even though the time series of GOK would look very similar to the one from WUK (see Figure 5.13). The shift of the trend line towards the one from WUK can be seen if the values for the three layers with the high concentrations are removed from the averaging one after the other, beginning with the deepest layer (510-520cm), followed by the two deepest layers (310-320cm and 510-520cm) and at last all three layers (110-120cm, 310-320cm and 510-520cm).

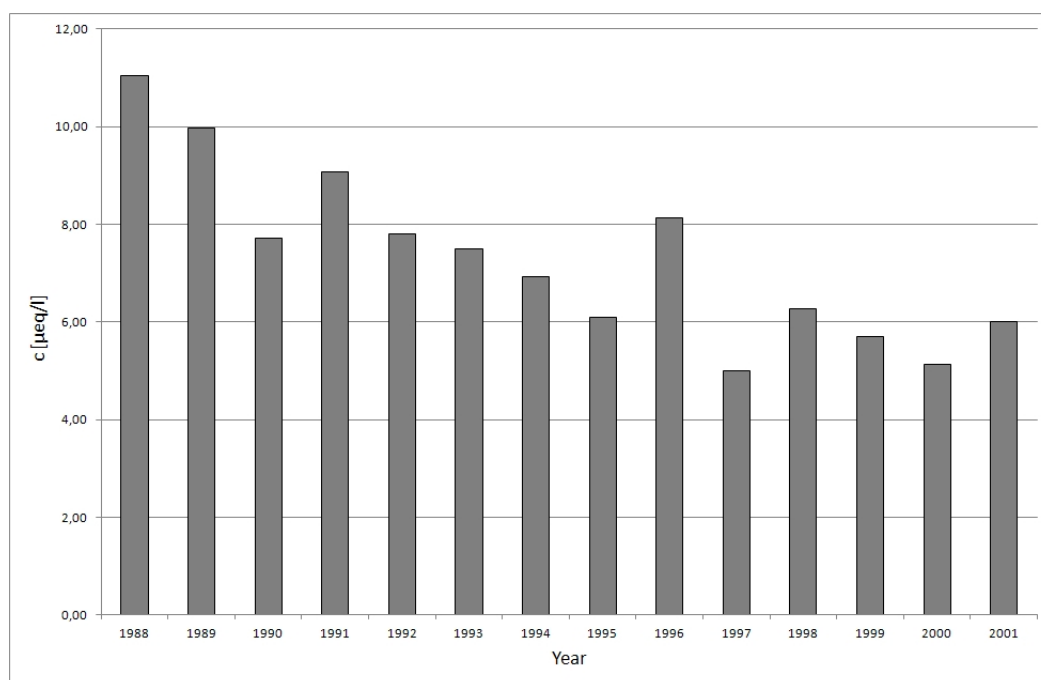


Figure 5.11.: WADOS time series of SO_4^{2-} concentration

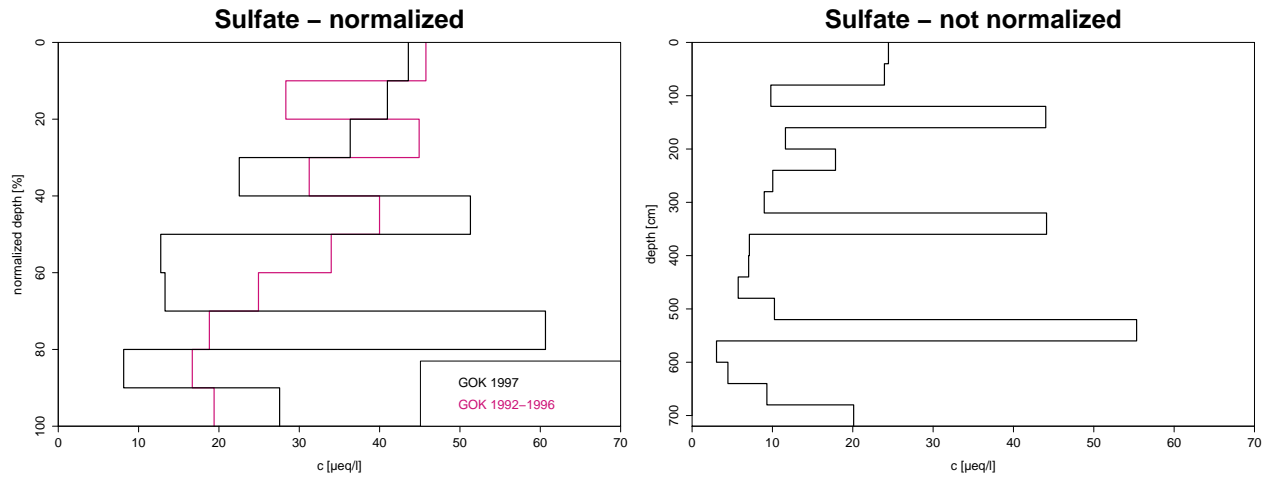


Figure 5.12.: Standardized profile (left) and non standardized profile (right) of SO_4^{2-} from GOK; Two layers (310-320cm and 510-520cm) may be outliers since the concentration of the single year profile is higher than of the averaged profile.

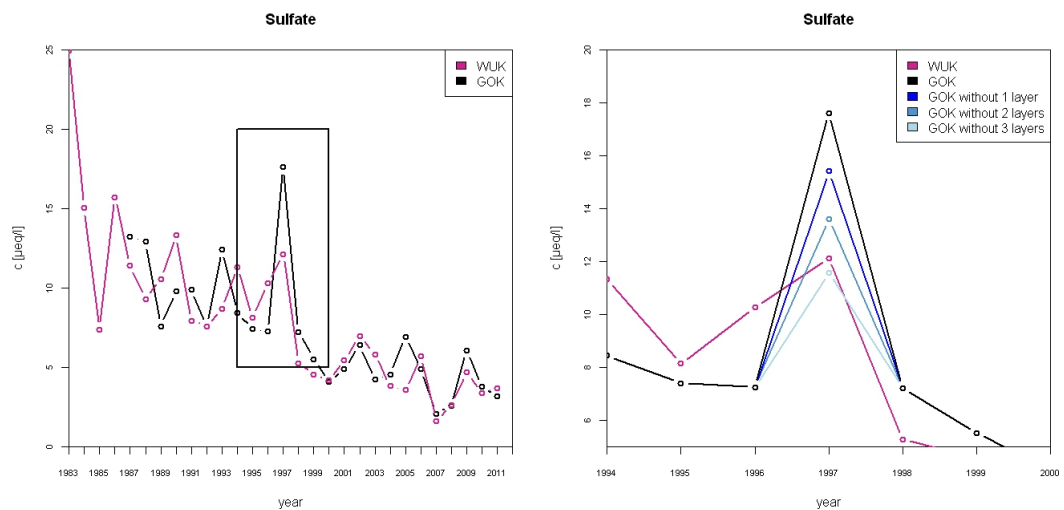


Figure 5.13.: Time series of WUK and GOK (left) and Zoom into the rectangular (right); If the three layers with the heightened values in the single year profile are removed from the data set, WUK and GOK time series would look very similar.

6. Main Findings and Conclusion

Since almost 30 years (from 1983 to 2011), snow samples were taken every spring at the maximum of the winter accumulation from snow pits at two Austrian glaciers, Goldbergkees (GOK) and Wurtenees (WUK) close to the Sonnblick Observatory (Nationalpark Hohe Tauern, approx. 3000m a.s.l., Austrian Alps). These samples were analyzed for the main components in high alpine snow, known to be Chloride (Cl^-), Nitrate (NO_3^-), Sulfate (SO_4^{2-}), Ammonium (NH_4^+), Sodium (Na^+), Potassium (K^+), Calcium (Ca^{2+}), Magnesium (Mg^{2+}) and the Hydron or Proton (H^+) to assess the temporal change of chemical composition and acidification. When analyzing the chemical composition of the samples taken, SO_4^{2-} and NO_3^- are identified as the main contributing anions with a proportion of 15% and 17% respectively. NH_4^+ (15%), Ca^{2+} (14%) and H^+ (17%) are found to be the dominating cations.

This work tried to identify the sources for the ions and to point out significant trends within the time series of acidification, concentration and deposition of the major ions. Additionally a comparison between the two sampling sites was done to see if the possible trends are significant for the researched region.

6.1. Main findings

For the identification of the source regions of the particular ions a Principal Component Analysis (PCA) with Varimax rotation was performed. The PCA converts the possibly correlated variables into groups of variables, linearly uncorrelated, called principal components or factors by maximizing the sum of the variances of the squared factor loads. The hierarchy of the principal components is then determined through the explained variance of each factor. For the ions in the snow cover, the PCA resulted in three factors with an explained cumulative variance of more than 70%.

1. The factor with the highest explained variance (~30%) represent the impact of Cl^- , Na^+ and K^+ .
2. The second factor (~24% explained variance) is loaded with SO_4^{2-} and NO_3^- as well as with NH_4^+ and H^+ .
3. The third factor (~17% explained variance) is correlated with Ca^{2+} and Mg^{2+} .

Similar studies assumed, that the ions of the first factor (Cl^- , Na^+ and K^+) originate from natural sources like sea salt aerosol. To prove this true, so called “non sea salt

concentrations”, based on the sea water ratios of every single ion with either Cl^- or Na^+ , were calculated. The result was, that Na^+ , Cl^- and K^+ are for 43%, 82% and 88% respectively not of maritime origin. It is assumed that these ions come from the impact of potash aerosols emitted during biomass combustion (especially charcoal) and K-fertilization in agriculture. The second factor, loaded with SO_4^{2-} , NO_3^- , NH_4^+ and H^+ , is known to be anthropogenically induced. The ions originate from the gas-to-particle conversion of gases emitted during fossil fuel combustion or biomass burning such as SO_2 and NO_x as well as NH_3 , emitted in animal husbandry or used for fertilization. The third factor (Ca^{2+} and Mg^{2+}) corresponds to dust aerosols, mainly from the Sahara, and is thus of natural origin. Hence, the PCA resulted in three factors where the two dominating once are of anthropogenic and only the last factor of natural origin.

Since the ions of the second factor, SO_4^{2-} , NO_3^- , NH_4^+ and H^+ are known to be responsible for the acidification (formation of the strong acid H_2SO_4 and the weak acid HNO_3) and partly for the neutralization (formation of the particular salts) of high alpine snow packs, this factor is the most important one for the estimation of the input of pollutants to the glaciers and their surrounding ecosystems. During the considered period, a significant decreasing trend in acidity of about 60%, and hence an increase in pH, was observed, which is attributed to a decrease in acidifying anions. According to this, both acidifying anions (SO_4^{2-} and NO_3^-) showed a significant decrease of 75% and 30%, respectively, during the analyzed time span. For the neutralizing ion NH_4^+ , no significant trend can be found, although the European NH_3 emissions and the N-fertilizer consumption show a decrease.

To see if the different orientation of the sampling sites in the terrain influences concentrations and deposition, the time series of the ions from both glaciers were compared. The trends for all ions on both glaciers is comparable even though several years could be identified in which differences occurred. Reasons for these differences are not identified yet and call for further investigations, especially concerning the analysis of the dominant flow in the particular years.

6.2. Conclusion and outlook

One of the main findings of the thesis is that the acidification of the snow and hence the input of acid melt water in surrounding ecosystems is regressive, caused through the decrease in concentration and deposition of acidifying ion such as SO_4^{2-} , NO_3^- and H^+ . The decline can be attributed to controlled emission reduction of their precursor gases SO_2 and NO_x . Even though the acidifying ions are loaded in the second factor of the PCA, they contribute the main part of ions in the snow cover and on the influence of acidification.

The second important outcome of this work was the finding, that the dominating factor of the PCA originates not from natural sources, like sea salt aerosols, but

from anthropogenic ones. Thus, the main part (7 out of 9 ions) of the ions are anthropogenic induced and only 2 ions (Ca^{2+} and Mg^{2+}) are of natural origin.

The analysis of the time series of the ion concentrations and deposition of the two sampling sites WUK and GOK, gave reasons for further investigations in interpreting the data. It would be interesting to analyze e.g. the seasonal input of ions or determine the amount which originates from rime and not from snow fall. Also further research in the identification of Saharan dust events seems to be necessary.

Bibliography

- Asman, W., A., H., and M. A. Sutton, 1998: Ammonia: emission, atmospheric transport and deposition, *New Phytologist*, Volume 139, p27-48
- Auer, I., R. Böhm, N. Hammer, W. Schöner, T. Wiesinger, W. Winiwarter, 1995: Glaziologische Untersuchungen im Sonnblickgebiet: Forschungsprogramm Wurtenkees, *Österreichische Beiträge zur Meteorologie und Geophysik*, Volume 12, Kapitel 5 (Schneechemie), p129-143
- Avila, A., 1996: Time trends in the precipitation chemistry at a mountain side in northeastern Spain for the period 1983-1994; *Atmospheric Environment*, Volume 30, No. 9, p1363-1373
- Barkan, J., P. Alpert, H. Kutiel, P. Kishcha, 2005: Synoptics of dust transportation days from Africa toward Italy and Central Europe; *Journal of Geophysical Research*, Volume 110, Issue D7, pD07208.1-D07208.14
- Barrie, L. A., 1985: Atmospheric particles: Their physical and chemical characteristics and deposition processes relevant to the chemical composition of glaciers; *Annals of Glaciology*, Volume 7, p100-108
- Chesworth, W., 2008: *Encyclopedia of soil science*, Springer, p245
- Colbeck, S. C., 1985: International Classification for seasonal snow on the ground, Hanover, Internat. Commission on Snow and Ice of the International Association of Scientific Hydrology
- De Angelis, M., A. Gaudichet, 1991: Saharan dust deposition over Mont Blanc (French Alps) during the last 30 years; *Tellus B*, Volume 43, Issue 1, p61-75
- Fellenberg, G., 1997: *Chemie der Umweltbelastung*, 3. Auflage, Stuttgart, B. G. Teubner
- Filippa, G., M. Freppaz, M. W. Williams, E. Zanini, 2010: Major element chemistry in inner alpine snow packs (Aosta Valley Region. NW Italy); *Cold Regions Science and Technology*, Volume 64, Issue 2, p158-166
- Fischer, H., D. Wagenbach, 1998: Sulfate and nitrate firn concentrations on the Greenland ice sheet 2. Temporal anthropogenic deposition changes; *Journal of Geophysical Research*, Volume 103, No. D17, p21.935-21.942
- Gabrielli, P., G. Cozzi, P. Cescon, C. Barbante, 2006: Source and origin of atmospheric trace elements entrapped in winter snow of the Italian Eastern Alps; *Atmospheric Chemistry and Physics Discussions*, Volume 6, p8781-8815

Intergovernmental Panel on Climate Change, Climate Change 2001, Cambridge University Press, p297-301

Jones, H. G., J. W. Pomeroy, D. A. Walker, R. W. Hohan, 2001: Snow Ecology, Cambridge University Press

Kalina, M. F., S. Stopper, E. Zambo, H. Puxbaum, 2001: Eintrag von Stickstoffverbindungen durch trockene, nasse und okkulte Deposition an zwei Höhenstufen in Achenkirch/Tirol (Mühleggerköpfl, 920m und Chritsumkopf, 1758m); FBVA-Berichte, No. 119, p73-83

Kuhn, M., J. Haslhofer, U. Nickus, H. Schellander, 1998: Seasonal development of ion concentration in a high alpine snow pack; Atmospheric Environment, Volume 32, No. 23, p4041-4051

Kumai, M., 1985: Acidity of snow and its reduction by alkaline aerosols; Annals of Glaciology, Volume 6, p92-94

Legrand, M., 1987: Chemistry of antarctic snow and ice; Journal de Physique, Volume 48, C1, pC1.77-C1.86

Maupetit, F., and R. J. Delmas, 1994: Snow chemistry of high altitude glaciers in the French Alps; Tellus B, Volume 46, Issue 4, p304-324

Maupetit, F., D. Wagenbach, P. Weddeling, J. Delmas, 1995: Seasonal fluxes of major ions to a high altitude cold alpine glacier; Atmospheric Environment, Volume 29, No. 1, p1-9

Mayer, D., 2008: Skriptum zur Vorlesung Allgemeine Meteorologie I

Möller, D., 2003: Luft, 1. Auflage, Berlin/New York, Walter De Gruyter

Mylona, S., 1996: Sulfur dioxide emissions in Europe 1880-1991 and their effect on sulfur concentrations and depositions, Tellus B, Volume 48, Issue 5, p662-689

Nickus, U., and M. Kuhn, 1993: Local Variance of Acid Deposition - A contribution to subproject ALPTRAC, The proceedings of EUROTRAC Symposium '92, edited by Borrell P.M., SPB Academic Publishing bv, p770-773

Nickus, U., M. Kuhn, U. Baltensberger, R. Delmas, H. Gäggeler, A. Kasper, H. Kromp-Kolb, F. Maupetit, A. Novo, F. Pichlmayer, S. Preunkert, H. Puxbaum, G. Rossi, W. Schöner, M. Schwikowski, P. Seibert, M. Staudinger, V. Trockner, D. Wagenbach, W. Winiwarter, 1997 : SNOSP: Ion deposition and concentration in high alpine snow packs; Tellus B, Volume 49, Issue 1, p56-71

Nickus, U., M. Kuhn, A. Novo, G. C. Rossi, 1998: Major element chemistry in alpine snow along a north-south transect in the Eastern Alps; Atmospheric Environment, Volume 32, No. 23, p4053-4060

Novo, A., and G. C. Rossi, 1998: A four-year record (1990-94) of snow chemistry at two glacier fields in the Italian Alps (Careser, 3090m; Colle Vincent, 4086m); Atmospheric Environment, Volume 32, No. 23, p4061-4073

- Paleczek, S., 1993: Analytische Charakterisierung von Aerosol-, Wolkenwasser- und Niederschlagsproben der hochalpinen Hintergrundmessstelle Sonnblick (3106m), Dissertation
- Pilson, M. E. Q., 1998: An introduction to the chemistry of the sea, Prentice-Hall Inc.
- Puxbaum, H., 1993: Luftchemie Skriptum
- Puxbaum, H., V. Simeonov, M. F. Kalina, 1998: Ten years trends (1984-1993) in the precipitation chemistry in Central Austria; *Atmospheric Environment*, Volume 32, No. 2, p193-202
- Rodriguez, S., A. Alastuey, S. Alonso-Pérez, X. Querol, E. Cuevas, J. Abreu-Afonso, M. Viana, N. Pérez, M. Pandolfi, J. de la Rosa, 2011: Transport of desert dust mixed with North African industrial pollutants in the subtropical Saharan Air Layer; *Atmospheric Chemistry and Physics*, Volume 11, p6663-6685
- Ruoho-Airola, T., S. Syri, G. Nordlund, 1998: Acid deposition trends at the Finnish Integrated Monitoring catchments in relation to emission reductions; *Boreal Environmental Research*, Volume 3, p205-219
- Schreiner, E., 2011: Spurenanalyse im Schnee, Bachelorarbeit
- Schöner, W., 1995: Schadstoffdeposition in einer hochalpinen winterlichen Schneedecke am Beispiel von Wurtenkees und Goldbergkees (Hohe Tauern), Dissertation
- Schwikowski, M., A. Novo, U. Baltensberger, R. Delmas, H. W. Gäggeler, A. Kasper, M. Kuhn, F. Maupetit, U. Nickus, S. Preunkert, H. Puxbaum, G. C. Rossi, W. Schöner, D. Wagenbach, 1997: Intercomparison of snow sampling and analysis within the alpine-wide snow pack investigation (SNOSP); *Water, Air and Soil Pollution*, Volume 93, p67-91
- Seilkop, S. K., and P. L. Finkelstein, 1987: Acid Precipitation Patterns and Trends in Eastern North America, 1980-84; *Journal of Climate and Applied Meteorology*, Volume 26, p980-994
- Spiridonov, V., and M. Curic, 2005: The Relative Importance of Scavenging, Oxidation and Ice-Phase Processes in the Production and Wet Deposition of Sulfate; *Journal of Atmospheric Sciences*, Volume 62, p2118-2135
- Staudinger, M., W. Schöner, H. Puxbaum, R. Böhm, 1997: Accumulation of Acidic Components in two Snowfields in the Sonnblick Region, Cloud multi-phase processes and high alpine air and snow chemistry, Springer, p219-224
- Vitovec, W., 1988: Untersuchungen zur Schneechemie des Wurtenkeesgletschers, Diplomarbeit
- Wagenbach, D., and K. O. Münnich, 1998: The anthropogenic impact of snow chemistry at Colle Gnifetti, Swiss Alps; *Annals of Glaciology*, Volume 10, p183-187
- Wallace, J., and P. Hobbs, 2006: *Atmospheric science - An introduction survey*, 2nd edition, Elsevier

Whitby, K.T., 1978: The physical characteristics of sulfur aerosols, *Atmospheric Environment*, Volume 12, Issues 1-3, p135-159 (compare PALECZEK, 1993)

Wiley, J. D., and R. H. Kiefer, 1990: A Contrast in Winter Rainwater Composition: Maritime versus Continental Rain in Eastern North Carolina; *Monthly Weather Review*, Volume 118, No. 2, p488-494

Winiwarter, W., H. Puxbaum, W. Schöner, R. Böhm, R. Werner, W. Vitovec, A. Kasper, 1998: Concentration of ionic compounds in the wintertime deposition: Results and trends from the Austrian Alps over 11 years (1983-1993); *Atmospheric Environment*, Volume 32, No. 23, p4031-4040

List of Figures

1.1.	The hydrological cycle; reveals interactions between different ecosystems and water reservoirs (Figure from the U.S. Geological Survey Homepage)	7
1.2.	Aerosol formation and deposition processes based on PALECZEK (1993). Small (<0,1µm) and big (>1µm) particles are deposited mainly through dry deposition processes such as diffusion and sedimentation, whereas particles between 0,1-1µm (mostly secondary aerosols) are deposited mainly through the mechanism of wet deposition.	12
1.3.	Goldberggruppe, part of the Nationalpark Hohe Tauern, Eastern Alps in Austria; Source: AMAP Austria - Bundesamt für Eich- und Vermessungswesen (BEV)	14
1.4.	Yellow dots represent the sampling sites on Goldbergkees (GOK) and Wurtenkees (WUK) in the Eastern Alps, Austria; Source: AMAP Austria - Bundesamt für Eich- und Vermessungswesen (BEV)	15
2.1.	Ion balance of samples from WUK and GOK for the period of 1983-2011 were concentrations of all ions are available. A cation excess is observed due to not measured carboxylic acids and organic anions.	21
2.2.	Measured vs. calculated Conductivity of samples from WUK and GOK for the period of 1983-2011 were concentrations of all ions are available. Measured conductivity showed higher values then the calculated one, perhaps due to carboxylic acids and organic anions not included in the calculation.	23
3.1.	Mean ion composition of the snow cover of the analyzed sites based on the ion concentrations	29
3.2.	Surface Seawater Composition [PILSON, 1998]	34
4.1.	Box-Whisker-Plot of measured conductivity including all layers where values are available from 1983-2011; left GOK, right WUK; A decreasing trend is present, due to the decrease of acidifying anions.	38
4.2.	Box-Whisker-Plot of acidity expressed in terms of the pH-value and the resulting proton concentration including all snow layers where values are available from 1983-2011; Top: GOK, Bottom: WUK; A decline in H ⁺ concentration and ,according to this, an increase in pH is observed.	39
4.3.	Box-Whisker-Plot of Sulfate and Nitrate of all layers where concentrations are available from 1983-2011; Top: GOK, bottom: WUK; A decrease in the concentration of both anions can be seen due to the emission reduction of their precursor gases.	40

4.4.	SO ₂ emissions (top) and NO _x emissions (bottom) of Europe, the European states with the highest emissions and Austria from 1986 - 2008; Data source: The EMEP Centre on Emission Inventories and Projections (CEIP); The reduction in emission is obvious.	41
4.5.	Estimated historical anthropogenic emissions of SO ₂ in Europe from 1880-1990. Reported total refers to emissions submitted by European countries to UN-ECE/EMEP [?]; Since the industrial revolution (1750-1850) the industrial SO ₂ emissions increased rapidly, but since the 1980's emissions are decreasing.	42
4.6.	Neutralization of acidic compounds (NO ₃ ⁻ and SO ₄ ²⁻) with NH ₄ ⁺ (left) or NH ₄ ⁺ and Ca ²⁺ (right); the 45° line represents neutralization of the samples; the shift towards neutralization is obvious when NH ₄ ⁺ and Ca ²⁺ are regarded as neutralizers	43
4.7.	Box-Whisker-Plot of Ammonium and Calcium of all layers where concentrations are available from 1983-2011; Top: GOK, bottom: WUK; No significant trends were observed for these ions.	44
4.8.	NH ₃ emissions (top) of Europe, the European states with the highest emissions and Austria from 1986 - 2008 and time trend of N-Fertilizer consumption (bottom) where values from 1987-2002 represent the consumption in tonnes whereas from 2002-2009 values represent the consumption in nutrients in tonnes of nutrients; Emission data source: The EMEP Centre on Emission Inventories and Projections (CEIP); Fertilizer data source: Food and Agriculture Organization of the United Nations (FAOSTATS)	45
4.9.	Schematic map of the general synoptic situation in periods of dust outbreaks from the Sahara to Europe (solid line: 700 hPa; dashed line: surface pressure) [BARKAN ET AL., 2005]	46
4.10.	Left: Average geopotential height of the dusty cases at 700 hPa, July 1979–1992; Right: Average geopotential height of the dusty period 5–9 July 1988 at 700 hPa [BARKAN ET AL., 2005]	46
4.11.	K-fertilizer consumption where values from 1987-2002 represent the consumption in tonnes whereas from 2002-2009 values represent the consumption in nutrients in tonnes of nutrients; Data source: Food and Agriculture Organization of the United Nations (FAOSTATS)	47
4.12.	Box-Whisker-Plot of Sodium, Chloride, Potassium of all layers where concentrations are available from 1983-2011; left: GOK, right: WUK; No significant trends were observed for the ions concerning potash.	48
4.13.	Box-Whisker-Plot of Magnesium of all layers where concentrations are available from 1983-2011; left: GOK, right: WUK; A significant decrease was observed only for GOK.	49
5.1.	Profile depth and Water equivalent of both sampling sites to show the similar tendency on both sampling sites. In the majority of the years the accumulation was higher on GOK due to the uplifting of incoming air masses which enables higher precipitation amounts.	52

5.2.	Left: Concentration in $\mu\text{eq/l}$ displayed as range from the mean \pm standard deviation; Right: Deposition in meq/m^2 of H^+ , SO_4^{2-} and NO_3^- ; In 1997 all three ions show a clear peak in deposition on both sites whereas only SO_4^{2-} shows a clear peak in the time series of concentration for 1997 especially for GOK, too. The high band in the concentration of H^+ arises is related with the high variation of H^+ , due to the high accuracy of 0,1-0,2 pH units.	54
5.3.	Left: Concentration in $\mu\text{eq/l}$ displayed as range from the mean \pm standard deviation; Right: Deposition in meq/m^2 of NH_4^+ , Ca^{2+} and Mg^{2+} ; In 1997 all three ions show a clear peak in deposition whereas concentrations do not. Additionally Ca^{2+} showed a peak in deposition and concentration for 1996. . . .	55
5.4.	Left: Concentration in $\mu\text{eq/l}$ displayed as range from the mean \pm standard deviation; Right: Deposition in meq/m^2 of Na^+ , Cl^- and K^+ . In 1997 all three ions show a clear peak in deposition, whereas concentration showed only a peak for the GOK sampling site. Additionally clear peaks in concentration and deposition were observed for all three ions on WUK in 2002 and 2006, and on GOK in 2006 and from 2008-2010.	56
5.5.	Depth profiles for Ca^{2+} in 1996; left: WUK, right: GOK	57
5.6.	Depth profiles for Na^+ , Cl^- and K^+ for the year 2002; top: WUK, bottom: GOK; It is shown that in this particular year it seems that WUK received more often air polluted with potash ions, originating mainly from biomass combustion (especially wood charcoal) and K-Fertilization.	58
5.7.	Depth profiles for Na^+ , Cl^- and K^+ for the year 2009; top: WUK, bottom: GOK; It is shown that in this particular year it seems that GOK received more often air polluted with potash ions, originating mainly from biomass combustion (especially wood charcoal) and K-Fertilization.	59
5.8.	Depth profiles for Na^+ , Cl^- and K^+ for the year 2006; top: WUK, bottom: GOK; In the WUK profile two layers (60-80cm) had increased concentrations ($> 50\mu\text{eq/l}$) of all three ions, relative to the rest of the profile. GOK showed slightly increased concentrations (10-40 $\mu\text{eq/l}$) over the whole profile.	60
5.9.	Comparison of an average profile from 1992-1996 (pink) and the profile of 1997 (black), both normalized to 100% depth; Single year concentrations are within the magnitude of the averaged profile, except for K^+	61
5.10.	Comparison of an average profile from 1992-1996 (pink) and the profile of 1997 (black), both normalized to 100% depth; Single year concentrations are always higher than the one from the averaged profile for Na^+ and Cl^- , but not for H^+ and NO_3^-	62
5.11.	WADOS time series of SO_4^{2-} concentration	63
5.12.	Standardized profile (left) and non standardized profile (right) of SO_4^{2-} from GOK; Two layers (310-320cm and 510-520cm) may be outliers since the concentration of the single year profile is higher than of the averaged profile.	64
5.13.	Time series of WUK and GOK (left) and Zoom into the rectangular (right); If the three layers with the heightened values in the single year profile are removed from the data set, WUK and GOK time series would look very similar.	64

D.1. from left to right 1983-1994	98
D.2. from left to right 1995-2006	99
D.3. from left to right 2007-2011	100
D.4. from left to right 1987-1998	101
D.5. from left to right 1998-2010	102
D.6. from left to right 2011	103

List of Tables

1.1. Primary particle emissions for the year 2000, source strength for emissions in the particular reference year of secondary aerosol precursors and estimates for secondary aerosol sources for the year 2000. Edited table, based on results from the Intergovernmental Panel on Climate Change (2001).	11
2.1. Sampling methods used in the particular years	17
2.2. Snow pit depth, water equivalent and number of samples for both sampling sides and all years from 1983-2011	18
2.3. pH and conductivity instruments	19
2.4. Instruments and adjustments of Ion chromatography	19
2.5. Comparison of limits of detection for the particular ions reported by SCHREINER (2011) (left) and VITOVEC (1988) (right)	19
2.6. Spearman Correlation coefficient and Kendall Trend Analysis of the Ion balance for the sites analyzed from 1983-2011; Significance levels: ^{a)} $p < 0,05$; ^{b)} $p < 0,01$; ^{c)} $p < 0,001$; n.s. = not significant	22
2.7. Equivalent Conductivity Λ_0 used for the calculation of the conductivity	22
2.8. Spearman correlation coefficients of measured and calculated Conductivity for both sampling sites from 1983-2012	23
2.9. Summary of the analytical and spatial coefficients of variation; bold values are used to calculate the total variability with the Gaussian error propagation (see Chapter 2.5.5); ^{a)} samples taken at grid distances of 10cm in a rectangle of 60x50cm; ^{b)} 20 samples in a vertical line at distances of 1m; ^{c)} 24 samples in a vertical line at distances of 10m	25
2.10. Total variability [%] calculated with the Gaussian error propagation from the analytic and mesoscale variability marked bold in Table 2.9	27
3.1. Spearman correlation matrix including ion concentrations of both sampling sites from 1983-2012	30
3.2. PCA WUK and GOK excl. H^+ and 3 factors	31
3.3. PCA WUK and GOK excl. H^+ and 4 factors	32
3.4. PCA WUK and GOK incl. H^+ and 3 factors	32
3.5. PCA WUK and GOK incl. H^+ and 4 factors	33
3.6. Non sea salt proportions given in [$\mu\text{eq/l}$] or [%] of the specific ion, based on the sea water ratio with Cl^- (Top) or Na^+ (Bottom) and either the mean or median of the time series	34

4.1. Kendall test for temporal trends of the annual volume weighted mean concentrations, the median or the deposition; colors account for different significance levels: n.s. = not significant; red: $p < 0,1$; orange: $p < 0,05$; yellow: $p < 0,01$; green: $p < 0,001$	37
5.1. Standard deviation in $\mu\text{eq/l}$ of the specific ions, based on the calculation of the total variability (sum of analytic and mesoscale variability).	51
5.2. Overview of the events clear peaks in the time series of WUK and GOK	53
A.1. Volume Weighted Means in $\mu\text{eq/l}$ of measured ions on both sampling sides	82
A.2. Median of the Volume Weighted concentrations $\mu\text{eq/l}$ of measured ions on both sampling sides	83
A.3. Deposition in meq/m^2 of measured ions on both sampling sides	84
B.1. Spearman correlation matrix WUK	86
B.2. PCA WUK incl. H^+ and 3 factors	86
B.3. PCA WUK incl. H^+ and 4 factors	86
B.4. PCA WUK excl. H^+ and 3 factors	87
B.5. PCA WUK excl. H^+ and 4 factors	87
B.6. Spearman correlation matrix GOK	87
B.7. PCA GOK incl. H^+ and 3 factors	88
B.8. PCA GOK incl. H^+ and 4 factors	88
B.9. PCA GOK excl. H^+ and 3 factors	88
B.10. PCA GOK excl. H^+ and 4 factors	89

Appendix

A. Mean, Median and Deposition

	GOK										WUK									
	Na ⁺	K ⁺	Cl ⁻	SO ₄ ²⁻	NO ₃ ⁻	NH ₄ ⁺	Ca ²⁺	Mg ²⁺	H ⁺		Na ⁺	K ⁺	Cl ⁻	SO ₄ ²⁻	NO ₃ ⁻	NH ₄ ⁺	Ca ²⁺	Mg ²⁺	H ⁺	
1983	-	-	-	-	-	-	-	-	-		-	-	12,29	24,95	7,88	-	-	-	-	39,48
1984	-	-	-	-	-	-	-	-	-		-	-	3,91	15,05	12,12	-	-	-	-	16,99
1985	-	-	-	-	-	-	-	-	-		-	-	3,69	7,38	6,57	-	-	-	-	7,91
1986	-	-	-	-	-	-	-	-	-		1,42	1,51	6,26	15,73	8,19	15,73	-	-	-	22,64
1987	2,20	1,07	2,32	13,22	9,22	5,29	8,01	2,43	11,22		1,19	1,97	1,59	11,41	8,47	4,64	5,49	0,69	11,94	
1988	3,36	1,97	4,38	12,91	9,99	7,82	-	-	26,52		2,87	1,32	3,80	9,29	10,05	6,52	-	-	-	37,05
1989	1,70	0,96	2,31	7,58	7,66	4,30	-	-	6,18		4,94	2,33	5,58	10,56	9,38	4,62	-	-	-	3,44
1990	2,41	1,53	3,26	9,77	6,06	8,96	-	-	7,39		2,02	1,05	3,24	13,31	10,25	9,72	-	-	-	8,12
1991	3,69	0,84	2,15	9,88	11,03	7,36	7,37	2,04	8,77		3,91	1,81	4,02	7,92	8,23	6,85	3,57	2,12	6,39	
1992	2,53	2,34	1,95	7,57	7,17	4,29	8,75	2,30	8,12		5,31	1,55	5,22	7,58	7,09	5,11	4,94	1,13	10,25	
1993	1,17	0,50	1,42	12,40	12,28	8,87	6,00	2,05	12,96		1,33	0,42	1,71	8,66	9,39	7,07	7,17	2,22	10,88	
1994	1,74	0,74	2,01	8,44	6,74	5,68	6,79	1,62	8,84		2,23	0,47	2,89	11,32	6,21	5,39	10,86	1,53	4,45	
1995	1,67	0,56	2,81	7,39	8,91	10,83	2,96	0,74	9,72		1,96	0,89	2,51	8,13	9,99	15,22	2,66	0,66	5,28	
1996	0,56	0,34	1,78	7,24	7,70	6,39	20,45	0,70	2,22		4,48	0,50	5,69	10,27	7,30	8,54	9,03	1,47	1,43	
1997	8,21	2,37	6,55	17,62	13,15	10,14	7,24	1,33	8,16		3,67	0,80	3,91	12,13	9,99	8,44	6,35	1,52	6,45	
1998	1,61	0,58	2,29	7,21	10,27	8,14	2,15	0,97	6,96		1,35	0,57	2,27	5,26	7,53	4,37	1,78	0,80	6,46	
1999	2,86	0,86	2,66	5,51	11,32	8,16	5,37	0,95	10,34		2,28	0,64	2,40	4,54	9,78	13,37	4,85	1,29	3,77	
2000	2,19	2,13	2,05	4,08	6,81	5,59	8,04	2,25	6,42		2,32	1,59	2,68	4,16	8,53	5,24	7,63	2,13	4,59	
2001	1,71	0,74	1,66	4,88	6,06	8,62	3,40	2,85	9,08		5,27	2,58	3,50	5,45	4,29	7,11	9,97	2,62	5,03	
2002	2,20	0,86	1,87	6,39	7,58	6,82	7,32	1,93	2,74		14,47	3,92	14,14	6,96	7,87	5,20	9,98	1,61	7,58	
2003	6,04	1,41	5,17	4,21	7,76	6,77	4,55	1,25	1,68		4,40	1,36	3,92	5,81	11,05	8,12	9,67	1,79	0,94	
2004	2,77	0,67	2,12	4,51	6,60	8,36	4,83	1,16	0,53		2,17	0,65	2,23	3,81	8,77	6,41	8,05	1,25	0,90	
2005	10,02	2,46	5,82	6,93	9,51	5,89	3,63	1,01	2,65		2,35	1,10	2,28	3,55	8,52	3,47	4,67	0,89	1,67	
2006	16,25	3,65	15,31	4,86	6,65	5,03	10,21	2,03	9,75		14,22	4,75	14,42	5,69	7,43	4,51	6,78	1,36	5,78	
2007	2,40	1,19	2,05	2,05	4,52	5,58	3,69	1,25	2,13		0,36	0,93	1,35	1,62	3,93	1,08	3,29	0,51	2,42	
2008	11,36	2,98	6,60	2,57	5,06	5,94	4,13	1,03	7,17		2,86	0,73	3,12	2,62	6,10	4,19	4,41	1,31	15,32	
2009	7,67	1,91	7,34	6,06	8,61	7,84	9,60	1,06	3,00		2,41	0,82	2,68	4,68	7,28	6,76	7,33	0,83	2,96	
2010	3,13	2,14	2,15	3,77	7,98	11,23	8,66	0,74	2,58		1,59	0,57	1,77	3,38	5,75	7,67	12,05	0,97	1,42	
2011	0,87	0,31	1,79	3,16	6,44	9,39	17,18	0,58	4,58		2,51	1,02	1,77	3,69	5,13	7,34	11,21	1,18	2,76	

Table A.1.: Volume Weighted Means in µeq/l of measured ions on both sampling sides

	GOK							WUK											
	Na ⁺	K ⁺	Cl ⁻	SO ₄ ²⁻	NO ₃ ⁻	NH ₄ ⁺	Ca ²⁺	Mg ²⁺	H ⁺	Na ⁺	K ⁺	Cl ⁻	SO ₄ ²⁻	NO ₃ ⁻	NH ₄ ⁺	Ca ²⁺	Mg ²⁺	H ⁺	
1983	-	-	-	-	-	-	-	-	-	-	-	8,74	22,55	6,69	-	-	-	-	31,62
1984	-	-	-	-	-	-	-	-	-	-	-	3,46	9,37	9,14	-	-	-	-	11,44
1985	-	-	-	-	-	-	-	-	-	-	-	3,55	7,08	5,89	-	-	-	-	6,69
1986	-	-	-	-	-	-	-	-	-	1,04	0,92	5,59	14,33	7,95	14,33	-	-	-	19,13
1987	1,40	0,77	1,38	9,25	6,80	3,70	6,20	0,89	7,28	1,23	1,03	1,09	7,94	9,22	3,69	4,59	0,45	9,32	
1988	2,30	1,11	2,96	8,87	7,51	4,47	-	-	9,30	2,54	0,96	3,39	7,50	8,97	4,73	-	-	-	11,06
1989	0,92	0,61	1,30	6,18	5,94	3,64	-	-	4,31	4,14	1,85	4,07	7,12	7,68	4,17	-	-	-	1,64
1990	1,55	0,81	2,38	6,00	4,68	6,65	-	-	2,72	1,66	0,83	2,70	9,39	8,24	7,54	-	-	-	5,87
1991	1,61	0,71	1,72	8,70	10,73	6,05	3,16	1,57	8,47	2,95	1,29	3,03	6,17	6,18	3,64	2,41	1,49	6,51	
1992	1,63	0,11	0,81	6,57	5,90	3,06	3,81	2,24	7,35	4,39	1,33	4,18	6,76	6,70	3,87	3,87	1,05	8,62	
1993	0,73	0,57	1,01	8,94	8,84	3,86	5,28	1,84	11,49	1,32	0,36	1,65	7,01	7,56	4,77	5,63	2,15	7,87	
1994	1,27	0,71	1,52	8,26	5,02	3,43	3,43	1,38	4,79	1,47	0,52	2,06	9,67	5,36	4,53	5,06	1,12	3,86	
1995	1,33	0,51	2,22	5,94	7,29	8,37	2,14	0,71	7,32	1,37	0,46	2,02	6,12	8,18	14,59	1,89	0,51	3,66	
1996	0,45	0,31	1,57	6,04	6,49	5,34	18,48	0,52	1,24	1,33	0,51	2,92	6,08	6,98	7,32	4,66	0,87	1,33	
1997	3,89	1,56	4,80	10,14	13,10	9,81	6,42	1,10	7,34	3,10	0,51	3,34	12,31	10,72	6,91	3,84	1,30	6,62	
1998	0,56	0,30	1,89	6,05	7,72	5,36	0,59	0,93	6,02	0,61	0,28	1,67	4,26	5,16	1,72	0,85	0,81	5,07	
1999	2,23	0,57	2,02	4,64	8,10	4,60	3,79	0,67	9,07	1,65	0,50	1,37	3,34	6,97	11,62	2,44	0,61	3,48	
2000	1,59	1,21	1,40	3,66	5,68	3,82	5,31	1,73	4,16	1,86	1,27	2,13	3,66	6,77	4,40	5,08	1,60	3,57	
2001	1,41	0,62	1,26	3,85	3,87	5,53	2,47	2,36	7,59	2,64	1,16	1,57	4,18	3,30	5,27	6,56	1,73	3,35	
2002	1,59	0,69	1,40	3,74	5,71	4,00	5,20	1,61	1,53	11,65	3,23	10,89	4,28	5,61	3,04	9,29	1,43	5,54	
2003	4,16	1,04	3,58	3,35	7,04	4,43	3,17	1,01	1,20	2,43	0,72	2,50	4,78	10,31	6,41	5,68	1,27	0,70	
2004	1,73	0,50	1,52	4,26	6,06	8,07	3,87	0,92	0,39	1,42	0,48	1,55	3,16	6,21	3,86	5,30	1,26	0,73	
2005	3,68	1,35	2,78	5,37	5,55	4,96	3,17	0,91	1,40	1,33	0,61	1,54	2,89	6,23	2,74	3,49	0,63	1,56	
2006	13,20	3,49	13,18	4,36	5,55	3,64	8,38	1,63	4,12	10,49	2,31	9,99	3,77	5,46	3,06	5,61	1,17	4,84	
2007	1,10	0,87	1,20	1,43	3,29	3,73	2,64	1,36	2,12	0,26	0,74	1,10	1,38	3,40	0,53	2,75	0,51	2,59	
2008	11,00	2,70	4,50	2,20	3,51	4,64	3,10	0,93	3,37	2,55	0,69	2,94	2,52	5,83	3,31	3,40	0,69	4,76	
2009	2,58	0,83	3,01	4,32	7,39	4,41	6,27	0,73	2,07	1,87	0,64	2,12	3,85	6,28	3,20	5,30	0,74	2,52	
2010	2,81	2,13	1,97	3,44	6,58	6,73	8,50	0,65	2,12	1,25	0,42	1,43	2,75	4,66	5,23	11,48	0,96	1,18	
2011	0,77	0,24	1,46	2,40	5,50	6,47	16,13	0,54	4,93	2,39	0,85	1,55	2,76	5,58	5,70	10,08	0,73	2,44	

Table A.2.: Median of the Volume Weighted concentrations µeq/l of measured ions on both sampling sides

	GOK									WUK									
	Na ⁺	K ⁺	Cl ⁻	SO ₄ ²⁻	NO ₃ ⁻	NH ₄ ⁺	Ca ²⁺	Mg ²⁺	H ⁺	Na ⁺	K ⁺	Cl ⁻	SO ₄ ²⁻	NO ₃ ⁻	NH ₄ ⁺	Ca ²⁺	Mg ²⁺	H ⁺	
1983	-	-	-	-	-	-	-	-	-	-	-	-	-	-	-	-	-	-	-
1984	-	-	-	-	-	-	-	-	-	-	-	-	-	-	-	-	-	-	-
1985	-	-	-	-	-	-	-	-	-	-	-	-	-	-	-	-	-	-	-
1986	-	-	-	-	-	-	-	-	-	-	-	-	-	-	-	-	-	-	-
1987	85,69	41,55	89,96	521,15	359,54	205,51	308,45	93,68	443,70	41,47	68,42	55,31	396,88	194,79	161,61	191,06	24,18	415,54	
1988	126,68	74,17	164,99	486,35	376,16	294,74	-	-	99,87	122,62	56,33	162,58	397,26	429,79	278,94	-	-	1584,58	
1989	64,52	37,58	87,57	287,68	290,67	163,02	-	-	234,33	189,42	89,27	214,17	405,25	359,82	177,08	-	-	131,82	
1990	99,15	62,83	134,30	402,10	249,56	369,01	-	-	313,23	83,95	43,86	135,02	554,43	426,84	404,86	-	-	338,26	
1991	140,97	32,09	82,30	377,40	421,13	281,06	281,61	77,81	334,95	129,70	56,35	133,27	262,53	272,93	227,12	114,52	70,26	211,77	
1992	81,58	75,43	62,79	243,82	231,05	138,21	281,82	73,99	261,48	212,59	63,81	214,61	311,38	291,42	204,63	202,88	46,37	421,22	
1993	42,79	18,29	51,88	453,62	449,22	324,63	219,52	75,03	474,22	48,73	15,50	62,70	318,20	344,82	259,61	263,34	81,39	399,59	
1994	66,60	28,24	76,79	322,98	258,12	217,53	260,03	61,98	338,58	87,03	15,50	62,70	318,20	344,82	259,61	263,34	81,39	399,59	
1995	63,58	21,36	107,30	281,86	339,69	413,04	112,88	28,38	377,39	76,03	18,35	112,68	442,24	242,66	210,43	424,16	57,60	173,73	
1996	20,77	12,63	66,40	270,20	287,17	238,46	762,76	26,13	83,00	181,84	20,50	231,36	417,34	296,59	347,14	366,80	59,80	58,36	
1997	1227,22	354,08	978,61	2634,87	1966,54	1515,66	1081,70	198,58	1219,29	643,83	140,92	686,37	2127,62	1751,72	1480,62	1114,67	266,55	1131,71	
1998	70,69	17,50	93,25	300,84	431,90	365,38	84,38	37,66	289,03	54,57	23,21	92,13	216,12	304,85	177,09	72,26	32,47	261,47	
1999	121,39	36,68	113,04	233,69	480,35	346,24	227,92	40,39	438,69	86,60	24,42	91,24	172,15	371,36	507,46	184,08	49,00	143,06	
2000	94,61	92,00	88,71	176,62	294,75	241,97	347,71	97,41	277,76	103,87	70,91	119,83	185,90	381,20	234,15	341,00	95,04	192,72	
2001	60,38	26,03	58,46	172,17	213,76	304,02	119,85	100,60	320,15	190,33	93,11	126,40	197,03	155,18	256,97	371,10	102,03	181,71	
2002	91,96	35,96	78,26	266,57	316,41	284,51	305,54	80,50	114,21	555,38	150,52	542,55	266,97	301,99	199,65	383,15	61,69	291,03	
2003	246,13	57,43	210,62	171,53	316,11	275,81	185,42	50,91	68,41	164,88	51,06	146,88	217,86	414,29	304,37	362,42	67,14	35,06	
2004	126,62	30,31	96,82	206,32	301,96	382,82	221,14	53,06	24,35	87,71	26,19	89,98	153,82	353,83	258,68	324,72	50,46	36,35	
2005	395,61	97,00	229,81	273,75	375,33	232,53	143,32	39,78	104,70	96,13	44,88	93,00	145,19	348,42	141,87	190,88	36,27	68,21	
2006	646,98	145,17	609,26	193,32	164,83	200,23	406,55	80,64	388,21	572,89	191,36	580,93	229,28	299,49	181,84	273,29	54,68	232,94	
2007	114,87	57,10	98,23	97,86	216,07	266,79	176,74	60,02	101,82	16,95	44,37	64,08	76,99	186,58	51,20	156,14	24,35	114,86	
2008	418,26	109,62	242,77	97,61	186,41	218,66	151,93	38,00	263,79	117,06	29,89	127,71	107,51	249,90	171,78	180,59	53,85	628,04	
2009	298,94	74,70	286,14	237,63	338,30	308,03	382,00	42,00	117,60	93,65	31,73	104,18	181,74	282,92	262,71	284,62	31,16	115,10	
2010	138,63	94,94	95,32	166,73	353,30	497,13	383,40	32,63	114,17	58,28	20,75	64,95	123,71	210,51	280,78	441,34	35,64	51,91	
2011	39,18	13,93	80,36	141,49	288,44	420,44	769,45	26,18	205,28	115,12	46,88	81,11	168,88	235,06	336,07	513,30	54,16	126,18	

Table A.3.: Deposition in meq/m² of measured ions on both sampling sides

B. Source Analysis

B.1. PCA WUK

	K ⁺	Na ⁺	Cl ⁻	SO ₄ ²⁻	NO ₃ ⁻	NH ₄ ⁺	Ca ²⁺	Mg ²⁺	H ⁺
K ⁺	1	0,693	0,619	0,149	0,038	-0,115	0,362	0,331	0,075
Na ⁺		1	0,815	0,133	0,088	0,073	0,471	0,412	-0,047
Cl ⁻			1	0,372	0,216	0,073	0,425	0,431	0,159
SO ₄ ²⁻				1	0,569	0,529	0,289	0,378	0,443
NO ₃ ⁻					1	0,495	0,225	0,236	0,316
NH ₄ ⁺						1	0,143	0,200	0,007
Ca ²⁺							1	0,583	-0,211
Mg ²⁺								1	-0,035
H ⁺									1

Table B.1.: Spearman correlation matrix WUK

	F1	F2	F3	Commonality
Cl ⁻	0,96	0,11	0,10	0,94
NO ₃ ⁻	-0,02	0,75	0,08	0,57
SO ₄ ²⁻	0,16	0,82	0,12	0,70
Na ⁺	0,93	-0,01	0,18	0,89
NH ₄ ⁺	-0,08	0,72	0,16	0,55
K ⁺	0,92	0,01	0,06	0,84
Mg ²⁺	0,14	0,12	0,83	0,71
Ca ²⁺	0,15	0,06	0,86	0,76
H ⁺	0,08	0,56	-0,34	0,43

	F1	F2	F3
SS loadings	2,69	2,09	1,62
Proportion Var.	0,30	0,23	0,18
Cumulative Var.	0,30	0,53	0,71

Table B.2.: PCA WUK incl. H⁺ and 3 factors

	F1	F2	F3	F4	Commonality
Cl ⁻	0,95	0,06	0,12	0,11	0,94
NO ₃ ⁻	0,01	0,78	0,04	0,16	0,63
SO ₄ ²⁻	0,14	0,64	0,20	0,51	0,72
Na ⁺	0,93	0,00	0,17	-0,04	0,90
NH ₄ ⁺	-0,02	0,89	0,03	-0,09	0,81
K ⁺	0,92	0,01	0,05	-0,01	0,85
Mg ²⁺	0,12	0,07	0,87	0,03	0,77
Ca ²⁺	0,13	0,06	0,87	-0,07	0,79
H ⁺	0,00	0,09	-0,08	0,95	0,93

	F1	F2	F3	F4
SS loadings	2,68	1,82	1,61	1,22
Proportion Var.	0,30	0,20	0,18	0,14
Cumulative Var.	0,30	0,50	0,68	0,82

Table B.3.: PCA WUK incl. H⁺ and 4 factors

B.2 PCA GOK

	F1	F2	F3	Commonality
Cl ⁻	0,96	0,10	0,12	0,94
NO ₃ ⁻	0,00	0,79	0,02	0,62
SO ₄ ²⁻	0,15	0,77	0,16	0,64
Na ⁺	0,93	0,00	0,17	0,89
NH ₄ ⁺	-0,04	0,83	0,02	0,69
K ⁺	0,92	0,02	0,06	0,85
Mg ²⁺	0,12	0,10	0,87	0,77
Ca ²⁺	0,13	0,07	0,87	0,79

	F1	F2	F3
SS loadings	2,68	1,93	1,59
Proportion Var.	0,33	0,24	0,20
Cumulative Var.	0,33	0,58	0,77

Table B.4.: PCA WUK excl. H⁺ and 3 factors

	F1	F2	F3	F4	Commonality
Cl ⁻	0,96	0,11	0,11	0,03	0,94
NO ₃ ⁻	0,02	0,33	0,05	0,93	0,97
SO ₄ ²⁻	0,14	0,87	0,14	0,08	0,80
Na ⁺	0,93	-0,02	0,18	0,03	0,90
NH ₄ ⁺	-0,05	0,80	0,01	0,30	0,73
K ⁺	0,92	0,04	0,05	-0,03	0,85
Mg ²⁺	0,11	0,15	0,86	-0,06	0,78
Ca ²⁺	0,13	0,00	0,88	0,12	0,81

	F1	F2	F3	F4
SS loadings	2,68	1,54	1,59	0,98
Proportion Var.	0,33	0,19	0,20	0,12
Cumulative Var.	0,33	0,52	0,72	0,84

Table B.5.: PCA WUK excl. H⁺ and 4 factors

B.2. PCA GOK

	K ⁺	Na ⁺	Cl ⁻	SO ₄ ²⁻	NO ₃ ⁻	NH ₄ ⁺	Ca ²⁺	Mg ²⁺	H ⁺
K ⁺	1	0,825	0,643	0,110	0,044	0,062	0,196	0,389	-0,034
Na ⁺		1	0,780	0,099	0,110	0,130	0,193	0,303	-0,103
Cl ⁻			1	0,295	0,308	0,248	0,263	0,272	-0,007
SO ₄ ²⁻				1	0,684	0,554	0,157	0,383	0,410
NO ₃ ⁻					1	0,592	0,187	0,215	0,431
NH ₄ ⁺						1	0,169	0,130	0,159
Ca ²⁺							1	0,378	-0,200
Mg ²⁺								1	0,035
H ⁺									1

Table B.6.: Spearman correlation matrix GOK

	F1	F2	F3	Commonality
Cl ⁻	0,94	0,08	0,11	0,90
NO ₃ ⁻	0,02	0,84	0,05	0,71
SO ₄ ²⁻	0,08	0,81	0,18	0,70
Na ⁺	0,96	0,01	0,06	0,93
NH ₄ ⁺	0,04	0,78	0,08	0,62
K ⁺	0,91	0,00	0,13	0,85
Mg ²⁺	0,16	0,06	0,79	0,66
Ca ²⁺	0,04	0,03	0,85	0,73
H ⁺	-0,03	0,53	-0,28	0,36

	F1	F2	F3
SS loadings	2,69	2,26	1,50
Proportion Var.	0,30	0,25	0,17
Cumulative Var.	0,30	0,55	0,72

Table B.7.: PCA GOK incl. H⁺ and 3 factors

	F1	F2	F3	F4	Commonality
Cl ⁻	0,94	0,09	0,10	0,00	0,-0
NO ₃ ⁻	0,02	0,82	0,03	0,20	0,72
SO ₄ ²⁻	0,07	0,77	0,18	0,25	0,70
Na ⁺	0,96	0,02	0,06	-0,02	0,93
NH ₄ ⁺	0,03	0,89	-0,03	-0,12	0,80
K ⁺	0,91	0,01	0,13	-0,02	0,85
Mg ²⁺	0,19	0,02	0,83	0,09	0,74
Ca ²⁺	0,04	0,10	0,83	-0,17	0,73
H ⁺	-0,04	0,20	-0,07	0,94	0,94

	F1	F2	F3	F4
SS loadings	2,68	2,11	1,46	1,05
Proportion Var.	0,30	0,23	0,16	0,12
Cumulative Var.	0,30	0,53	0,70	0,81

Table B.8.: PCA GOK incl. H⁺ and 4 factors

	F1	F2	F3	Commonality
Cl ⁻	0,94	0,10	0,11	0,90
NO ₃ ⁻	0,01	0,85	0,02	0,72
SO ₄ ²⁻	0,07	0,81	0,16	0,69
Na ⁺	0,96	0,02	0,06	0,93
NH ₄ ⁺	0,03	0,85	-0,02	0,72
K ⁺	0,91	0,01	0,14	0,85
Mg ²⁺	0,19	0,05	0,82	0,71
Ca ²⁺	0,04	0,06	0,85	0,73

	F1	F2	F3
SS loadings	2,68	2,11	1,45
Proportion Var.	0,33	0,26	0,18
Cumulative Var.	0,33	0,60	0,78

Table B.9.: PCA GOK excl. H⁺ and 3 factors

B.2 PCA GOK

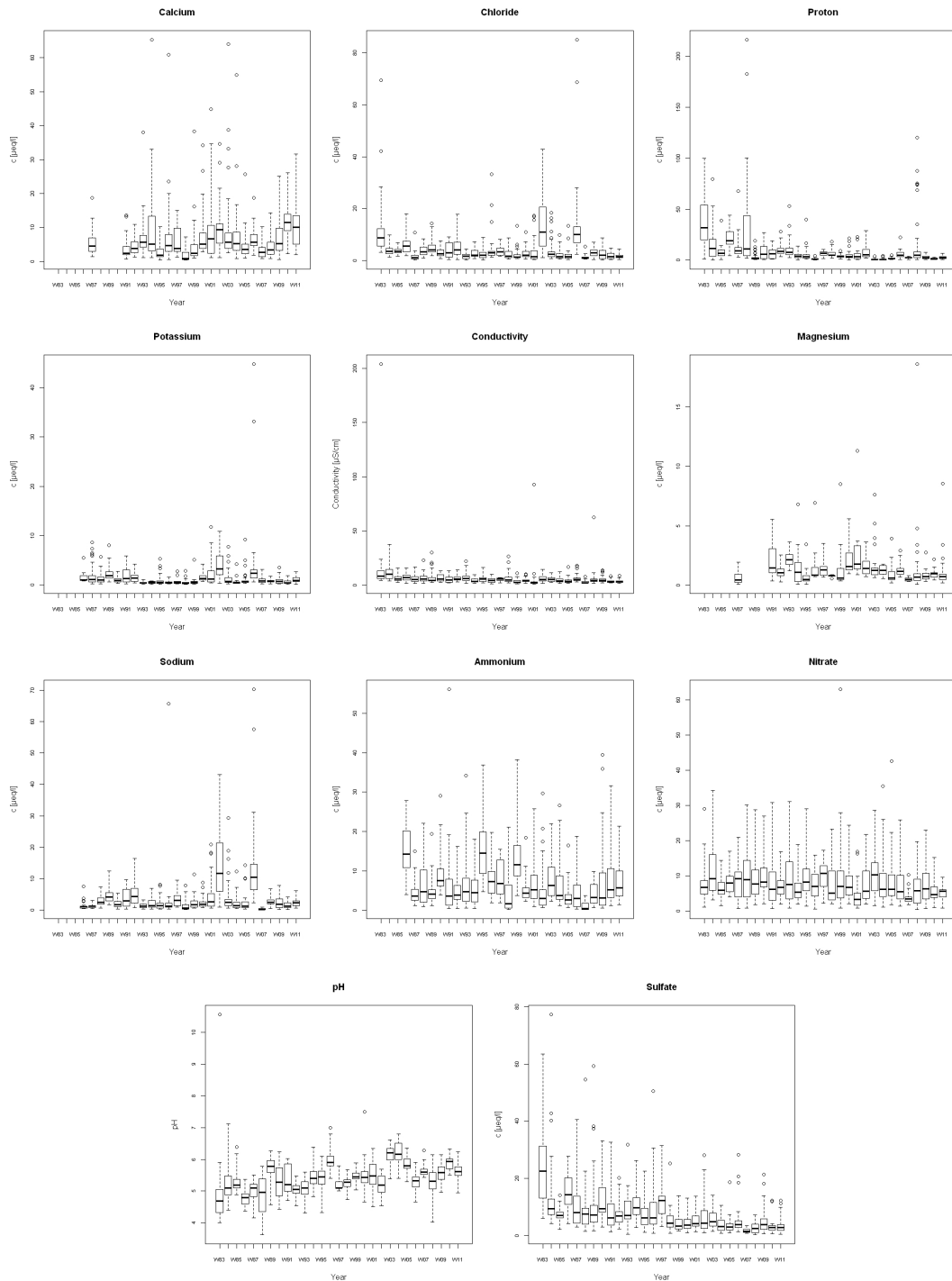
	F1	F2	F3	F4	Commonality
Cl ⁻	0,94	0,09	0,05	0,09	0,91
NO ₃ ⁻	0,02	0,85	0,03	-0,01	0,72
SO ₄ ²⁻	0,06	0,81	-0,07	0,30	0,76
Na ⁺	0,96	0,02	0,00	0,06	0,93
NH ₄ ⁺	0,05	0,85	0,11	-0,14	0,75
K ⁺	0,91	0,01	0,08	0,10	0,85
Mg ²⁺	0,17	0,04	0,25	0,92	0,94
Ca ²⁺	0,08	0,06	0,96	0,23	0,98

	F1	F2	F3	F4
SS loadings	2,68	2,11	1,01	1,03
Proportion Var.	0,34	0,26	0,13	0,13
Cumulative Var.	0,34	0,60	0,73	0,85

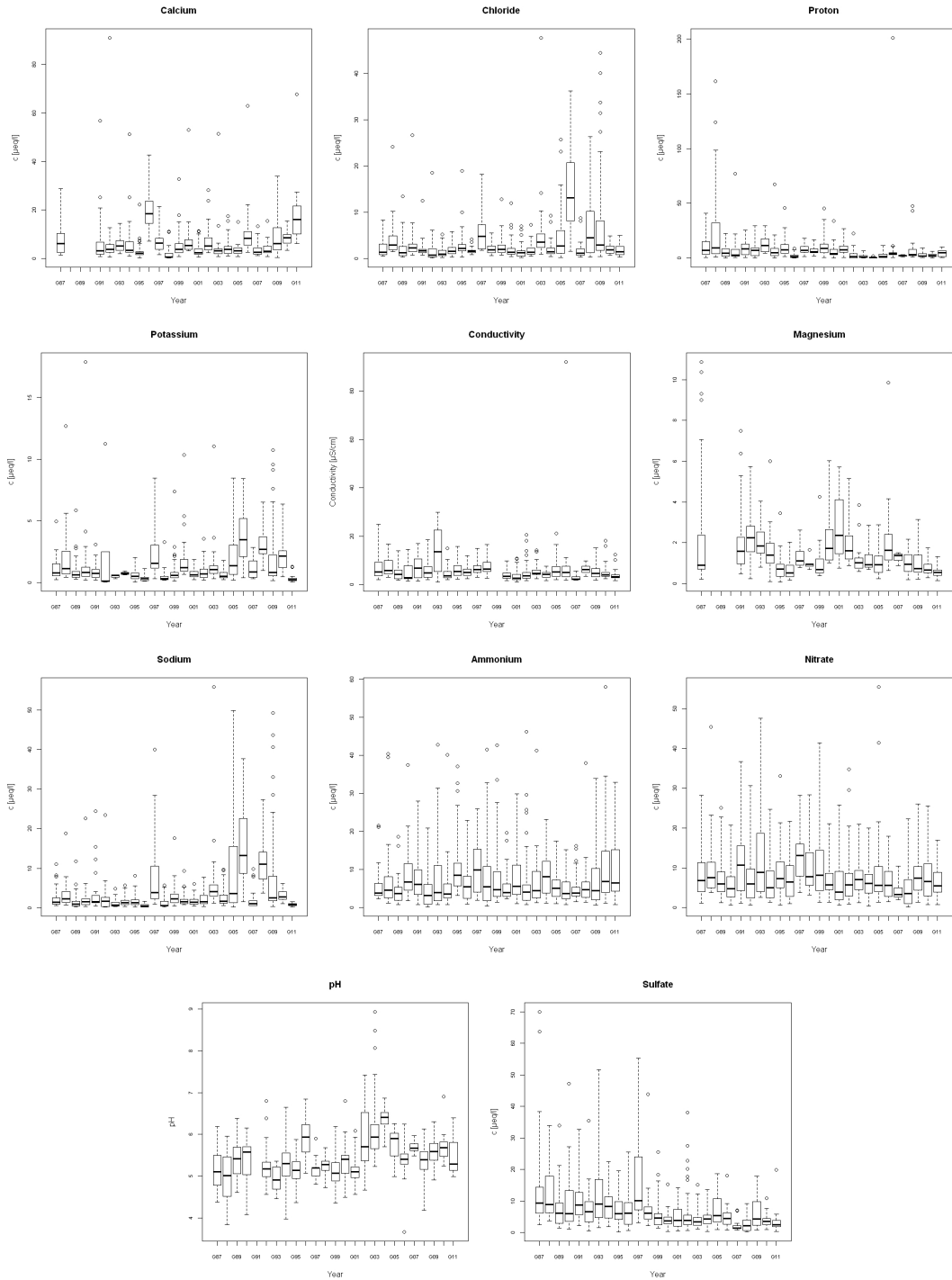
Table B.10.: PCA GOK excl. H⁺ and 4 factors

C. Boxplots

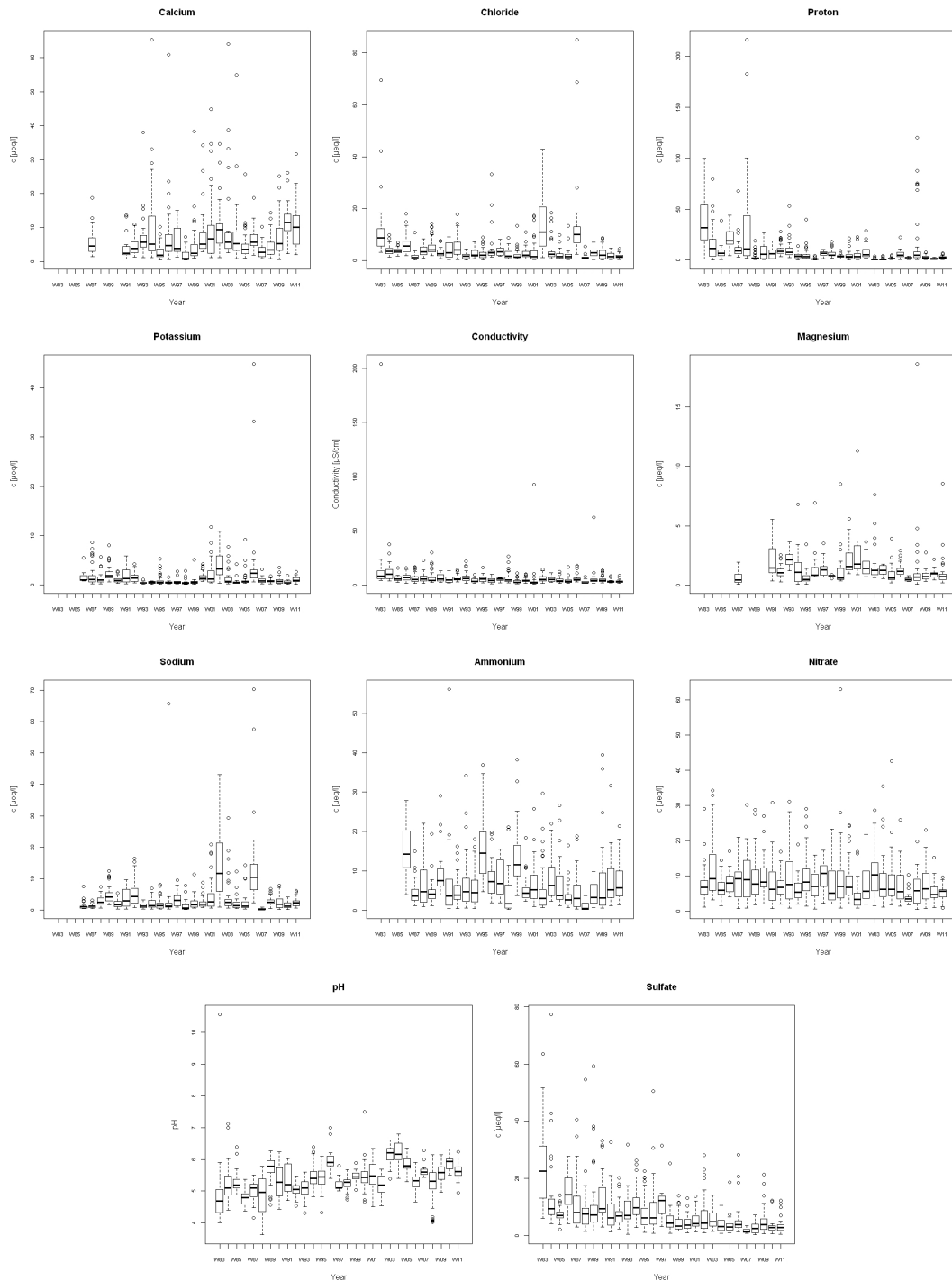
C.1. 3*Interquantil range (WUK)



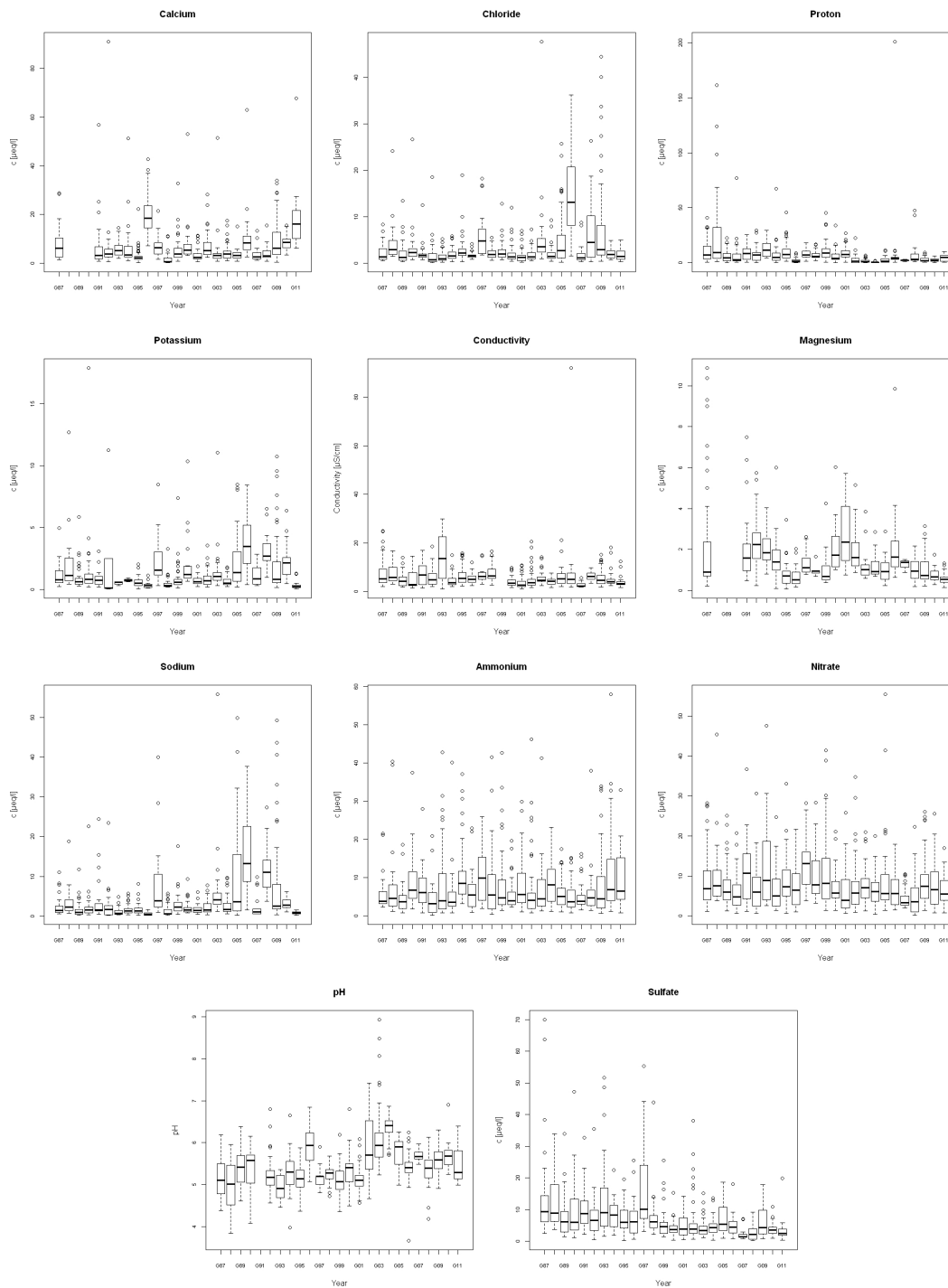
C.2. 3*Interquantil range (GOK)



C.3. 1,5*Interquantil range (WUK)



C.4. 1,5*Interquantil range (GOK)



D. Depth profiles for all years

D.1. WUK

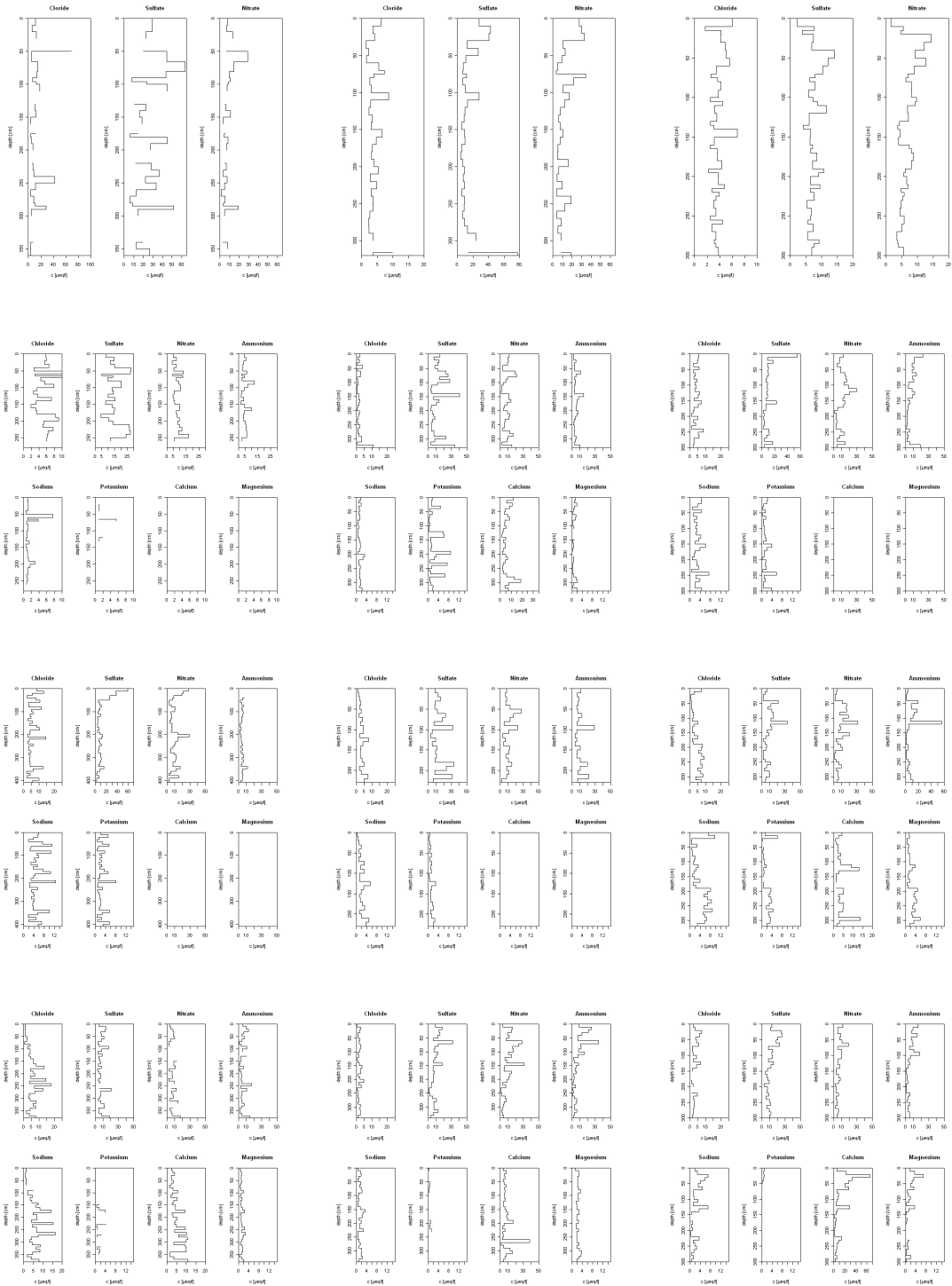


Figure D.1.: from left to right 1983-1994

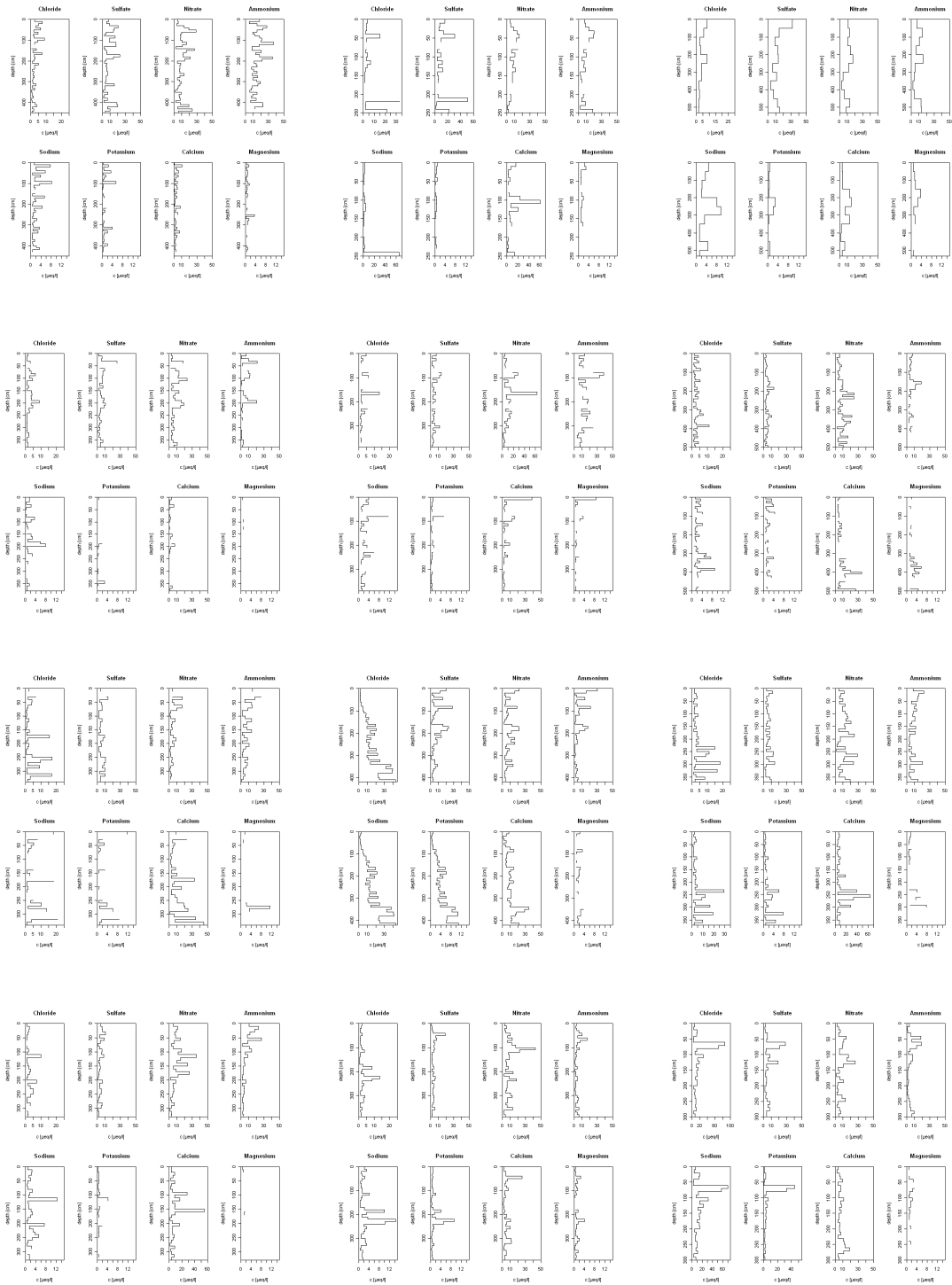


Figure D.2.: from left to right 1995-2006

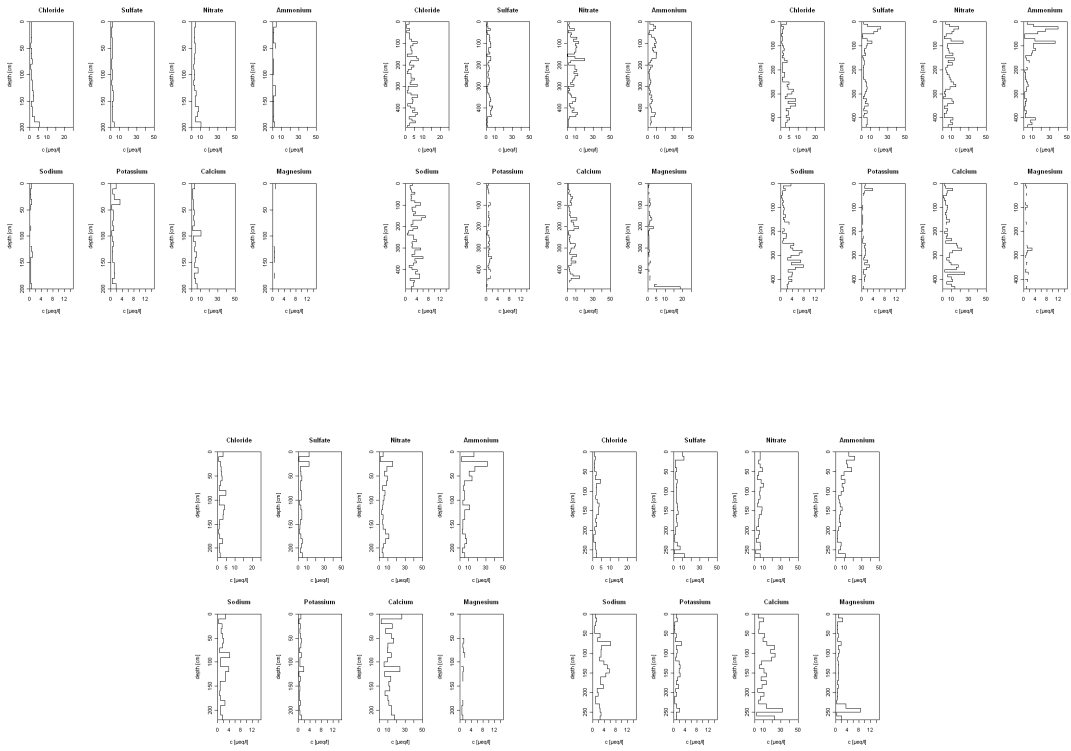


Figure D.3.: from left to right 2007-2011

D.2. GOK

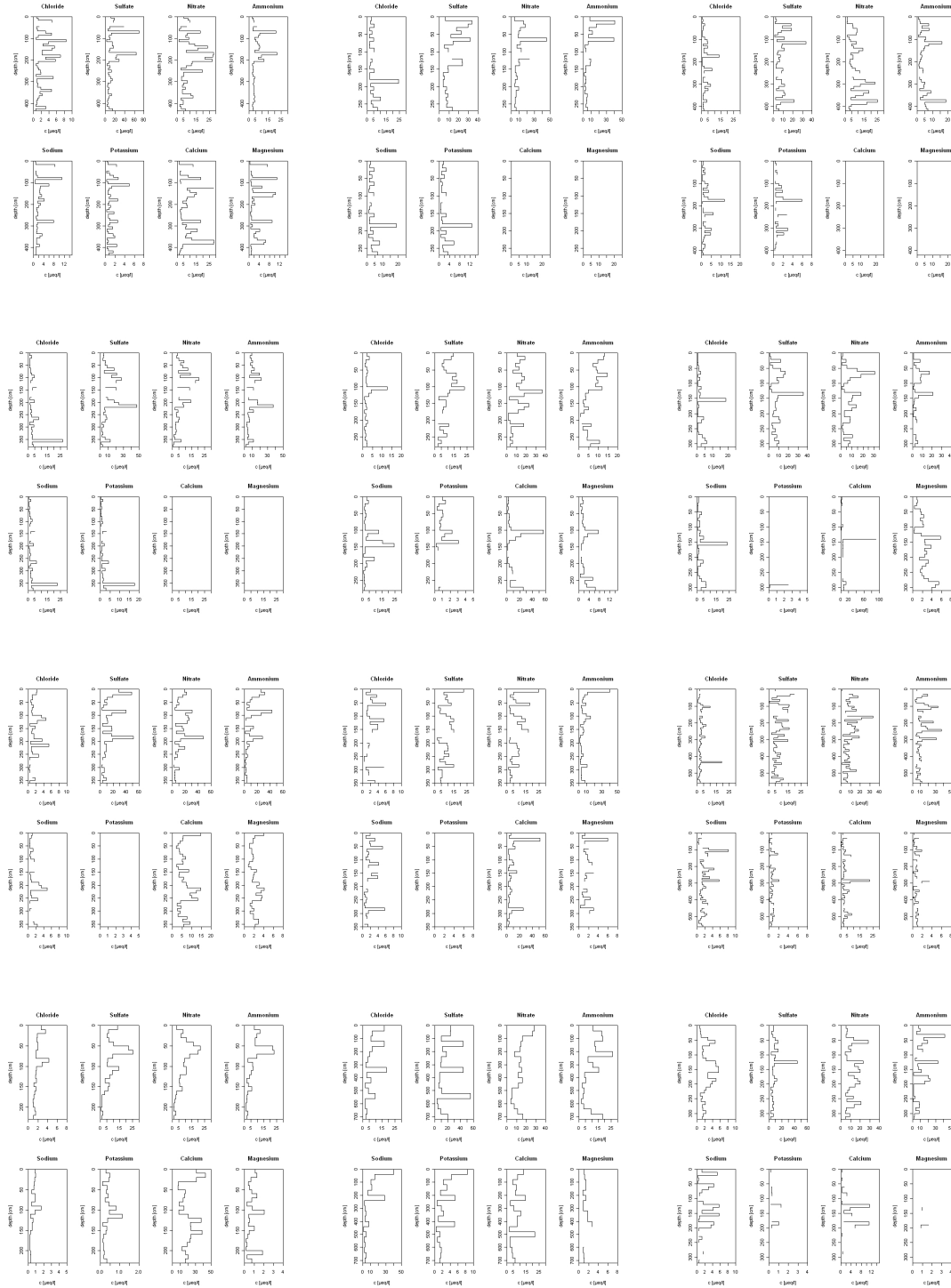


Figure D.4.: from left to right 1987-1998



Figure D.5.: from left to right 1998-2010

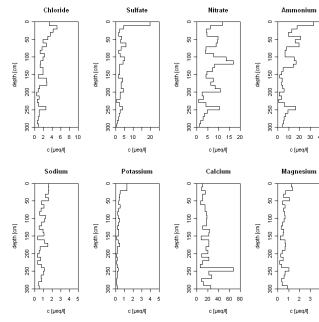


Figure D.6.: from left to right 2011

Curriculum Vitae

ING. MARION ROTHMÜLLER
17.09.1984, Vienna, Austria

Education

- 1990–94 ELEMENTARY SCHOOL
Carl Prohaska Platz 1, 1100 Vienna
- 1994–98 SECONDARY SCHOOL
*Realgymnasium unter besonderer Berücksichtigung der musischen Aus-
bildung*
Pichelmayergasse 1, 1100 Vienna
- 1998–03 HIGHER TECHNICAL SCHOOL FOR CHEMISTRY
*Höhere Lehr- und Versuchsanstalt für chemische Industrie mit Ausbil-
dungsschwerpunkt technische Chemie und Umwelttechnik*
Rosensteingasse 79, 1170 Vienna
- SINCE 2007 UNIVERSITY OF VIENNA
Meteorology

Employment History

- 2003–11 TECHNICIAN
*University of Natural Resources and Life Sciences (BOKU)
Institute of Applied Microbiology*
- 2007 TEMPORARY JOB FOR INVENTORY TAKING
Essilor Austria GmbH
- 2003 INTERNSHIP JULY AND AUGUST
Anker Snack & Coffee GmbH
- 2002 INTERNSHIP AUGUST
Boehringer Ingelheim Austria GmbH
- 2002 TEMPORARY JOB FOR INVENTORY TAKING
Essilor Austria GmbH
- 2001 INTERNSHIP AUGUST
Boehringer Ingelheim Austria GmbH
- 2000 INTERNSHIP JULY
MA 38 - Magistrat für Lebensmitteluntersuchung

Tutorial Jobs

- 2010 FIELDPRACTICA II - *Stormchasing in Vienna*
Kestrel, Mikroregenradar, Distrometer
- 2009 FIELDPRACTICA I - *Traflberg, Gutensteiner Alps*
Messlift, SONIC, MAWS, HOBO

Attended Field Practica

- 2011 GLACIER PRACTICAL COURSE
Hoher Sonnblick, Hohe Tauern, Austria
Snowprofiles, Stratigraphic description, Sampling for snow chemistry analysis
- 2011 METEOROLOGICAL EXCURSION
Costa Rica
Climatology of Costa Rica, small scale observations with Kestrel
- 2010 GLACIER PRACTICAL COURSE
Wurtenkees, Hohe Tauern, Austria
Snowprofiles, Stratigraphic description, Sampling for snow chemistry analysis
- 2010 METEOROLOGICAL EXCURSION
Glider airfield in Lower Austria
Radiosonde, Theodolite, Synop report, thermal forecast
- 2009 ECOLOGICAL EXCURSION
Sibiria
Soil, Water and Vegetation Analysis from the forrest to the tundra

Research Publications

- 2010 *“Identification and characterisation of novel Pichia pastoris promoters for heterologous protein production”*
Stadlmayr G., Mecklenbräuker A., Rothmüller M., Maurer M., Sauer M., Mattanovich D., Gasser B.
Journal of Biotechnology, Volume 150, Issue 4, December 2010, Pages 519–529

Skills

Microsoft Office - high level

The R Project for Statistical Computing - basics

English - advanced in spoken and written

Research Interests

Atmospheric Chemistry, Snow Chemistry, Climate Change

Interests

Skiing, Mountain Climbing, Dancing